Field-Flow Fractionation of Amphiphilic Block Copolymers

by

Guilaume Hermanus Greyling

Dissertation presented for the degree of

Doctor of Philosophy in Polymer Science in the

Faculty of Science at Stellenbosch University

Supervisor: Prof. Harald Pasch

March 2016

Declaration

By submitting this dissertation electronically, I declare that the entirety of the work contained therein is my own, original work, that I am the sole author thereof (save to the extent explicitly otherwise stated), that reproduction and publication thereof by Stellenbosch University will not infringe any third party rights and that I have not previously in its entirety or in part submitted it for obtaining any qualification.

March 2016

Declaration for Publications

With regards to the manuscripts in the dissertation, the nature and the scope of the candidate's contributions were as follows:

Nature of Contributions	Extent of Contributions (%)
Experimental work, Data analysis, Manuscript preparation, Addressing of reviewers' comments	90

The following co-author contributed to the manuscripts in the dissertation as follows:

Name	E-mail address	Nature of Contributions	Extent of Contributions (%)
Harald Pasch		Supervision and mentoring, Revision and correcting of manuscripts for publication.	10

March 2016

Declaration by co-author:

1. The declaration above accurately reflects the nature and extent of the contributions of the candidate and co-author to the manuscripts in the dissertation.
2. In addition to the co-author specified above, no other authors contributed to the manuscripts in the dissertation, and
3. Potential conflicts of interest have been disclosed to all parties and that all parties consented to the inclusion of the results presented in the manuscripts into the dissertation.

March 2016

Abstract

Complex polymers have multiple distributions with respect to molecular weight, chemical composition, functionality as well as molecular topology and architecture. Moreover, these distributions affect polymer properties thus making it necessary to develop fractionation techniques capable of providing comprehensive information regarding these distributions. As a result, field-flow fractionation (FFF) has emerged as a main stream fractionation technique for the characterisation of complex macromolecular, colloidal and particulate materials as it has significant advantages over current column-based techniques. Of the various FFF subtechniques, thermal field-flow fractionation (ThFFF) shows sensitivity towards chemical composition and as such has successfully been applied to address the analytical challenges associated with chemical composition determination.

The work presented in this study demonstrates that the separation capabilities of ThFFF are not limited to size and chemical composition, but can also be extended to include microstructure-based separations. It is further demonstrated that ThFFF is currently the only fractionation technique capable of separating dynamic polymer self-assemblies (such as micelles) according to corona microstructure while simultaneously providing information regarding shape, aggregation number, diffusion, thermal diffusion and Soret coefficients as well as size, molecular weight, chemical composition and their respective distributions. Moreover, the determination of chemical composition distributions was accomplished by a novel approach coupling ThFFF to FTIR via a LC-Transform interface.

Opsomming

Komplekse polimere het verskeie verspreidings ten opsigte van molekulêre eienskappe, soos molekulêre massa, funksionaliteit, chemiese samestelling, mikrostruktuur, molekulêre argitektuur en molekulêre topologie. Hierdie verspreidings kan die toepassings van polimere direk beinvloed en dus is dit nodig om fraksioneringstegnieke te ontwikkel wat ‘n omvattende beeld van hierdie verspreidings kan lewer. As ‘n gevolg het veldvloeifraksionering (FFF) as ‘n hoofstroom polimeerkarakteriseringstegniek ontwikkel vir die analiese van makromolekulêre en partikulêre materiale omdat dit verskeie voordele het bo huidige metodes. Termiese veldvloeifraksionering (ThFFF) is n fraksioneringstegniek wat sensitief is vir die chemiese samestelling van polimeriese materiale en as sulks word dit gebruik om die uitdagings wat verband het met die bepaling van chemiese samestellings, aan te pak.

Die werk wat hier beskryf word bewys dat die fraksioneringsvermoë van ThFFF is nie net beperk tot molekulêre groote en chemiese samestelling nie, maar dat dit ook mikrostruktuur insluit. Dit word ook gewys dat ThFFF is huidiglik die enigste fraksioneringstegniek wat die form, saampakgetal, diffusie, termies diffusie en Soret koëffisiënte asook molekulêre groote, molekulêre massa en chemiese samestelling verspreidings van micelles kan bepaal terwyl dit die hulle skei volgens chemiese samestelling. Die bepaling van chemiese samestelling verspreidings word gedoen deur n nuwe metode wat ThFFF koppel met FTIR deur gebruik te maak van n LC-Transform apparaat.

Acknowledgements

Firstly, I would like to thank my supervisor Prof. Harald Pasch for giving me the opportunity and freedom to explore the field of thermal field-flow fractionation. I am very grateful for the opportunities that I have been given to broaden my scientific knowledge. I appreciate your advice, insight, financial and academic support.

I would also like to thank all the researchers of our group as well as the staff members at the Department of Chemistry and Polymer science for the assistance whenever I needed it.

I would like to thank my friends and family for all of their support and encouragement.

TABLE OF CONTENTS

List of Figures

List of Symbols and Abbreviations

A	Proportionality constant
ACN	Acetonitrile
AF4	Asymmetric flow field-flow fractionation
AFM	Atomic force microscopy
BuMA	Poly(butyl methacrylate)
tBuMA	Poly(t-butyl methacrylate)
nBuMA	Poly(n-butyl methacrylate)
c	Concentration of analyte
c_0	Concentration of analyte at accumulation wall
C_∞	Characteristic ratio
CCD	Chemical composition distribution
CH	Cyclohexane
CMC	Critical micelle concentration
CMT	Critical micelle temperature
δ	Hildebrand solubility parameter
D	Diffusion coefficient
DCM	Dichloromethane
D_h	Hydrodynamic diameter

DLS	Dynamic light scattering
DMF	Dimethylformamide
dn/dc	Specific refractive index increment
DOX	Dioxane
dRI	Differential refractive index
dT/dx	Applied temperature gradient, also see ΔT
D_T	Thermal diffusion coefficient
F	Force
FFF	Field-flow fractionation
FlFFF	Flow field-flow fractionation
FTIR	Fourier transform infrared spectroscopy
^{1}H-NMR	Proton nuclear magnetic resonance spectroscopy
k	Boltzmann constant
ℓ	Analyte cloud equilibrium mean layer thickness
LCCC	Liquid chromatography at critical conditions
MALLS	Multiangle laser light scattering
MEK	Methyl ethyl ketone
MMD	Molecular weight distribution
M_w	Molecular weight

NMR	Nuclear magnetic resonance spectroscopy
P'	Snyder polarity index
PB	Polybutadiene
1,2-PB	1,2-polybutadiene
1,4-PB	1,4-polybutadiene
PB-PS	Polybutadiene-polystyrene block copolymer
1,2 PB-PS	1,2-polybutadiene-polystyrene block copolymer
1,4 PB-PS	1,4-polybutadiene-polystyrene block copolymer
PI	Polyisoprene
1,4-PI	1,4-polyisoprene
3,4-PI	3,4-polyisoprene
PMMA	Poly(methyl methacrylate)
PMMA-PS	Poly(methyl methacrylate)-polystyrene block copolymer
iPMMA-PS	Isotactic poly(methyl methacrylate)-polystyrene block copolymer
sPMMA-PS	Syndiotactic poly(methyl methacrylate)-polystyrene block copolymer
PS	Polystyrene
PSD	Particle size distribution
R_g	Radius of gyration
R_g/R_h	Shape factor

R_h	Hydrodynamic radius
SEC	Size exclusion chromatography
SEM	Scanning electron microscopy
SLS	Static light scattering
SSBR	Solution styrene-butadiene-rubber
S_T	Soret coefficient
T	Temperature
t_o	Elution time of an unretained analyte
t_r	Elution time
ΔT	Applied temperature gradient
TEM	Transmission electron microscopy
THF	Tetrahydrofuran
ThFFF	Thermal field-flow fractionation
U	Field-induced migration
UV	Ultraviolet
w	Channel thickness
x	Distance from the accumulation wall
Z	Aggregation number

Chapter 1

Introduction and Objectives

1.1 Introduction

The high demand for new materials with improved performance and tailored properties is one of the major driving forces behind the development of novel and complex synthetic polymers. Polymers are highly complex multicomponent materials which have various distributions in properties such as molecular weight (chain length), chemical composition, microstructure as well as molecular architecture and topology.[1,2] As property distributions can significantly influence applications, proper monitoring and characterisation of these distributions is needed in order to improve polymer performance.[1,2] In order to determine the various distributions, separation is required. Thus, for complex polymers separation according to molecular weight as well as according to composition and microstructure is essential.[2]

Polymer microstructure can greatly influence properties such as glass transition temperature, viscosity, solubility as well as mechanical and viscoelastic properties.[3–5] However, separating polymers according to chemical composition and microstructure is challenging with traditional column-based techniques and although separation of polymers regarding different molecular parameters has been accomplished by techniques such as size exclusion chromatography (SEC) and liquid chromatography at critical conditions (LCCC), SEC separates according to hydrodynamic size in solution which is mainly determined by polymer chain length.[6–8] The effect of different microstructures on size is rather small and, therefore, SEC is not suitable for the separation of polymers based on microstructure. Furthermore, while the separation of polymers according to chemical composition and

microstructure is feasible by LCCC, optimisation of mobile phase composition and column temperature is very tedious and time consuming.[9] In addition to these limitations, column-based techniques are further limited in their suitability for the characterisation of high molecular weight and fragile analytes as interaction with the stationary phase and column frits could cause shear degradation.[10,11]

Field-Flow Fractionation (FFF) is a family of channel-based fractionation techniques that has attracted significant attention for the fractionation and characterisation of complex macromolecular, colloidal and particulate materials.[12,13] The open channel design makes FFF more suitable for the characterisation of high molecular weight and fragile compounds than traditional column-based techniques as the absence of a stationary phase significantly reduces shear degradation.[10–12] Additionally, sample preparation steps such as filtering, which could affect sample composition, are not often required prior to FFF analysis. Of the various FFF subtechniques, thermal field-flow fractionation (ThFFF) is the best suited method to obtain information regarding chemical composition and as such has been applied to the characterisation of a variety of analytes including polymer blends, copolymers, colloids and aggregates.[12,14–19] More importantly, this sensitivity to composition could potentially make ThFFF a suitable technique for microstructure-based fractionation.

In addition to possessing complex property distributions, polymers also exhibit complex behaviours in solution such as the self-assembly of block copolymers into various kinds of nanostructures. Moreover, the solution behaviour of block copolymers has been at the forefront of the modern nanotechnology revolution.[20] The ability of block copolymers to self-assemble into various nanostructures (such as micelles) when dissolved in a selective solvent (i.e. a good solvent for one of the blocks but a precipitant for the other) has attracted much attention as polymeric

micelles provide a versatile platform that can readily be modified for a wide range of applications.[20–22] Block copolymer micelles consist of a core formed by the insoluble block and a corona formed by the soluble block (Figure 1 A).[23] The critical concentration at which the block copolymers start to self-assemble into micelles is called the critical micelle concentration, CMC. Below the CMC only molecularly dissolved copolymer chains (or unimers) are found whereas above the CMC, micelles are in equilibrium with unimers.[22,23] Closely related to the CMC is the critical micelle temperature, CMT. The CMT is the temperature above which micelles disassemble into unimers due to decreasing solvent selectivity with increasing temperature.[23,24]

Micelles are appealing for applications in fields such as colloid stabilization, microreactors, drug delivery and biomedical applications due to their stability, versatility and relative ease of preparation.[21–23,25] Micelles consisting of two or more different block copolymers and thus mixed compositions (i.e. mixed micelles), have attracted significant attention in recent years as a convenient method to improve micelle stability and prepare micelles with unique morphologies and properties (Figure 1 B).[25,26] Mixed micelles can be formed by either triggering micelle formation in the presence of various block copolymers or by the exchange of unimers between micelles of different compositions.[25] Moreover, mixed micelles enable the incorporation of various functionalities into the system without the synthetic challenge of preparing a single copolymer with the desired functionalities.[25] However, the successful application of micelles greatly depends on their comprehensive characterisation in terms of properties such as size, aggregation number, morphology, corona composition and molecular weight.[22,25] Additionally,

the distributions of these properties also need to be determined as they significantly influence applications.[25,27]

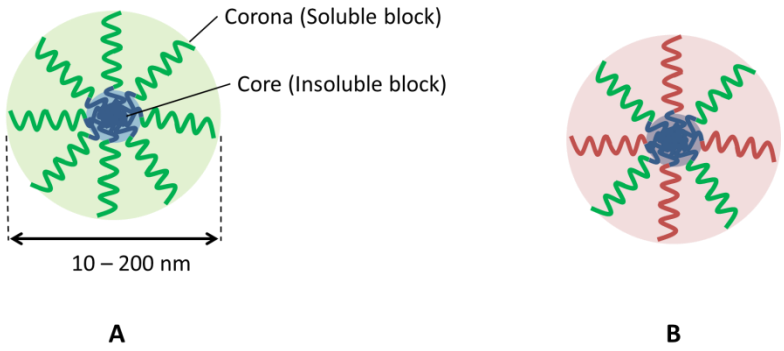

Figure 1. Schematic representations of different types of block copolymer micelles. A) Micelles consisting of a single type of block copolymer. B) Mixed micelles consisting of different types of block copolymers.

Micelles are traditionally characterised in terms of size, molecular weight and chemical composition by techniques such as electron microscopy (SEM and TEM), atomic force microscopy, dynamic and static light scattering, NMR and fluorescence spectroscopy.[22,23] However, while microscopy and light scattering techniques are suitable to determine particle size and its distribution, these techniques cannot directly determine molecular weight, chemical composition or their respective distributions.[28] With regards to NMR and fluorescence spectroscopy, although these techniques can be used to determine corona composition and number average molecular weight, they yield no information regarding composition or molecular weight distributions.[26,29,30] Moreover, traditional micelle characterisation techniques become less reliable for samples exhibiting complex or multiple size, molecular weight or composition distributions.[31] Thus, currently there are no suitable techniques which can monitor and characterise micelles in terms of chemical composition, size, molecular weight and their respective distributions. Consequently,

a single technique that can directly determine these properties and their respective distributions is highly desirable.[26,28]

To address this issue, FFF and SEC have been used to separate and characterise micelles. However, SEC showed analyte trapping in the column, disassembly of micelles and adsorption on the column packing occurring during analysis.[23,32] On the other hand, various FFF subtechniques such as asymmetric flow field-flow fractionation (AF4), flow field-flow fractionation (FlFFF) and ThFFF were shown to be capable of successfully characterising self-assemblies (such as micelles) in terms of size, molecular weight and their respective distributions.[27,33,34] However, although FlFFF, AF4 and ThFFF can all separate analytes according to size and determine molecular weight and size distributions, only ThFFF can additionally separate analytes according to chemical composition. Thus, only ThFFF can potentially be applied to separate micelles according to corona composition while simultaneously determining size, molecular weight and chemical composition distributions.[12,35,36]

1.2 Research Hypothesis

To date it has been shown that ThFFF can separate analytes according to size and chemical composition and the question whether separations according to microstructure can be achieved, has not yet been addressed. Thus, the subsequent questions were posed:

1) Is ThFFF sensitive towards microstructure, and if so,
2) Which microstructures (such as tacticity and topology) could be separated?

ThFFF has the most potential of current fractionation techniques to successfully separate polymer self-assemblies according to chemical composition while simultaneously providing comprehensive information on shape, aggregation number,

diffusion, thermal diffusion and Soret coefficients as well as corona composition, size, molecular weight and their respective distributions. Hence, the following questions concerning block copolymer micelles were posed:

1) Does corona microstructure influence micelle stability and retention behaviour in ThFFF, and if so,
2) Is microstructure-based fractionation of block copolymer micelles feasible by ThFFF?

Lastly, the lack of suitable analytical techniques which can monitor and characterise the formation of mixed micelles in terms of chemical composition, size, molecular weight and their respective distributions posed the following question:

1) Can ThFFF monitor and characterise the formation of mixed micelles according to corona microstructure while simultaneously determining size, molecular weight, chemical composition and their respective distributions?

1.3 Objectives

This first objective of this study was to determine if the separation capabilities of ThFFF are limited to size and chemical composition or if separations based on polymer microstructure could be achieved. The sensitivity of ThFFF towards microstructure was investigated by the analyses of polymers with similar molecular weights but different microstructures including:

1) 1,4- and 3,4-polyisoprene
2) 1,4- and 1,2-polybutadiene
3) Isotactic and syndiotactic poly(methyl methacrylate)
4) Poly(n-butyl methacrylate) and poly(t-butyl methacrylate)

The second objective was divided into two parts. The first part was to determine the influence of corona microstructure on the stability and retention behaviour of micelles in ThFFF while the second part subsequently investigated the capability of ThFFF to separate micelles according to corona composition. The suitability of ThFFF to characterise and separate micelles of similar sizes according to corona composition was investigated by preparing micelles with similar polystyrene cores but different corona compositions such as:

1) 1,4- and 1,2-polybutadiene
2) Isotactic and syndiotactic poly(methyl methacrylate)

The third objective was to subsequently investigate if the unique fractionation capabilities of ThFFF could be employed to monitor (in addition to size and molecular weight) changes in chemical composition and its distribution during the formation of mixed micelles. To this end, mixed micelles were prepared from micelles with different corona microstructures while changes in chemical composition were monitored by ThFFF coupled to FTIR (via a LC-Transform approach).

1.4 Layout of Dissertation

This dissertation is divided into the following chapters:

Chapter 1

A brief introduction to concepts relevant to the study, including the objectives and outline of the dissertation are given.

Chapter 2

A concise discussion of the historical background and theory related to FFF and ThFFF for the molecular characterisation of complex polymers and their self-assemblies.

Chapter 3

The experimental part contains the analysis conditions and instrument parameters for all the techniques used as well as micelles preparation methods.

Chapter 4

The results of this study, according to the three main objectives of this work are presented here in the form of published articles. The first section contains the results obtained by ThFFF analysis of polymers with various microstructures. The second section shows the results of ThFFF analysis of block copolymer micelles with various corona compositions while the third section explains a novel analytical approach (ThFFF-FTIR) in which the chemical composition distribution of mixed micelles as a function of elution time is determined by coupling FTIR spectroscopy to ThFFF via an LC-Transform interface.

Chapter 5

The conclusions of all three sections of this study are summarised and recommendations are proposed for future studies within this field of research.

Chapter 6

All the bibliographic references relevant to the current dissertation are given here.

Chapter 2

Historical and Theoretical Background

2.1 Field-Flow Fractionation

Field-Flow Fractionation (FFF) is a family of channel-based fractionation techniques that was first introduced in 1966.[37] Since its inception, FFF has been used to characterise numerous analytes including nanotubes, bacteria, nanoparticles, whole cells, viruses, polymers, liposomes, colloids, polysaccharides, aggregates and proteins.[13,18,38–41] The range of possible applications for FFF is enormous.

FFF is an elution based technique in which separation occurs in a single liquid phase where smaller molecules are the first to elute.[12,42] Moreover, FFF also exhibits other important characteristics such as low shear rates (ideal for investigating fragile species), low sample loss, adjustable selectivity and speed as well as the ability to separate analytes according to different physicochemical properties.[12,18,42,43]

In FFF an external field is applied perpendicular to a carrier liquid flowing through an open, thin ribbon-like channel. Due to the high aspect ratio of the channel, a laminar parabolic flow velocity profile forms which results in faster flow streams towards the centre of the channel and slower streams towards the channel walls.[12,42] Elution from the channel is determined by the analyte cloud's average distance from the accumulation wall and thus its position in the flow velocity profile (Figure 2).[18,42]

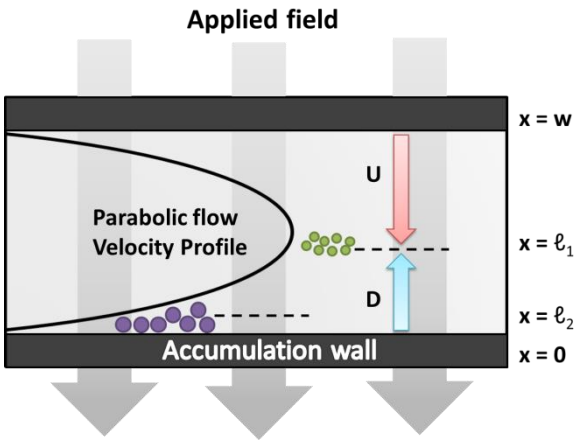

Figure 2. Schematic representation of the FFF separation mechanism. Elution is governed by the balance between the field-induced migration (U) of the analytes towards the accumulation wall and the diffusion (D) of analytes away from the accumulation wall due to a concentration build up. Furthermore, x = 0 represent the accumulation wall while x = w is the channel thickness and ℓ_1 and ℓ_2 are the analyte clouds' mean layer thicknesses.

Therefore, the further the analyte cloud is from the accumulation wall (faster flow streams), the shorter the elution time. The analyte cloud's average distance from the accumulation wall is determined by the balance between the field-induced migration of analytes towards the accumulation wall and the diffusion of analytes away from this wall due to a concentration build-up.[12] When equilibrium between the two transport processes is reached, the analyte concentration, c, exhibits an exponential function of distance, x, from the accumulation wall given by:[12,42,44]

$$c = c_0 exp^{\left(\frac{-x}{\ell}\right)} \qquad (1)$$

where c_0 is the analyte concentration at the accumulation wall, x is the distance from the accumulation wall and ℓ is the equilibrium mean layer thickness of the analyte cloud. Ideally, each analyte will have a unique ℓ value which corresponds to a different position in the parabolic flow velocity profile and thus different elution time

(Figure 2).[12,42] Therefore, separation is achieved when the ℓ values differ for different analytes. Furthermore, ℓ can also be expressed as the ratio of diffusion coefficient (D) and the field-induced migration, U:[12,42]

$$\ell = \frac{D}{|U|} \qquad (2)$$

It can be seen that larger analytes (smaller D values) and/or stronger interaction with the applied field (U) result in smaller ℓ values and thus longer elution times. Moreover, the relationship between ℓ, elution time (t_r) and the force (F) exerted on an analyte by the applied field can be approximated by:[12,42]

$$\frac{t_r}{t_0} = \frac{w}{6\ell} = \frac{|F|w}{6kT} \qquad (3)$$

where t_0 is the void time, w is the channel thickness, k is Boltzmann's constant and T is absolute temperature. Assuming that all particles are non-interacting point masses and that w >> ℓ, equation 3 shows that F governs both retention and separation as differences in the force experienced by analytes will result in roughly proportional differences in t_r.[12,42]

The magnitude of F depends on analyte properties, field strength and the type of field employed.[42] Thus, almost any type of field can be applied, provided it interacts with some physicochemical property of the analytes to drive them to the accumulation wall. This has given rise to multiple techniques within the FFF family of which thermal, sedimentation, and cross-flow FFF are the most commonly used FFF techniques.[18]

2.2 Thermal Field-Flow Fractionation

ThFFF is the oldest of the FFF subtechniques and utilises a temperature gradient to drive analytes to the accumulation wall.[44] The ThFFF setup consists of a ribbon-like channel which is clamped between two heat conductive blocks. The temperature of one block is controlled by a heating element while the other block's temperature is controlled by circulating chilled water or coolant.[12] Furthermore, ThFFF was successfully miniaturised by the introduction of micro-ThFFF.[45]

ThFFF was originally applied to the characterisation of synthetic polymers in organic solvents but has been expanded to nanoparticles in aqueous as well as nonaqueous solvent mixtures.[16,46] In ThFFF, the effective driving force is given by:[12,42]

$$F = kT\frac{D_T}{D}\frac{dT}{dx} \qquad (4)$$

where D_T is the thermal diffusion coefficient and dT/dx is the applied temperature gradient (also expressed as ΔT). Substituting equations 3 and 4 yields equation 5 which shows that t_r is proportional to the field strength (ΔT) and the Soret coefficient (D_T/D). Furthermore, equation 5 also shows that measuring t_r yields direct information on the Soret coefficient, S_T.

$$\frac{t_r}{t_0} = \frac{D_T\,\Delta T}{6D} \qquad (5)$$

When S_T is known, then if D_T is also known (material constant), D can be calculated which yields information on molecular weight (M_w) through the relationship $D = A(M_w)^{-b}$ where A is an experimentally determined proportionality constant and b is ~0.6 for a thermodynamically good solvent.[13,47] Alternatively, if D is known (for example from FlFFF or SEC), D_T can be obtained which can yield information on chemical composition.[48,49] Thermal diffusion of macromolecular materials in liquids

is still poorly understood and lacks clear theoretical definition to predict elution times and directly relate D_T to sample composition.[35,48,50] Despite this, ThFFF has successfully been applied for the fractionation and characterisation of various polymers and particles in aqueous and organic solvents. Moreover, ThFFF is an excellent tool for the study of thermal diffusion of macromolecular materials in solution.[12,49]

Some of the earliest empirical observations regarding D_T of homopolymers in various organic solvents showed that D_T is virtually independent of molecular weight for high molecular weight polymers but strongly dependent on the chemical composition of both the polymer and solvent.[51] The analysis of polystyrene–polyisoprene diblock copolymers and polystyrene–poly(methyl methacrylate) random copolymers showed that D_T varies linearly with the mole fraction of one of the constituent homopolymers in a thermodynamically good solvent. [52–54] In contrast, for block copolymers which segregate in a selective solvent, D_T is governed by monomers located at the surface of the solvated macromolecule.[52–54] Furthermore, it was later shown that, in addition to composition, D_T is also influenced by factors such as solvent viscosity and polymer chain stiffness.[51,55,56]

The sensitivity of D_T towards chemical composition has made ThFFF a powerful technique to address the analytical challenges associated with polymer and nanoparticle composition. ThFFF has been successfully used for the characterisation of various homopolymers, polymer blends, copolymers, gel containing samples, particles and aggregates.[15,16,19,33,52,57–62] The capabilities of ThFFF to separate homopolymers according to chemical composition was demonstrated early on by the analysis of various polymers and polymer blends such as polystyrene, polyisoprene,

polybutadiene, poly(methyl methacrylate), poly(dimethylsiloxane), poly(α-methylstyrene) and poly(vinyl acetate).[17,47,48,61]

With regards to block copolymers, ThFFF was used to characterise a polystyrene-poly(t-butyl acrylate)-poly(methyl methacrylate) triblock copolymer according to composition and yield information about impurities.[63] Moreover, separate studies that coupled ThFFF online to NMR in order to separate and characterise tri- and diblock copolymers, further highlighted ThFFF's promising abilities to separate polymers according to composition and determine trends in composition distributions.[14,64] The first study characterised a polystyrene-b-poly(methyl methacrylate) diblock copolymer (and its constituent homopolymers) while the second study characterised triblock copolymers consisting of polybutadiene, poly(2-vinylpyridine) and poly(t-butyl methacrylate) blocks to determine trends in composition and molecular weight distributions.[14,64] NMR provided an independent measurement of copolymer composition and confirmed compositional fractionation by ThFFF. Furthermore, analysis of polystyrene–poly(n-butyl acrylate) and polystyrene–poly(methyl acrylate) copolymers showed that ThFFF can be used to evaluate a copolymer's composition by its D_T value, provided D is measured independently.[57] However, although ThFFF has successfully addressed various challenges regarding polymer composition, the suitability of ThFFF for microstructure-based separation is still unclear and remains an area of interest.

In addition to characterising polymers with regards to chemical composition, it was demonstrated by the use of D_T and S_T values that the number of chain ends could also be determined by ThFFF.[65] Experimentally measured D_T and S_T values were used in conjunction with theoretical values to construct calibration curves from which the numbers of arms of poly(methyl methacrylate) star polymers were determined.

This study showed that the determination of chain ends is feasible without the need for linear polymer analogues.[65]

Another very promising application for ThFFF is the characterisation of fragile ultrahigh molecular weight and gel/microgel containing samples. ThFFF is well suited for such fragile samples as shear degradation is virtually negligible in the open channel. The ability of ThFFF to maintain sample integrity was demonstrated by reinjecting well-retained fractions of a polymer standard with a molecular weight of 20×10^6 g mol^{-1}.[11] Furthermore, sample preparation steps (such as filtration) which could potentially encourage sample loss or degradation, are not often required prior to analysis. As a result, ThFFF was used to separate and characterise polyvinyl acetate and solution styrene-butadiene rubber (SSBR) samples containing ultrahigh molecular weight polymers and microgels.[17,66] Moreover, determining the macrostructure and gel content provided insight into the physical behaviour of SSBR.[66]

The unique separation capabilities of ThFFF have not solely been applied to the characterisation of polymers, but they were also broadened to include the characterisation of nanoparticles and polymer self-assemblies such as block copolymer micelles. It was demonstrated by the composition-based separation of various latex, inorganic, metallic and core-shell particles, that ThFFF is sensitive to the surface composition of particles.[16] The retention of these particles were found to be influenced by several factors including ionic strength, carrier solution composition, pH and field strength.[15,67,68] With regards to polymer self-assemblies, the gentle separation conditions (which are suitable for fragile compounds) as well as its sensitivity to composition should make ThFFF a powerful technique for the characterisation of polymeric micelles. Indeed, it was demonstrated that block

copolymer micelles with different core compositions could successfully be characterised by ThFFF.[33] However, although it was shown that ThFFF separates particles according to surface composition, the composition-based separation of polymeric micelles (and the subsequent determination of corona composition distribution) is still an unexplored area of interest.

Chapter 3

Experimental

3.1 Thermal Field-Flow Fractionation

The ThFFF system TF2000 (Postnova Analytics, Landsberg, Germany) was coupled online to UV (PN 3212 at 254 nm, Postnova Analytics), MALLS (PN 3070, Postnova Analytics), dRI (PN 3150, Postnova Analytics) and DLS detectors (Zen 1600, Malvern Instruments, Worcestershire, UK). The TF2000 channel had a tip-to-tip length of 45.6 cm, breadth of 2 cm, thickness of 127 µm and void volume of 1.14 mL. Carrier flow is generated by an isocratic pump (PN 1130, Postnova Analytics) and the samples are introduced into the channel via a Rheodyne manual injection valve. Unless otherwise stated, the temperature of the cold wall was 25 °C and a constant ΔT of 60 degrees was used to achieve fractionation. Furthermore, values for S_T were calculated as shown in Chapter 2, equation 5, while values for D_T were calculated from equation 6:

$$D_T = \frac{6Dt_r}{\Delta T t_0} \qquad (6)$$

where t_o is the void time, t_r is the elution time of the sample and ΔT is the temperature difference between the hot and cold wall. D_h and D values were determined by DLS analysis while solvent flow rates were adjusted to meet system pressure requirements. Samples were injected through a 100 µL capillary sample loop and triplicate analyses of each sample were performed under non-overloading sample concentrations.

3.2 ^{1}H NMR

The NMR experiments were conducted on a 400 MHz Varian Unity Inova spectrometer (Agilent/Varian, Palo Alto, California, USA). The measurements were performed with a 5 mm dual broadband pulsed field gradient probe. Two-hundred and fifty-six scans using 45° pulses were acquired with an acquisition time of 2.0 s and a relaxation delay of 1 s. The polymer samples were fractionated by ThFFF, collected in 25 to 30 runs, and evaporated at room temperature. The collected fractions were dissolved in 0.7 mL $CDCl_3$ and subsequently analysed. Data were processed by use of MestReNova software version 7.1.1. Quantitative information obtained from the spectra is accurate within 5 %.

3.3 Micelle Preparation

3.3.1 Nanoprecipitation method

Twenty milligrams of polymer was dissolved in 0.4 mL of acetone. This solution was added dropwise to the selective solvent under stirring over 10 min. The solution was then further stirred for 30 min and heated to evaporate acetone.

3.3.2 Cosolvent method

Thirty two milligrams of polymer was dissolved in 0.6 mL tetrahydrofuran. To the solution, 8 mL of selective solvent was added dropwise. After the addition of the selective solvent, the solution was then heated to 60 °C for 2h to remove the remaining tetrahydrofuran.

3.4 Analyte Deposition by LC-Transform Interface

An LC-Transform series model 300 (Lab Connections) was coupled to the ThFFF system and the analytes were deposited on a germanium disk rotating at a speed of

10° min^{-1}. The disk stage and nozzle temperatures of the LC-Transform were set to 100 and 85 °C, respectively.

3.5 FTIR Analyses of the Deposited Analytes

FTIR analyses were performed on a Thermo Nicolet iS10 Spectrometer (Thermo Scientific, Waltham, MA), equipped with the LC-Transform FTIR interface connected to a standard transmission baseplate. Spectra were recorded at a resolution of 8 cm^{-1} with 16 scans being recorded for each spectrum. Thermo Scientific OMNIC software (version 8.1) was used for data collection and processing.

Chapter 4

Results and Discussion

4.1 Separation of Polymers According to Microstructure, Tacticity and Molecular Topology.

The first part of this study describes the separation of various isomers of polyisoprene (PI), polybutadiene (PB), poly(methyl methacrylate) (PMMA) and poly(butyl methacrylate) (BuMA) according to microstructure, tacticity and molecular topology.

4.1.1 Polyisoprene and Polybutadiene

G. Greyling, H. Pasch, *Macromol. Rapid Commun*. **2014**, *35*, 1846–1851.

As mobile phase composition and viscosity are important parameters in ThFFF, the influence of these parameters on the separation of PI and PB isomers was investigated.[51,61] In a first step of the experiments, ThFFF analysis of a number of PI and PB samples were conducted in tetrahydrofuran (THF) as mobile phase and the results demonstrated that samples with different microstructures elute at distinctly different elution times. THF is a low viscosity, thermodynamically good solvent for both PI and PB and thus serves as a good starting point for the separation of these samples. It was found that the 1,4- and 3,4-PI isomers elute at distinctly different elution times of 6.4 and 7.8 min, respectively. Moreover, it was found that the 1,4- and 1,2-PB isomers also showed distinct retention behaviours with elution times of 6.1 and 7.7 min, respectively. The ThFFF data also showed that the S_T values of the various microstructures are very similar, where the differences in the S_T values for the PI and PB samples were found to be 0.023 and 0.02, respectively.

To determine the influence of solvent viscosity on the separation of the PI and PB isomers, cyclohexane (CH) was used as mobile phase. CH is a high viscosity, thermodynamically good solvent for both PI and PB. It was found that the 1,4- and 3,4-PI isomers exhibited longer elution times of 10.9 and 15.0 min, respectively, while the 1,4- and 1,2-PB isomers also showed longer elution times of 9.4 and 16.0 min, respectively, than in THF. When using CH as the mobile phase the differences in S_T are more pronounced exhibiting values of 0.063 and 0.077 for the PI and PB isomers respectively. These increased differences in S_T suggest that microstructure-based separations can be improved when a higher viscosity solvent is used as the mobile phase.

During the study, the samples were also separated with a THF/CH mixture as mobile phase. It was found that the mixed solvent system exhibited an intermediate viscosity and that the 1,4- and 3,4-PI samples showed elution times of 10.3 and 13.1 min, respectively, while the 1,4- and 1,2-PB samples showed elution times of 10.1 and 14.3 min, respectively. Furthermore, the mixed solvent system yielded S_T values of 0.034 and 0.058 for the PI and PB isomers respectively. Thus, these S_T values show that the THF/CH mixed solvent system yields a better separation than pure THF.

To further confirm microstructure-based separations, each of the PI and PB samples was fractionated by ThFFF (with CH as mobile phase) and the collected fractions were analysed by ^{1}H NMR. The NMR data showed an enrichment of the PI isomers across the elution profile which correlated with their ThFFF retention behaviours. Similar correlations between the NMR and ThFFF data were found for the PB isomers. These results demonstrated that, in addition to size and chemical composition, ThFFF is capable of fractionating polymers according to microstructure.

Moreover, fractionating polymers based on microstructure highlights ThFFF's sensitivity towards subtle differences in molecular structure such as microstructure where the only differences between the samples are in the arrangement of the monomers in the backbone of the chain. This sensitivity towards subtle differences in molecular structure is not observed for column-based techniques such as SEC as SEC separates according to hydrodynamic size. The effect of different microstructures on size is rather small and, therefore, SEC is not suitable for the separation of polymers based on microstructure

Macromolecular
Rapid Communications

Macromolecular Journals

Communication

Multidetector Thermal Field-Flow Fractionation as a Novel Tool for the Microstructure Separation of Polyisoprene and Polybutadiene

Guilaume Greyling, Harald Pasch*

For the first time, it is demonstrated that thermal field-flow fractionation (ThFFF) is an efficient tool for the fractionation of polyisoprene (PI) and polybutadiene (PB) with regard to molecular microstructure. ThFFF analysis of 1,4- and 3,4-PI as well as 1,4- and 1,2-PB samples in tetrahydrofuran (THF), THF/cyclohexane, and cyclohexane reveals that isomers of the same polymer family having similar molar masses exhibit different Soret coefficients depending on microstructure for each solvent. The separation according to microstructure is found to be based on the cooperative influence of the normal and the thermal diffusion coefficient. Of the three solvents, cyclohexane has the greatest influence on the fractionation of the isomers. In order to determine the distribution of isomeric structures in the PI and PB samples, the samples are fractionated by ThFFF in cyclohexane and subsequently analyzed by ^{1}H NMR. The isomeric distributions determined from NMR data correlate well with ThFFF retention data of the samples and thus further highlight the unique fractionating capabilities of ThFFF. The interplay of the normal and thermal diffusion coefficients that are influenced by temperature and the mobile phase opens the way to highly selective fractionations without the drawbacks of column-based separation methods.

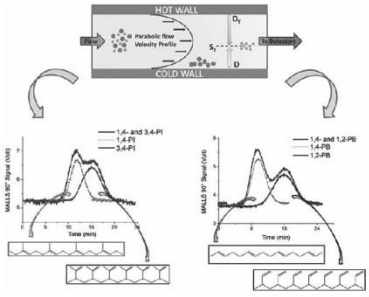

1. Introduction

Thermal field-flow fractionation (ThFFF) and, more recently, micro-thermal field-flow fractionation (micro-TFFF, pioneered by Janca) are subtechniques of field-flow fractionation (FFF) that apply a temperature gradient perpendicular to a carrier liquid flowing through an open, ribbon-like channel in order to fractionate a large variety of polymers.[1,2] Polymers subjected to such a thermal gradient migrate from the hot to the cold wall (accumulation wall) of the channel. This migration under a thermal gradient is termed thermal diffusion and is characterized by the thermal diffusion coefficient, D_T.[3] Thermal diffusion is counteracted by ordinary diffusion, D, which is the migration of molecules away from the accumulation wall toward the center of the channel due to increasing analyte concentration at the accumulation wall (Figure S1, Supporting Information).[4,5]

Laminar flow conditions within the channel result in a parabolic flow velocity profile across the channel with the fast flow streams toward the center of the channel

G. Greyling, Prof. H. Pasch
Department of Chemistry and Polymer Science,
University of Stellenbosch, Private Bag X1 7602, Matieland,
South Africa
E-mail: hpasch@sun.ac.za

DOI: 10.1002/marc.201400405

and the slower streams near the channel walls.[4,6] As with all FFF subtechniques, elution from the channel is determined by the analyte's average distance from the accumulation wall and thus their position in the velocity profile.[3] The analyte's distance from the accumulation wall is governed by its Soret coefficient, S_T, which is the ratio D_T/D (Figure S1, Supporting Information).[4] Therefore, polymers with similar S_T values will co-elute from the channel. Diffusion is dependent on the size of the polymer in solution, whereas thermal diffusion is dependent on the chemical nature of the polymer and solvent.[7] The influence of solvent composition on retention has been reported in numerous publications.[5,7,8] It was demonstrated that solvent composition can greatly influence retention of block terpolymers and that, although thermal diffusion is not viscosity dependent, viscosity is also an important parameter influencing retention.[7,9–11]

ThFFF can thus separate molecules not only according to size but also according to chemical composition. The retention mechanism in ThFFF has been described in detail in numerous publications.[6,12,13] Furthermore, ThFFF's sensitivity toward polymer composition and architecture was illustrated when it was used to determine the composition and number of arms of PS-PBA miktoarm star copolymers as well as the molecular heterogeneity of PB-*b*-PVP-*b*-P*t*BMA triblock copolymers.[14,15] To date, ThFFF's capability to fractionate polymers according to size and/or chemical composition in order to gain comprehensive information on molecular weight and copolymer structures has well been established and an excellent overview on ThFFF applications for polymers has been presented by Messaud et al.[16] The fractionation according to microstructure by ThFFF has not yet been addressed.

Fractionation of polyisoprene (PI) isomers regarding different molecular parameters has been accomplished by size-exclusion chromatography (SEC) and liquid chromatography at critical conditions (LCCC).[17–19] SEC separates according to hydrodynamic size in solution, which is mainly determined by the polymer chain length. The effect of different microstructures is rather low and, therefore, SEC is not suitable for the separation of PI or polybutadiene (PB) of similar molar masses based on microstructure. Furthermore, SEC has significant limitations in the analysis of very high-molecular-weight compounds.[16] For such samples, shear degradation might occur due to interactions with the stationary phase and the column frits. ThFFF is thus a powerful alternative to column-based chromatography as it can fractionate very high-molecular-weight compounds according to size and chemical composition without degradation taking place.

The question whether it is possible to fractionate PI and PB isomers by ThFFF according to microstructure has yet to be answered.[20] In the present study, we shall demonstrate that, in addition to fractionation according to size and chemical composition, ThFFF is capable of fractionating these polymers according to microstructure. This work, for the first time, describes the characterization and fractionation of PI and PB isomers according to microstructure by means of ThFFF coupled to multiangle laser light scattering (MALLS), differential refractive index (dRI), and dynamic light scattering (DLS) detection as well as by ^{1}H NMR. The multidetector approach enables the simultaneous online determination of the molecular weight distributions by MALLS as well as the diffusion and thermal diffusion coefficients of the eluting polymers by DLS. The dRI detector was required as universal concentration detector.

2. Experimental Section

2.1. Materials

The 1,4-PI (47.3 kDa) and 3,4-PI (53.3 kDa) as well as the 1,4-PB (87.5 kDa) and 1,2-PB (97.4 kDa) standards were purchased from PSS GmbH (Mainz, Germany) and prepared in 3 mg mL^{-1} concentrations using HPLC grade THF and cyclohexane purchased from Sigma–Aldrich (South Africa).

2.2. Thermal Field-Flow Fractionation

The thermal FFF system TF2000 (Postnova Analytics, Landsberg, Germany) was coupled online to UV (PN 3212 at 254 nm, Postnova Analytics), MALLS (PN 3070, Postnova Analytics), dRI (PN 3150, Postnova Analytics), and DLS detectors (Zen 1600, Malvern Instruments, Worcestershire, UK). The experimental details of ThFFF are summarized in the Supporting Information. Furthermore, dn/dc values for the samples in the various solvents were determined according to literature.[21, 22]

2.3. ^{1}H NMR

The NMR experiments were conducted on a 400 MHz Varian Unity Inova spectrometer (Agilent/Varian, Palo Alto, California, USA). The experimental details of ^{1}H NMR including the fractionation of the samples are summarized in the Supporting Information.

3. Results and Discussion

3.1. ThFFF Analysis of the PI and PB Isomers

The selection of the samples was such that their average molecular weights were as similar as possible to make sure that the differences in ThFFF behavior are not caused by differences in molecular weight. In a first step of the experiments, ThFFF fractionations of a number of PI and PB samples were conducted in THF as the mobile phase. These experiments indicated that samples with different microstructures elute at distinctively different elution times as

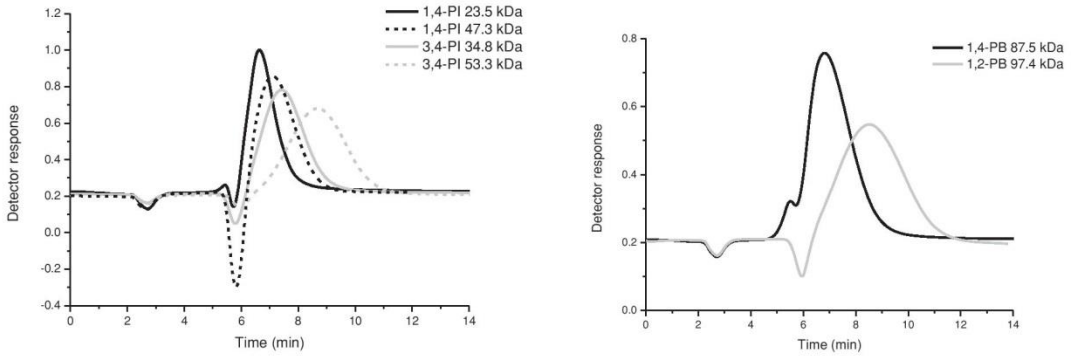

Figure 1. ThFFF fractograms of 1,4-PI and 3,4-PI (left) as well as 1,2-PB and 1,4-PB (right), mobile phase: THF, detector: dRI.

can be seen in Figure 1. In all cases, it was found that 1,4-PI eluted before 3,4-PI and 1,4-PB eluted before 1,2-PB.

To study this new phenomenon more in detail, samples were compared that had rather similar molar masses but different microstructures. As it has been pointed out in the introduction, solvent composition and viscosity are important parameters in ThFFF. With the aim of determining the influence of solvent composition and viscosity on the fractionation of two PI and PB isomers, the samples were consecutively analyzed in THF, in a THF/cyclohexane mixture (THF/CH), and in pure cyclohexane (CH). The solvent viscosities are 0.455, 0.640, and 0.90 cP for THF, THF/CH, and CH, respectively, and calculated according to the literature.[7] In order to evaluate the different elution behaviors quantitatively, the diffusion coefficients and the Soret coefficients for all samples were determined in THF, CH, and THF/CH. Values for D, D_T, and S_T for each of the four samples in each solvent and listed in Table 1.

The comparison of the diffusion coefficient data reveals some interesting correlations. In THF as the mobile phase, the differences in the diffusion coefficients for different microstructures are rather low. The consequence is that the Soret coefficients for the different microstructures are not very different; for PI, the difference is 0.023 while for PB the difference is 0.02. As compared with THF, in CH as the mobile phase the differences are more pronounced, being 0.063 for PI and 0.077 for PB. These increased differences in the Soret coefficients suggest that the microstructure fractionation can be improved when CH instead of THF is used as the mobile phase.

ThFFF analysis of a mixture of the 1,4- and 3,4-PI samples in THF showed the presence of a shoulder accompanying the primary peak in the fractogram of the MALLS 90° signal. The 1,4- and 3,4-PI samples were analyzed individually by ThFFF and an overlay of the MALLS 90° fractograms of each sample and the mixture reveals that the retention times, t_r, of the primary peak and the shoulder correspond to the 1,4- and 3,4-PI samples, respectively (Figure 2A). The 1,4-PI peak and 3,4-PI shoulder in the mixture elute at 6.1 and 7.9 min, respectively, while the individual 1,4- and 3,4-PI samples elute at 6.4 and 7.8 min, respectively. As has been pointed out before, in order to determine the factors governing the

Table 1. Soret (S_T), diffusion (D), and thermal diffusion (D_T) coefficients for the 1,4- and 3,4-polyisoprene samples as well as for 1,4- and 1,2-polybutadiene samples determined in THF, THF/cyclohexane, and cyclohexane (CH).

Sample[a]	D [10^{-7} cm^2 s^{-1}]			D_T [10^{-7} cm^2 s^{-1} K^{-1}]			S_T [K^{-1}]		
	THF	THF/CH	CH	THF	THF/CH	CH	THF	THF/CH	CH
1,4-PI	5.89 ± 1.19	5.77 ± 0.11	3.97 ± 0.15	0.821 ± 0.149	0.813 ± 0.110	0.565 ± 0.081	0.139 ± 0.001	0.141 ± 0.001	0.142 ± 0.001
3,4-PI	5.67 ± 0.44	5.37 ± 0.15	3.31 ± 0.18	0.838 ± 0.070	0.938 ± 0.065	0.678 ± 0.060	0.148 ± 0.002	0.175 ± 0.001	0.205 ± 0.001
1,4-PB	3.87 ± 0.13	3.17 ± 0.09	2.19 ± 0.11	0.492 ± 0.016	0.443 ± 0.019	0.281 ± 0.013	0.127 ± 0.001	0.140 ± 0.001	0.128 ± 0.001
1,2-PB	3.63 ± 0.22	2.36 ± 0.11	1.50 ± 0.19	0.532 ± 0.030	0.468 ± 0.021	0.307 ± 0.015	0.147 ± 0.001	0.198 ± 0.001	0.205 ± 0.001

[a]Molecular weights of the samples: 1,4-PI (47.3 kDa), 3,4-PI (53.3 kDa), 1,4-PB (87.5 kDa), 1,2-PB (97.4 kDa).

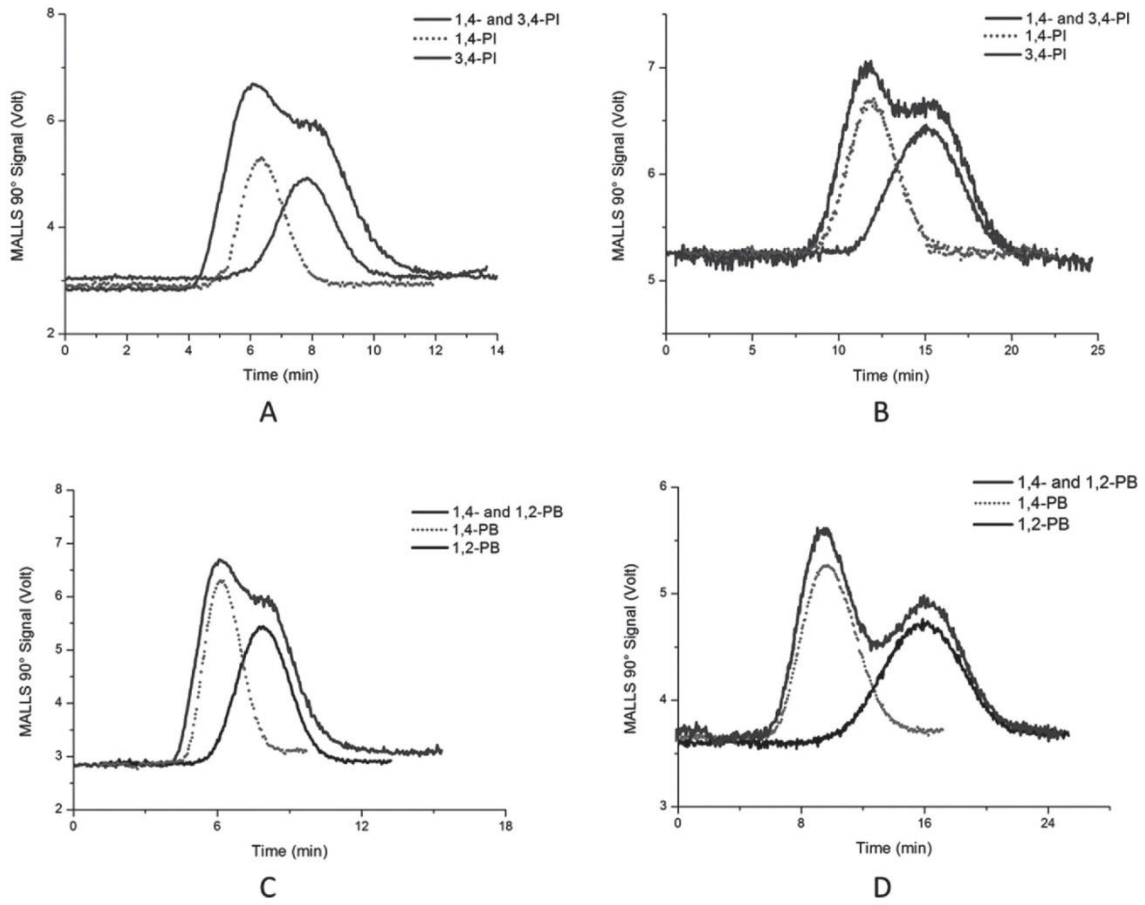

Figure 2. Overlays of fractograms of the MALLS 90° signal for the mixed and individual samples in THF and cyclohexane. A) 1,4- and 3,4-PI in THF, B) 1,4- and 3,4-PI in cyclohexane, C) 1,4- and 1,2-PB in THF, and D) 1,4- and 1,2-PB in cyclohexane.

fractionation in ThFFF, it is imperative to determine D and D_T of the respective samples. The former was determined by DLS measurements, whereas the latter was determined from diffusion and ThFFF retention data of the samples (Table 1). A difference in S_T is indicative of a separation.

In addition to the PI samples, two PB samples were analyzed by ThFFF in THF. A mixture of the 1,4- and 1,2-PB was injected and the fractogram of the MALLS 90° signal revealed a similar shoulder as seen in the corresponding PI fractogram (Figure 2C). The primary peak and shoulder elute at 5.9 and 7.8 min, respectively, while the individual 1,4- and 1,2-PB samples elute at 6.1 and 7.7 min, respectively. This confirms that the primary peak and shoulder correspond to the elution of the 1,4- and 1,2-PB samples, respectively. Values for D, D_T, and S_T were subsequently determined and, as seen with the PI samples, the PB samples have different S_T values which is indicative of fractionation.

S_T values for the PI and PB samples in THF/CH indicate that separations takes place between the isomers of the same polymer family (Table 1). The t_r of the 1,4- and 3,4-PI samples are 10.3 and 13.1 min, respectively, while the t_r of the 1,4- and 1,2-PB samples are 10.1 and 14.3 min, respectively. Not only has the solvent increased the t_r of the four samples but also it has slightly increased the resolution of the PI and PB samples by 0.9 and 2.6 min, respectively, when compared with THF. Therefore, increasing solvent viscosity appears to enhance the fractionation selectivity.

ThFFF analyses of the PI and PB samples in CH had a noticeable effect on the retention behavior of the samples. The fractogram of the MALLS 90° signal of a mixture of PI samples in CH revealed a similar 3,4-PI shoulder as seen

in THF. However, the fractogram in CH shows a noticeable increase in the peak resolution (Figure 2B). This influence of the solvent is also reflected in the increase in t_r of the peaks. The 1,4-PI peak and 3,4-PI shoulder of the mixture elute at 10.6 and 14.3 min, respectively, which corresponds to an increase in resolution of almost 2 min compared with that in THF. The t_r of the individual 1,4- and 3,4-PI samples were determined as 10.9 and 15.0 min, respectively. Moreover, values for D, D_T, and S_T confirm that fractionation is according to microstructure (Table 1). The fractogram of the MALLS 90° signal of a mixture of PB samples in CH shows a dramatic increase in resolution of the two peaks (Figure 2D). The t_r of the 1,4- and 1,2-PB samples in the mixture are 9.4 and 16.0 min, respectively. These values correspond to an increase in peak resolution by 4.6 min relative to that determined in THF. Therefore, increasing solvent viscosity greatly enhanced the selectivity.

3.2. ^{1}H NMR Analysis of the Fractionated PI and PB Isomers

The available samples of the PI and PB isomers contain small amounts of the other isomeric moieties. The 1,4-PI samples contain small amounts of the 3,4-PI isomer, whereas the 3,4-PI samples contains some 1,2- and 1,4-PI isomers. The 1,4- and 1,2-PB samples both contain a small amount of the other isomer. In the previous section, it was demonstrated that ThFFF can fractionate the PI and PB samples with respect to microstructure. Thus, to determine the isomeric content of the PI and PB samples, each of the four individual samples was fractionated by ThFFF into three fractions with CH as solvent (Figure S2 and Table S1, Supporting Information). Each of the three fractions was subsequently analyzed by ^{1}H NMR and the isomeric contents were calculated from the signal intensities (Figure 3).

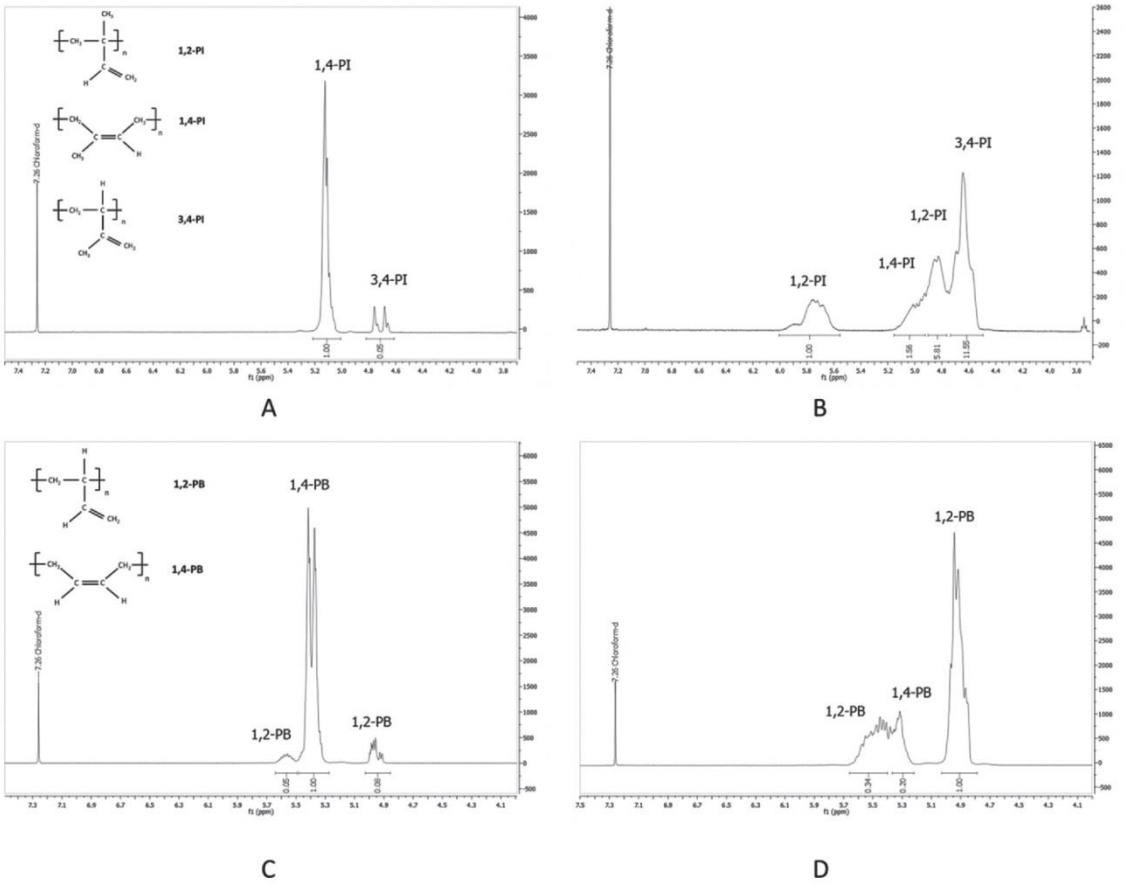

Figure 3. Expansions of the ^{1}H NMR spectra for fractions 1 of the PI and PB samples collected in cyclohexane. A) 1,4-PI, B) 3,4-PI, C) 1,4-PB, and D) 1,2-PB.

The NMR results confirm that the 1,4-PI sample is quite pure with some 3,4-PI isomer present (Table S2, Supporting Information). The 3,4-PI isomer content increases from 4.8% in fraction 1 to 7.2% in fraction 3, while the 1,4-PI isomer content decreases from 95.2% in fraction 1 to 92.8% in fraction 3.

Furthermore, the 3,4-PI sample contained predominantly 3,4-isomers with significant 1,2- and some 1,4-PI isomers present. The 3,4-PI isomer content shows an increase from 58.0% to 60.3% in fractions 1 and 3, respectively, while the 1,4-PI isomer content exhibits an decrease from 7.7% to 5.5% in fractions 1 and 3, respectively (Table S2, Supporting Information). This is in agreement with the NMR results of the 1,4-PI sample. The NMR data are in agreement with the results from the ThFFF analysis. NMR data show an enrichment of the 1,4-isomer content at the peak front (fraction 1) and an enrichment of the 3,4-PI isomer content at the peak tail (fraction 3). This observation is reflected in ThFFF by a shorter t_r for the 1,4-PI sample (10.9 min) compared with the 3,4-PI sample (15 min).

With regard to the 1,4-PB sample, the NMR data showed that the 1,2-PB isomer content increases from 3.8% to 5.7% in fractions 1 and 3, respectively, and the 1,4-PB content decreases from 96.2% to 94.3% in fractions 1 and 3, respectively (Table S3, Supporting Information). Moreover, NMR data for the 1,2-PB sample showed a similar trend with the 1,2-PB isomer content increasing from 82% to 84% in fractions 1 and 3, respectively, and the 1,4-PB isomer content decreasing from 18% to 16% in fractions 1 and 3, respectively. Thus, the NMR results of the PB samples indicate that the 1,4-PB and 1,2-PB samples both exhibit an enrichment of the 1,4-PB isomer content at the peak front (fraction 1) and an enrichment of the 1,2-PB isomer at the peak tail (fraction 3). This is in agreement with the shorter t_r for the 1,4-PB sample (9.4 min) compared with the 1,2-PB sample (16.0 min) observed in ThFFF.

4. Conclusions

For the first time, it has been demonstrated that ThFFF can fractionate 1,2-, 1,4-, and 3,4-polyisoprene isomers as well as the 1,4- and 1,2-polybutadiene isomers based on differences in microstructure. ^{1}H NMR data of fractions collected in cyclohexane showed an enrichment of specific isomers across the elution peak that correlates to the ThFFF retention data of the respective isomers. It was also demonstrated that solvent composition influenced the resolution of the peaks and dramatically enhanced the fractionation selectivity.

Supporting Information

Supporting Information is available from the Wiley Online Library or from the author.

Acknowledgements: The authors thank Dr. Magaretha Brand for the ThFFF training and Dr. Pritish Sinha for discussions on NMR of polyisoprene isomers.

Received: July 21, 2014; Revised: August 7, 2014; Published online: September 15, 2014; DOI: 10.1002/marc.201400405

Keywords: microstructure; polybutadiene; polyisoprene; thermal field-flow fractionation

[1] Y. S. Gao, K. D. Caldwell, M. N. Myers, J. C. Giddings, *Macromolecules* **1985**, *18*, 1272.
[2] J. Janca, *Microthermal Field-Flow Frationation*, HNB Publishing, New York **2008**.
[3] M. E. Schimpf, *J. Chromatogr. A* **1990**, *517*, 405.
[4] J. R. Runyon, S. K. R. Williams, *J. Chromatogr. A* **2011**, *1218*, 6774.
[5] C. A. Rue, M. E. Schimpf, *Anal. Chem.* **1994**, *66*, 4054.
[6] M. E. Schimpf, J. C. Giddings, K. Caldwell, *Field-Flow Fractionation Handbook*, Wiley-Interscience, New York **2000**.
[7] R. M. Sisson, J. C. Giddings, *Anal. Chem.* **1994**, *66*, 4043.
[8] A. C. Van Asten, W. T. Kok, R. Tjissen, H. Poppe, *J. Polym. Sci., Part B: Polym. Phys.* **1996**, *34*, 283.
[9] G. E. Kassalainen, S. K. R. Williams, *J. Chromatogr. A* **2003**, *988*, 285.
[10] C. A. Ponyik, D. T. Wu, S. K. R. Williams, *Anal. Bioanal. Chem.* **2013**, *405*, 9033.
[11] J. J. Kirkland, L. S. Boone, W. W. Yau, *J. Chromatogr. A* **1990**, *517*, 377.
[12] J. J. Gunderson, J. C. Giddings, *Macromolecules* **1986**, *19*, 2618.
[13] A. Van Asten, E. Venema, W. Kok, H. Poppe, *J. Chromatogr. A* **1993**, *644*, 83.
[14] J. Runyon, S. Williams, *Polym. Prepr.* **2011**, *52*, 230.
[15] W. van Aswegen, W. Hiller, M. Hehn, H. Pasch, *Macromol. Rapid Commun.* **2013**, *34*, 1098.
[16] F. A. Messaud, R. D. Sanderson, J. R. Runyon, T. Otte, H. Pasch, S. K. R. Williams, *Prog. Polym. Sci.* **2009**, *34*, 351.
[17] M. Hehn, W. Hiller, T. Wagner, J. Thiel, H. Pasch, *Macromol. Chem. Phys.* **2012**, *213*, 401.
[18] P. Sinha, W. Hiller, V. Bellas, H. Pasch, *J. Sep. Sci.* **2012**, *35*, 1731.
[19] H. Pasch, B. Trathnigg, *Multidimensional HPLC of Polymers*, Springer-Verlag, Berlin-Heidelberg-New York **2013**.
[20] W. Hiller, P. Sinha, M. Hehn, H. Pasch, T. Hofe, *Macromolecules* **2011**, *44*, 1311.
[21] J. E. Mark, *Polymer Data Handbook*, Oxford University Press, New York **1999**.
[22] W. Machtle, H. Fisher, *Angew. Makromol. Chem.* **1969**, *7*, 147.

4.1.2 Isotactic and Syndiotactic Poly(methyl methacrylate)

G. Greyling, H. Pasch, *Anal. Chem.* ***2015***, *87*, 3011–3018.

The investigation into microstructure-based separations was subsequently extended to PMMA samples exhibiting different tacticities. By using THF as mobile phase, it was shown that isotactic and syndiotactic PMMA exhibit different retention behaviours with elution times of 19.4 and 15.7 min, respectively. Since solvent viscosity could improve microstructure-based separations, a more viscous solvent such as dioxane (DOX) was subsequently used as mobile phase. As expected, it was found that viscosity improved the separation. To further explore the influence of solvent composition, acetonitrile (ACN) (which is a theta solvent for PMMA) was used as mobile phase. It was found that, although DOX yielded the longest elution times, ACN yielded the best resolution of isotactic and syndiotactic PMMA. It was determined that this interesting phenomenon was due to differences in polymer chain stiffness between isotactic and syndiotactic PMMA.

Chain stiffness played a larger role in fractionating PMMA with the theta solvent as mobile phase because PMMA could adopt different size conformations in ACN depending on polymer chain stiffness. This was reflected in both D and D_T values for the samples of different tacticities. The DLS data showed that the D values are larger for syndiotactic PMMA than for isotactic PMMA in ACN. Therefore, syndiotactic PMMA adopts a smaller conformation in ACN than isotactic PMMA. With regards to D_T, isotactic PMMA exhibits larger D_T values than syndiotactic PMMA which indicates differences in chain stiffness.[51,55] These experimental results were also confirmed by molecular dynamic calculations and reported Kuhn lengths of 0.47 and 0.41 nm for isotactic and syndiotactic PMMA, respectively.[69–71] In addition, an atactic PMMA sample was also characterised and showed similar retention

behaviours to syndiotactic PMMA. From ^{1}H NMR it was determined to mostly consist of syndiotactic segments, thus explaining the similar retention behaviours.

To confirm a microstructure-based separation, an atactic PMMA sample was fractionated by ThFFF (with ACN as mobile phase) and the collected fractions were analysed by ^{1}H NMR. The NMR results showed an enrichment of isotactic and syndiotactic PMMA across the elution profile which corresponds to their ThFFF retention behaviours. These results showed that ThFFF can be applied to probe polymer chain stiffness and that microstructure-based fractionations can be extended to include tacticity.

Moreover, these results further demonstrate ThFFF's sensitivity towards subtle differences in molecular structure where the only differences between the samples are in the relative arrangements of pendent groups along the polymer backbone. Traditional column-based techniques (such as SEC) do not exhibit this kind of sensitivity to microstructure as it only has a small influence on hydrodynamic size.

analytical chemistry

Article

pubs.acs.org/ac

Tacticity Separation of Poly(methyl methacrylate) by Multidetector Thermal Field-Flow Fractionation

Guilaume Greyling and Harald Pasch*

Department of Chemistry and Polymer Science, University of Stellenbosch, Private Bag X1, 7602 Matieland, South Africa

ABSTRACT: For the first time, thermal field-flow fractionation (ThFFF) has been used for the separation of poly(methyl methacrylate) (PMMA) with regard to molecular microstructure. PMMA exists in three different isomeric forms, namely, isotactic, syndiotactic, and atactic. ThFFF analysis of the different PMMA isomers in tetrahydrofuran, acetonitrile (ACN), and dioxane reveals that isomers with similar molecular weights exhibit different Soret coefficients, and thus different retention times, under identical experimental conditions. Of the three solvents, ACN shows the greatest influence on fractionation of the isomers. The separation according to molecular microstructure is found to be based on the cooperative effects of the normal and thermal diffusion coefficients. Furthermore, it is found that blends of different PMMA isomers with similar molecular weights can be fractionated into their respective isomeric components. The distribution of the isomeric content in an atactic PMMA sample is determined quantitatively by fractionating the sample with ThFFF and subsequently analyzing the fractions by ^{1}H NMR. The isomeric distributions determined from NMR data correlate well with ThFFF retention data of the samples and thus further highlight the unique fractionating capabilities of ThFFF.

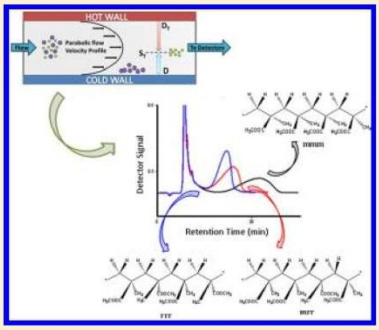

Thermal field-flow fractionation (ThFFF) is a channel-based fractionation technique that applies a temperature gradient perpendicular to a carrier liquid flowing through an open, ribbonlike channel in order to fractionate polymers according to size or chemical composition.[1,2] Polymers subjected to such a thermal gradient migrate from the hot to the cold wall (accumulation wall) of the channel. This migration under a thermal gradient is termed thermal diffusion and is characterized by the thermal diffusion coefficient, D_T.[3] Thermal diffusion is counteracted by ordinary diffusion, which is the migration of molecules away from the accumulation wall toward the center of the channel due to increasing analyte concentration at the accumulation wall.[4,5] The parameter that describes normal diffusion is the normal diffusion coefficient, D.

In the separation channel, a parabolic flow velocity profile forms, which results in faster flow streams toward the center of the channel and slower streams toward the accumulation wall.[4,6] Elution from the channel is determined by the analytes' average distance from the accumulation wall and thus their position in the flow velocity profile.[3] The analytes' average distance from the accumulation wall is determined by the Soret coefficient, S_T, which is the ratio of D_T/D and describes the interaction between the two forces.[4] Diffusion is dependent on the size of the polymer in solution, whereas thermal diffusion is dependent on the chemical nature of the polymer as well as on the solvent type and composition.[7] The influence of solvent composition on retention has been reported previously, and it was demonstrated that solvent composition can greatly influence the retention of block copolymers.[5,7,8] It has been shown that solvent viscosity is also an important parameter influencing retention.[7,9−12]

In numerous publications, it has been shown that ThFFF can separate macromolecules according to not only size but also chemical composition.[6,13−16] To date, the capability of ThFFF to fractionate polymers according to size and/or chemical composition to gain comprehensive information on molecular weight and chemical composition distributions has well been established, and an excellent overview on ThFFF applications for polymers has been presented by Messaud et al.[17]

The fractionation of polymers regarding different molecular parameters can be accomplished by more traditional methods, such as size exclusion chromatography (SEC) and various other types of liquid interaction chromatography.[18] SEC separates according to hydrodynamic size in solution, which is mainly determined by the polymer chain length. The effect of different microstructures is rather small and, therefore, SEC is not suitable for the separation of polymers according to microstructure. Furthermore, SEC has significant limitations in the analysis of very high molecular weight compounds. For such samples, shear degradation might occur due to interactions with the stationary phase and the column frits. ThFFF is thus a powerful alternative to column-based chromatography as it can fractionate very high molecular weight compounds without the occurance of degradation.[19]

The question of whether it is possible to fractionate polymeric isomers by ThFFF according to microstructure is still an unexplored area. An interesting preliminary result was obtained recently showing that polyisoprene and polybutadiene isomers can be fractionated according to microstructure.[12] Using a ThFFF setup coupled to multiangle laser light scattering (MALLS), differential refractive index (dRI), and dynamic light

Received: December 15, 2014
Accepted: February 5, 2015
Published: February 5, 2015

DOI: 10.1021/ac504651p
Anal. Chem. 2015, 87, 3011−3018

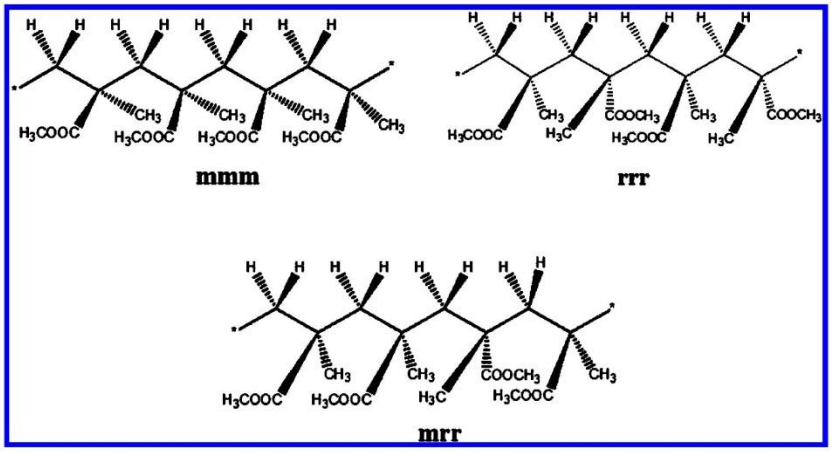

Figure 1. Structure of isotactic (mmm), syndiotactic (rrr), and atactic (mrr) PMMA.

scattering (DLS) detectors, it was proven that the fractionation was based on differences solely in the polymer microstructure. Polyisoprene was fractionated into the 1,4-, 1,2- and 3,4-isomers, and polybutadiene was fractionated into the 1,4- and 1,2-isomers.

The present investigation is aimed at testing the capabilities of ThFFF to fractionate the various poly(methyl methacrylate) (PMMA) isomers according to microstructure. PMMA exists in three different isomeric forms, namely, isotactic, syndiotactic, and atactic (Figure 1). PMMA is widely used in optical applications, such as fiber optics, and properties like glass transition temperature greatly depend on the microstructure content of the polymer.[20−22] Thus, determining the microstructure content is of great importance to determining a polymer's suitability for its intended application. In this study, samples with similar molecular weights are analyzed to demonstrate the selectivity of ThFFF based on molecular microstructure.

■ EXPERIMENTAL SECTION

Materials. The isotactic (135 kDa), syndiotactic (131 kDa), and atactic (139 kDa) PMMA standards were purchased from Polymer Source Inc. (Montreal, Canada). The samples were prepared in 3 mg mL^{-1} concentrations using HPLC grade tetrahydrofuran (THF), acetonitrile (ACN), and dioxane (DOX) purchased from Sigma-Aldrich (South Africa). The viscosities of THF, ACN, and DOX are 0.55 cP, 0.33 cP, and 1.2 cP, respectively.

Thermal Field Flow Fractionation. The thermal FFF system TF2000 (Postnova Analytics, Landsberg, Germany) was coupled online to MALLS (PN 3070, Postnova Analytics), dRI (PN 3150, Postnova Analytics), and DLS detectors (Zen 1600, Malvern Instruments, Worcestershire, UK). The dn/dc values for the samples in the various solvents were determined according to the literature.[23,24] The TF2000 channel had a tip-to-tip length of 45.6 cm, breadth of 2 cm, thickness of 127 μm, and void volume of 1.14 mL. The temperature of the cold wall was 24 °C, and a constant ΔT of 60 °C was used to achieve fractionation. THF, ACN, and DOX were used as carrier liquids with corresponding flow rates of 0.3 mL min^{-1}, 0.3 mL min^{-1}, and 0.2 mL min^{-1}, respectively. Diffusion data were gathered online via a quartz flow cell with THF and ACN as solvents but gathered off-line with a glass cuvette with DOX as solvent. Off-line diffusion data were collected at concentrations of 3 mg mL^{-1}, 1.5 mg mL^{-1}, 0.75 mg mL^{-1}, and 0.375 mg mL^{-1} and plotted by OriginPro 8 software. The slope and intercept determined from linear regression, in combination with the elution concentration determined from dRI, were used to graphically determine D values. Values for D_T were calculated according to eq 1.

$$D_T = \frac{6Dt_r}{\Delta T t^0} \quad (1)$$

where t^0 is the void time, t_r is the retention time of the sample, and ΔT is the temperature difference between the hot and cold wall. Samples were injected through a 100 μL capillary sample loop, and triplicate analysis of each sample was performed under nonoverloading sample concentrations.

^{1}H NMR Spectroscopy. The NMR experiments were conducted on a 400 MHz Varian Unity Inova spectrometer (Agilent/Varian, Palo Alto, California, USA). The measurements were performed with a 5 mm dual broadband pulsed field gradient probe. Two-hundred and fifty-six scans using 45° pulses were acquired with an acquisition time of 2.0 s and a relaxation delay of 1 s. The polymer samples were fractionated by ThFFF, collected in 25 runs, and evaporated at room temperature. The collected fractions were dissolved in 0.7 mL $CDCl_3$ and subsequently analyzed. Data were processed by use of MestReNova software version 7.1.1. Quantitative information obtained from the spectra is accurate within 5%.

■ RESULTS AND DISCUSSION

PMMA samples with different tacticities and similar molecular weights were selected for the experiments. The tacticity content of each of the samples was determined by ^{1}H NMR and is reported in Table 1.

Table 1. Isotactic, Syndiotactic, and Atactic Content Found in the PMMA Samples As Calculated from ^{1}H-NMR

PMMA	nominal molecular weight [kDa]	isotactic content [mol %]	atactic content [mol %]	syndiotactic content [mol %]
isotactic	135	92.6	1.9	5.5
syndiotactic	131	0.8	18.5	80.7
atactic	139	4.5	39	56.5

DOI: 10.1021/ac504651p
Anal. Chem. 2015, 87, 3011−3018

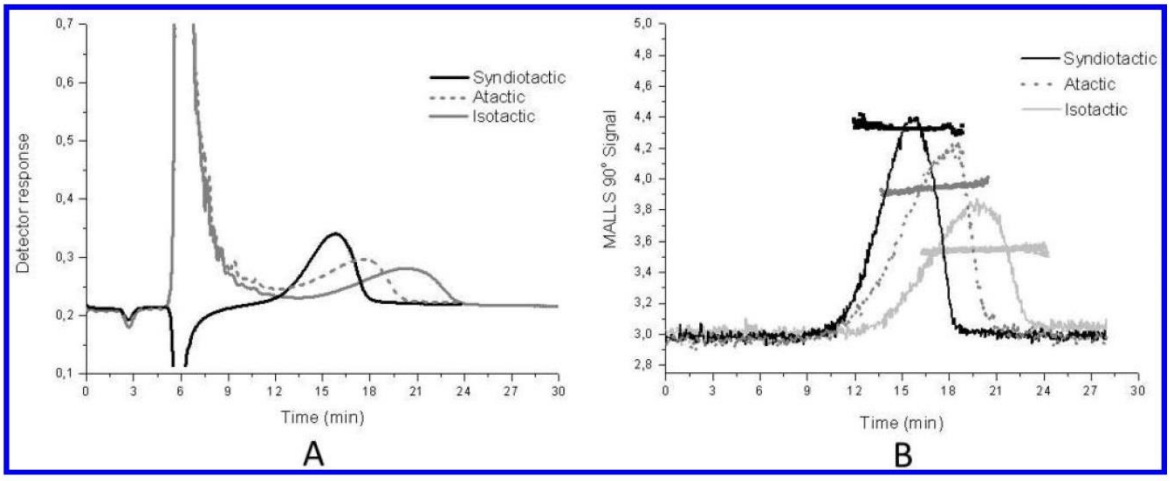

Figure 2. Fractogram overlays and the respective molecular weight distribution of the samples across the elution peak for the syndiotactic (black solid line), atactic (gray broken line), and isotactic (gray solid line) PMMA samples. Molecular weight distributions are shown on relative scales for clarity. Mobile phase: THF. Detectors: dRI (A) and MALLS 90° (B).

Because the solvent (mobile phase) is assumed to have a significant influence on the separation, solvents of different thermodynamic qualities and viscosities were investigated. The solvents to be tested were THF (a thermodynamically good solvent for PMMA with a low viscosity), ACN (a theta solvent for PMMA with a low viscosity), and DOX (a thermodynamically good solvent for PMMA with a high viscosity). In the first set of experiments, isotactic, syndiotactic, and atactic PMMA samples of similar molecular weights were analyzed by ThFFF in THF.

ThFFF Analysis in Tetrahydrofuran. The ThFFF fractograms of the samples recorded with dRI and MALLS detection are presented in Figure 2. From Figure 2B, it can be seen that the molecular weight distributions of the sample remain constant across the elution profile as expected for narrowly dispersed standards. Furthermore, the molecular weights determined from MALLS correlate well with the nominal molecular weights reported by the manufacturer (see Tables 1 and 2).

The retention times for the different samples in the various solvents are reported in Table 2. THF is a thermodynamically good solvent for PMMA with a low viscosity. It is therefore expected that the PMMA samples would exhibit relatively large diffusion coefficients (D) and thus shorter retention times compared to other more viscous solvents. This low viscosity, thermodynamically good solvent thus serves as a good starting point for the present study. The difference in retention times between the isotactic and syndiotactic samples is 3.7 min, indicating that for isomers of similar molecular weights ThFFF fractionation is driven by the polymer microstructure. The atactic PMMA sample elutes between the isotactic and syndiotactic samples, as expected. It should be noted that the retention time difference between the atactic and isotactic samples as well as between the atactic and syndiotactic samples is roughly 2 min in each case, which is as expected considering that the atactic sample is comprised of 56.5 mol % syndiotactic triads.

The diffusion, thermal diffusion, and Soret coefficients of the samples in THF are presented in Table 2. From Table 2, it can be seen that the S_T values for each of the samples are different. A difference in S_T is indicative of a separation, as illustrated in Figure 2.

In agreement with the retention behavior of the samples, the highest diffusion coefficient is obtained for syndiotactic PMMA followed by atactic and isotactic PMMA. At the same time, the thermal diffusion coefficients decrease in the order isotactic-atactic-syndiotactic. This indicates that the molecular structure of the samples influences the normal and thermal diffusion coefficients in different ways. As net retention is determined by the Soret coefficient, the lowest S_T is obtained for syndiotactic PMMA followed by atactic and isotactic PMMA. Furthermore, the difference between the S_T values of the isotactic and syndiotactic samples increase from 0.066 in THF to 0.086 in dioxane, which clearly illustrates that the separation improves with the change of solvent. Acetonitrile, however, shows an unexpectedly large difference of 0.139. This observation is addressed in the following section.

ThFFF Analysis in Acetonitrile. Following the analysis in THF, the samples were analyzed in ACN, which is a low viscosity theta solvent for PMMA. It was expected that the theta solvent would lead to a decreased coil size of the macromolecules in solution, resulting in a higher diffusion coefficient. This in turn would be observed as a decrease in ThFFF retention time compared to THF. The ThFFF fractograms of the samples recorded with dRI and MALLS detection in ACN are presented in Figure 3.

As can be seen in Figure 3 and Table 2, the retention times for the syndiotactic and atactic samples in ACN are observed to be decreased relative to those in THF, whereas for isotactic PMMA an increase in retention time is observed. Comparison of D, D_T and S_T values for the isotactic, syndiotactic, and atactic samples in THF and ACN give some interesting results. For the isotactic sample, both D and D_T increase with the solvent change from THF to ACN. This results in an increase in the Soret coefficient and a corresponding increase in the retention time. The syndiotactic sample, on the other hand, also shows an increase in both D and D_T but shows a decrease in S_T. Furthermore, the atactic sample shows little change in D but a decrease in both D_T and S_T. These results indicate that the interplay between D and D_T influence the retention behavior of the samples.

On the basis of the lower viscosity of ACN compared to THF, an increase in D is expected for the samples assuming

DOI: 10.1021/ac504651p
Anal. Chem. 2015, 87, 3011−3018

Table 2. Retention Times (t_r), Diffusion (D), Thermal Diffusion (D_T), and Soret (S_T) Coefficients for the Isotactic, Syndiotactic, and Atactic PMMA Samples Determined in THF, Acetonitrile (ACN), and Dioxane (DOX)

PMMA	molecular weights[a] [kDa]		t_r [min]			D [10^{-7} cm^2 s^{-1}]			D_T [10^{-7} cm^2 s^{-1} K^{-1}]			S_T [K^{-1}]		
	THF		THF	ACN	DOX	THF	ACN	DOX	THF	ACN	DOX	THF	ACN	DOX
isotactic	145.7		19.4	21.0	31.0	3.95 ± 0.556	4.85 ± 0.198	1.51 ± 0.218	1.47 ± 0.197	1.99 ± 0.097	0.65 ± 0.104	0.372 ± 0.003	0.41 ± 0.004	0.431 ± 0.006
syndiotactic	145.6		15.7	13.6	24.8	4.53 ± 0.222	5.54 ± 0.227	1.84 ± 0.140	1.39 ± 0.083	1.50 ± 0.082	0.635 ± 0.495	0.306 ± 0.003	0.271 ± 0.006	0.345 ± 0.007
atactic	153.1		17.6	15.3	27.0	4.25 ± 0.035	4.37 ± 0.180	1.79 ± 0.348	1.44 ± 0.019	1.31 ± 0.051	0.671 ± 0.133	0.339 ± 0.004	0.299 ± 0.002	0.375 ± 0.001

[a]Molecular weights determined by MALLS in THF.

that their hydrodynamic sizes are similar in both solvents. However, this is not the case as ACN is a theta solvent for PMMA, and changing solvents from THF to ACN leads to a decrease in the hydrodynamic diameter, D_h. A decrease in D_h should increase D even further, which is evidently not the case for all samples. To determine the cause of the observed retention behavior of the PMMA samples in ACN, the samples were analyzed by off-line DLS at various temperature intervals. The temperature range was chosen to mimic the conditions in the ThFFF channel: an initial temperature of 25 °C (accumulation wall temperature), which was increased by 5 °C increments to 80 °C. The effect of temperature on D_h and D for the isotactic, atactic, and syndiotactic samples are shown in Figure 4.

From Figure 4A, it can be seen that the syndiotactic and atactic samples undergo a change in D_h as a function of temperature that is greater than for the isotactic sample. Furthermore, it can also be seen that the syndiotactic sample undergoes a change in D as a function of temperature that is greater than both the isotactic and atactic samples (Figure 4B). The isotactic and atactic samples appear to undergo similar changes in D as a function of temperature.

Isotactic PMMA has a hydrodynamic diameter that is larger than that of syndiotactic PMMA at the same molecular weight (same number of repeating units) and is thus more rigid than syndiotactic PMMA, which is confirmed by Kuhn lengths of 0.47 and 0.41 nm that have been reported for isotactic and syndiotactic PMMA, respectively.[25] It was also reported that the unperturbed dimensions of PMMA increase with increasing isotactic content.[26] Therefore, it is expected that the isotactic sample undergoes a smaller change in D_h as a function of temperature as at the initial temperature it is in a more extended conformation than the syndiotactic and atactic samples. This has been confirmed by molecular dynamics simulations, which demonstrated that syndiotactic PMMA is coiled more strongly than the extended isotactic PMMA.[27] Therefore, the syndiotactic and atactic samples, which contain less isotactic segments, form more compact conformations at the initial temperature and thus undergo larger changes in D_h as a function of temperature.

The observations mentioned above can be used to explain the retention behavior of PMMA in ACN. Because the syndiotactic and atactic samples undergo a change in D_h and D across the temperature gradient that is greater than in the isotactic sample, they are expected to elute earlier than the isotactic sample as D becomes more dominant in the D_T/D ratio as a function of temperature. Additionally, the S_T values, which are calculated directly from ThFFF retention data, for the isotactic, syndiotactic, and atactic samples are 0.41, 0.271, and 0.299 K^{-1}, respectively (Table 2). The S_T values for the syndiotactic and atactic samples being smaller than that of the isotactic sample clearly demonstrate that D is dominating the D_T/D ratio. This is in agreement with the data obtained from DLS measurements. Therefore, the dominating influence of D on S_T accounts for the decrease in retention times for the syndiotactic and atactic samples in ACN compared to THF.

In the case of the isotactic sample, the relatively large S_T value of 0.41 K^{-1} indicates that D_T is dominating the D_T/D ratio. The dominating influence of D_T on S_T is due to the relative rigidity of the isotactic sample as it has been reported that rigidity increases the D_T of a polymer.[28] This is seen by the D_T value of 1.99×10^{-7} cm^2 s^{-1} K^{-1} for the isotactic sample that is larger than the values of 1.50×10^{-7} and 1.31×10^{-7} cm^2 s^{-1} K^{-1} of the syndiotactic and atactic samples,

DOI: 10.1021/ac504651p
Anal. Chem. 2015, 87, 3011−3018

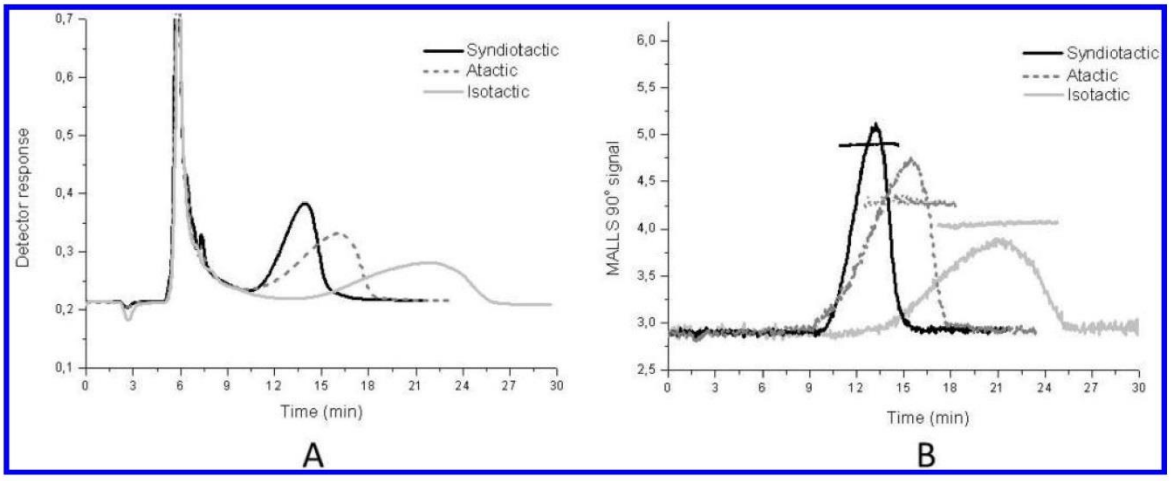

Figure 3. Fractogram overlays and the respective molecular weight distributions of the samples across the elution peak for the syndiotactic (black solid line), atactic (gray broken line), and isotactic (gray solid line) PMMA samples. Molecular weight distributions are shown on relative scales for clarity. Mobile phase: Acetonitrile. Detectors: dRI (A) and MALLS 90° (B).

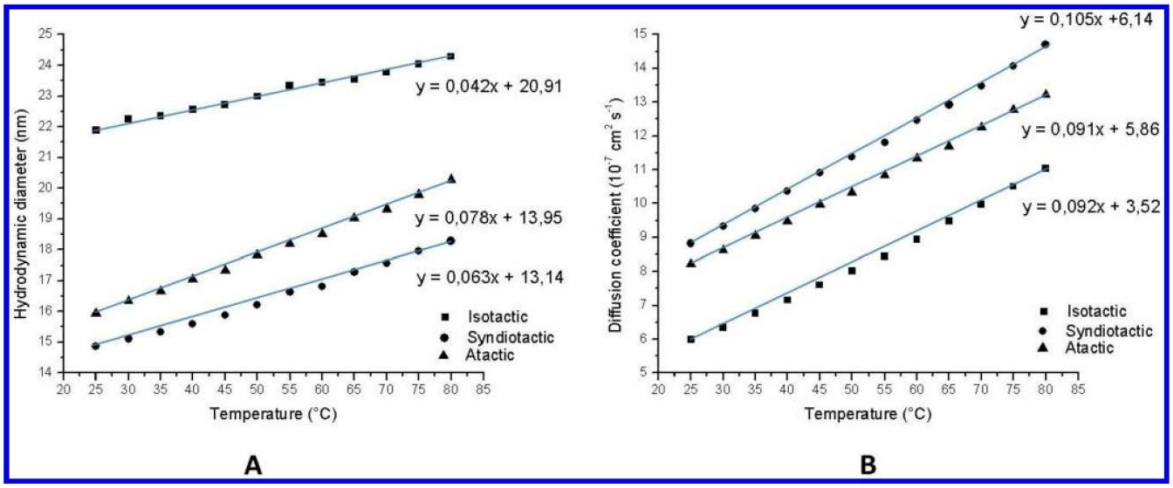

Figure 4. Plots of hydrodynamic diameter (A) and diffusion coefficient (B) versus temperature for the isotactic (squares), syndiotactic (circles), and atactic (triangles) PMMA samples in acetonitrile. Linear regression lines are drawn to aid interpretation of the data and illustrate general trends as a function of temperature.

respectively (Table 2). The stronger influence of D_T on S_T results in the retention time of the isotactic sample in ACN being increased relative to THF. Therefore, the respective influences of D and D_T on S_T account for the contrasting retention behaviors observed for the various PMMA samples in ACN.

ThFFF Analysis in Dioxane. Dioxane is a high viscosity thermodynamically good solvent for PMMA, and as expected, the retention times of the samples increased greatly compared to THF (Figure 5).

The increase in viscosity decreased D and D_T for the samples whereas S_T increased with regard to THF. Furthermore, the increase in viscosity increased the retention time difference between the isotactic and syndiotactic samples from 3.7 min in THF to 6.2 min in dioxane (Figures 2 and 5). Thus, the more viscous solvent retains the polymer longer in the thermal gradient and in doing so exploits the differences in D_T between the samples. The analysis of a 1:1 mixture of the isotactic and syndiotactic samples in dioxane shows a bimodal distribution with the first peak eluting at 22.5 min and the second peak at 30.2 min (Figure 6). The individual syndiotactic and isotactic samples elute at 24.8 and 30.1 min, respectively (Table 2).

The 1:1 ratio of isotactic/syndiotactic PMMAs was chosen to avoid potential stereocomplexes, which are reported to form when a 2:1 ratio of isotactic/syndiotactic PMMA is used in solvents with strong complexing power.[29] Thus, even though ACN yields better resolution than dioxane, dioxane and ACN are known to be weakly and strongly complexing solvents, respectively. To further avoid potential stereocomplexes (and self-aggregation), low concentrations of the samples were prepared, resulting in the noisy MALLS 90° fractogram.

DOI: 10.1021/ac504651p
Anal. Chem. 2015, 87, 3011−3018

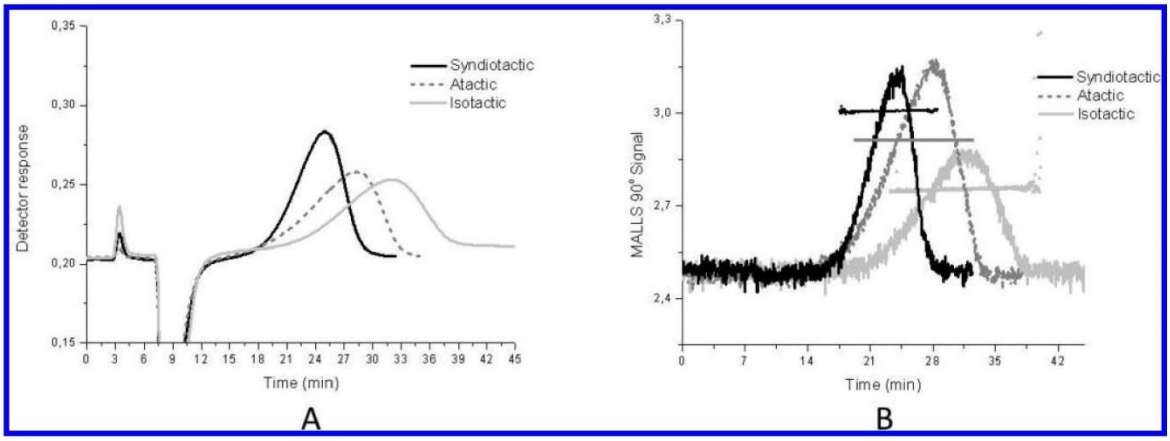

Figure 5. Fractogram overlays and the respective molecular weight distributions of the samples across the elution peak for the syndiotactic (black solid line), atactic (gray broken line), and isotactic (gray solid line) PMMA samples. Molecular weight distributions are shown on relative scales for clarity. Mobile phase: Dioxane. Detectors: dRI (A) and MALLS 90° (B).

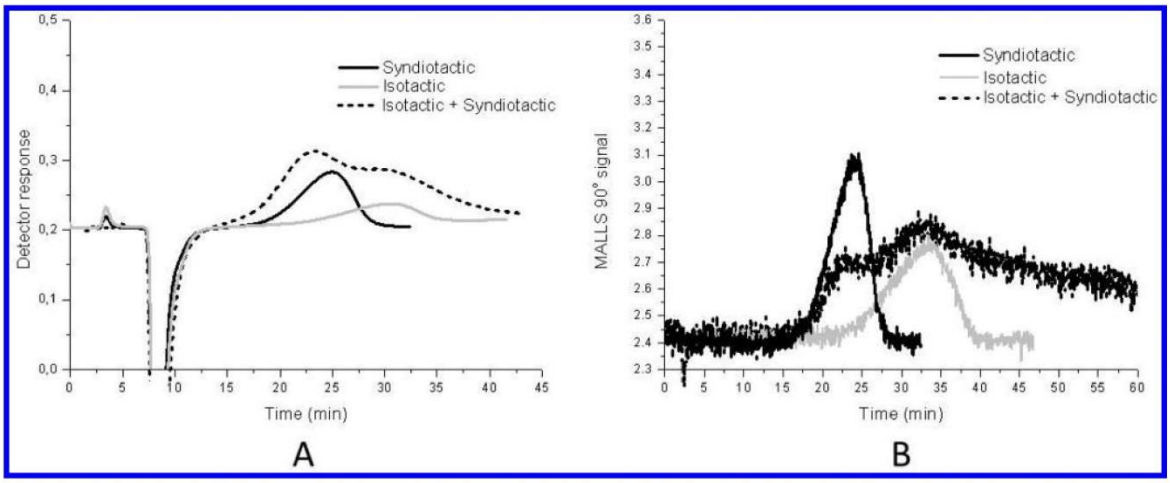

Figure 6. Fractogram overlays of the syndiotactic (black solid line) and isotactic (gray solid line) PMMA samples as well as a 1:1 mixture of the isomers (black broken line). Mobile phase: Dioxane. Detectors: dRI (A) and MALLS 90° (B).

In light of the obtained separations with respect to microstructure, a 139 kDa atactic PMMA sample was fractionated into four fractions by ThFFF with ACN as solvent. ACN was selected as solvent because it gave the best resolution between the isotactic and syndiotactic PMMA standards. The four collected fractions were subsequently sent for ^{1}H NMR analysis to determine the respective isotactic, atactic, and syndiotactic contents. The calculated isotactic, atactic and syndiotactic contents for each fraction are reported in Table 3, and the NMR spectra are shown in Figure 7.

From Table 3, it can be seen that the isotactic content increases by 2.3% from fraction 1 to fraction 4, whereas the atactic and syndiotactic contents decrease from fraction 1 to fraction 4 by 0.9 and 1.4%, respectively. Thus, the NMR data show an enrichment of the syndiotactic isomer content at the peak front (fraction 1) and an enrichment of the isotactic isomer content at the peak tail (fraction 4). The NMR data are in agreement with the results obtained from the ThFFF analysis in which the retention data show a retention time for the isotactic sample (21 min) that is longer than that of the syndiotactic sample (13.6 min) in ACN. Figure 8 illustrates the elution times of the four collected fractions as well as an overlay of the general elution trend of the different tacticities. The elution times for each of the collected fractions are as follows: fraction 1, 9.0−12.5 min; fraction 2, 12.5−15.0 min; fraction 3, 15.0−17.3 min; and fraction 4, 17.3−20.0 min.

Table 3. Isotactic, Atactic, and Syndiotactic Contents Determined from ^{1}H NMR Spectra for Fractions Collected from ThFFF in Acetonitrile[a]

fraction	isotactic content [mol %]	atactic content [mol %]	syndiotactic content [mol %]
1	3.5	38.7	57.8
2	4.6	38.2	57.2
3	5.1	38.4	56.5
4	5.8	37.8	56.4

[a]Tacticity content was calculated by integrating the mm, mr, and rr triad sequences.

DOI: 10.1021/ac504651p
Anal. Chem. 2015, 87, 3011−3018

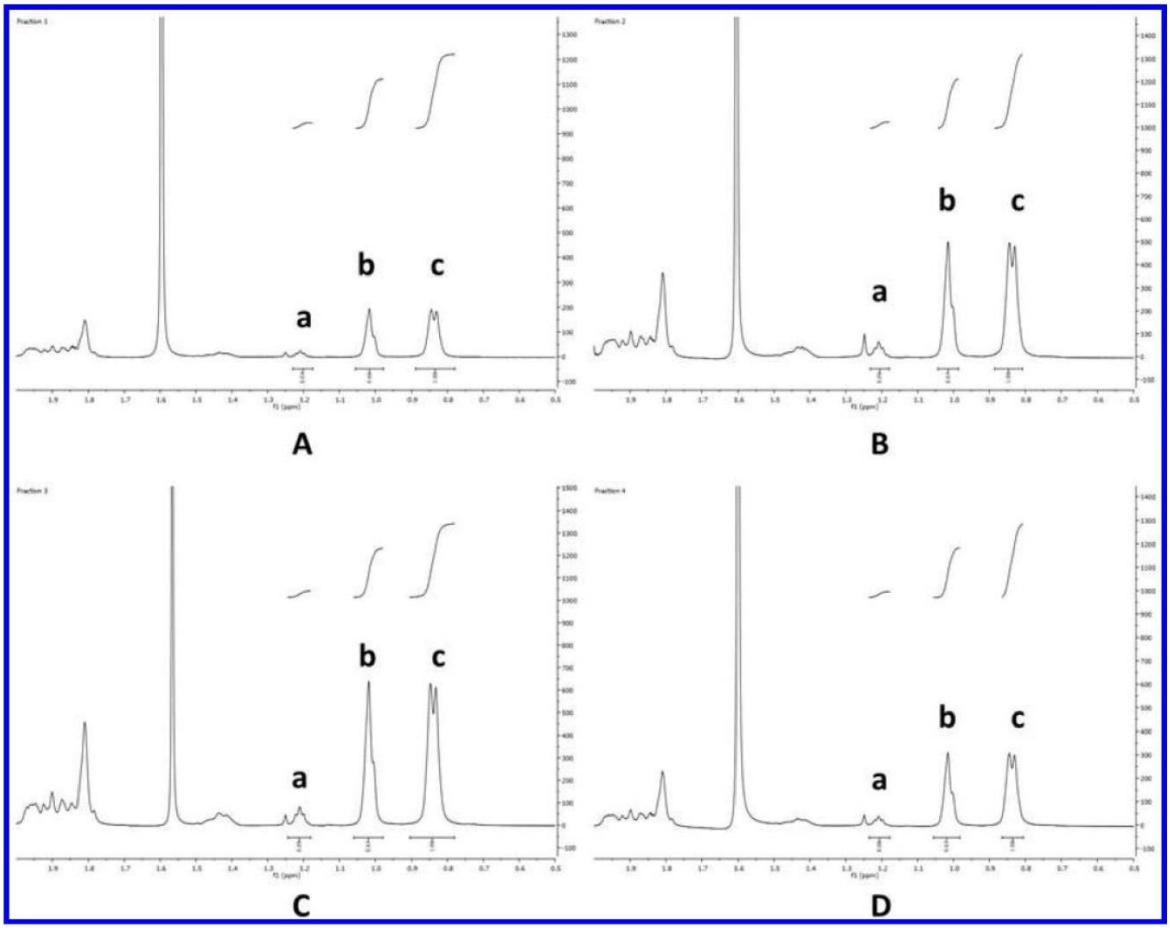

Figure 7. ^{1}H NMR spectra of the fractions collected by ThFFF in acetonitrile. (A) Fraction 1, (B) fraction 2, (C) fraction 3, and (D) fraction 4. Labels a, b, and c designate the chemical shifts corresponding to the mm (isotactic), mr (atactic), and rr (syndiotactic) triad sequences at 1.2, 1.0, and 0.9 ppm, respectively.

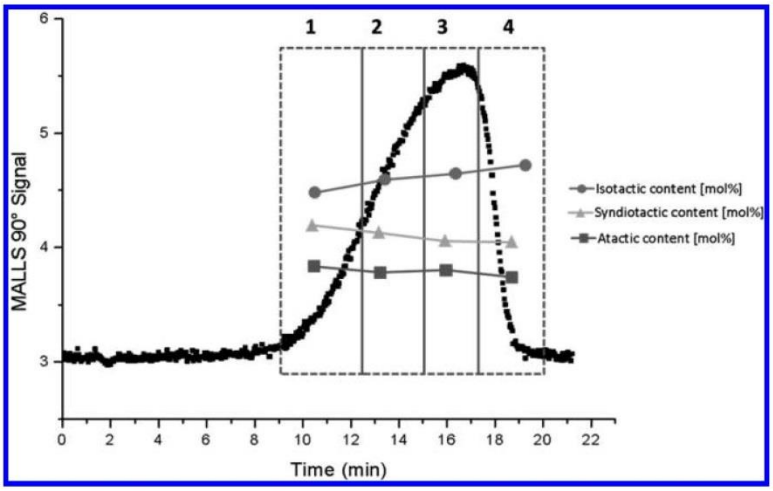

Figure 8. Fractionation of atactic PMMA (139 kDa) by ThFFF in acetonitrile for ^{1}H NMR analysis. General trends in isotactic (circle), syndiotactic (triangle), and atactic (square) content are overlaid on the elution profile.

DOI: 10.1021/ac504651p
Anal. Chem. 2015, 87, 3011−3018

CONCLUSIONS

For the first time, it has been demonstrated that ThFFF has the capability of fractionating polymers on the basis of tacticity. It has been shown that ThFFF fractionates isotactic, syndiotactic, and atactic PMMA isomers based on differences in microstructure. ^{1}H NMR data of fractions collected in acetonitrile showed an enrichment of isomers across the elution peak that correlates to ThFFF retention data. It was also demonstrated that polymer microstructure can influence the Soret coefficient in favor of either D (low retention) or D_T (high retention). In addition to the influence of microstructure on the separation, it was shown that solvent composition influences the resolution of the peaks and dramatically enhances the fractionation selectivity.

AUTHOR INFORMATION

Corresponding Author

*E-mail: hpasch@sun.ac.za.

Notes

The authors declare no competing financial interest.

ACKNOWLEDGMENTS

The authors thank Sasol for financial support.

REFERENCES

(1) Gao, Y. S.; Caldwell, K. D.; Myers, M. N.; Giddings, J. C. *Macromolecules* **1985**, *18*, 1272.
(2) Janča, J. *Microthermal Field-Flow Fractionation*; HNB Publishing: New York, 2008.
(3) Schimpf, M. E. *J. Chromatogr. A* **1990**, *517*, 405.
(4) Runyon, J. R.; Williams, S. K. R. *J. Chromatogr. A* **2011**, *1218*, 6774.
(5) Rue, C. A.; Schimpf, M. E. *Anal. Chem.* **1994**, *66*, 4054.
(6) Schimpf, M. E.; Caldwell, K.; Giddings, J. C., Eds. *Field-Flow Fractionation Handbook*; Wiley-Interscience: New York, 2000.
(7) Sisson, R. M.; Giddings, J. C. *Anal. Chem.* **1994**, *66*, 4043.
(8) Van Asten, A. C.; Kok, W. T.; Tjissen, R.; Poppe, H. *J. Polym. Sci., Part B: Polym. Phys.* **1996**, *34*, 283.
(9) Ponyik, C. A.; Wu, D. T.; Williams, S. K. R *Anal. Bioanal. Chem.* **2013**, *405*, 9033.
(10) Kassalainen, G. E.; Williams, S. K. R. *J. Chromatogr. A* **2003**, *988*, 285.
(11) Kirkland, J. J.; Boone, L. S.; Yau, W. W. *J. Chromatogr. A* **1990**, *517*, 377.
(12) Greyling, G.; Pasch, H. *Macromol. Rapid Commun.* **2014**, *35*, 1846.
(13) Gunderson, J. J.; Giddings, J. C. *Macromolecules* **1986**, *19*, 2618.
(14) Van Asten, A.; Venema, E.; Kok, W.; Poppe, H. *J. Chromatogr. A* **1993**, *644*, 83.
(15) Runyon, J.; Williams, S. *Polym. Prepr.* **2011**, *52*, 230.
(16) Van Aswegen, W.; Hiller, W.; Hehn, M.; Pasch, H. *Macromol. Rapid Commun.* **2013**, *34*, 1098.
(17) Messaud, F. A.; Sanderson, R. D.; Runyon, J. R.; Otte, T.; Pasch, H.; Williams, S. K. R. *Prog. Polym. Sci.* **2009**, *34*, 351.
(18) Pasch, H.; Trathnigg, B. *Multidimensional HPLC of Polymers*; Alig, I., Pasch, H., Eds.; Springer-Verlag: Heidelberg, Germany, 2013.
(19) Podzimek, S. *Light Scattering, Size Exclusion Chromatography and Asymmetric Flow Field Flow Fractionation: Powerful Tools for the Characterization of Polymers, Proteins and Nanopoarticles*; John Wiley & Sons, Inc.: Hoboken, New Jersey, 2011.
(20) Garcia, B.; Ocampo, M. A.; Luna-Bárcenas, G.; García, R.; Mejia, I.; Rodríguez Melgarejo, F.; Fernández Loyola, C.; Sánchez Catalán, K.; Flores Ramírez, N.; Vásquez, G.; Salomón, R.; Ortiz-Estrada, C.; Garcia-Gaitan, B.; Zavala, R. *Macromol. Symp.* **2009**, *342*, 283.
(21) Zaikov, G. E.; Kozlowski, R., Eds. *Chemical and Physical Properties of Polymers*; Nova Science Publishers: Hauppauge, New York, 2005.
(22) Salamone, J.C., Ed. *Polymeric Materials Encyclopedia, Twelve Vol. Set*; CRC Press: Boca Raton, FL, 1996.
(23) Mark, J. E., Ed. *Polymer Data Handbook*; Oxford University Press: Oxford, U.K., 1999.
(24) Machtle, W.; Fisher, H. *Angew. Makromol. Chem.* **1969**, *7*, 147.
(25) Wunderlich, B. *Thermal Analysis of Polymeric Materials*; Springer-Verlag: Heidelberg, Germany, 2005.
(26) Cowie, J.; McEwen, L. *J. Chem. Soc., Faraday Trans. 1* **1976**, *72*, 526.
(27) Apel, U.; Hentschke, R.; Helfrich, J. *Macromolecules* **1995**, *28*, 1778.
(28) Schimpf, M. E.; Giddings, J. C. *J. Polym. Sci., Part B: Polym. Phys.* **1989**, *27*, 1317.
(29) Wypych, G., Ed. *Handbook of Solvents*; ChemTec Publishing: Toronto, Canada, 2001.

DOI: 10.1021/ac504651p
Anal. Chem. 2015, 87, 3011−3018

4.1.3 Poly(n-butyl methacrylate) and Poly(t-butyl methacrylate)

G. Greyling, H. Pasch, *Macromol. Rapid Commun*. **2015**, *36*, 2143-2148

The final investigation into microstructure-based separations for this study addressed the separation of poly(n-butyl methacrylate) (nBuMA) and poly(t-butyl methacrylate) (tBuMA) according to the topology of the butyl group. Analysis in THF showed that nBuMA and tBuMA exhibit different retention behaviours as they showed elution times of 9.3 and 13.9 min, respectively. Moreover, the ThFFF data also showed that nBuMA is less rigid than tBuMA, which was confirmed by reported characteristic ratios (C_∞) of 8.8 and 10.2, respectively.[72,73]

It was reported that tBuMA and nBuMA exhibit different Hildebrand solubility parameters (δ) of 16.9 and 17.8 $MPa^{1/2}$, respectively.[74] Therefore, the different δ values for tBuMA and nBuMA indicate that the samples exhibit different polarities. Thus, the retention behaviours in ThFFF could be influenced by solvent polarity rather than solvent viscosity. Consequently, solvents of various polarities and viscosities such as cyclohexane (CH), dichloromethane (DCM), tetrahydrofuran (THF), methyl ethyl ketone (MEK), dioxane (DOX) and dimethylformamide (DMF) were used to determine the effect of solvent polarity on the separation of nBuMA and tBuMA. It was demonstrated that the separation improves in order of DCM-THF-MEK-DOX-DMF which showed increasing differences in elution times of 3.2, 4.5, 5.1, 6.3 and 7.2 min, respectively. This trend showed that solvent polarity can influence polymer retention behaviour to a greater extent than solvent viscosity as DMF (0.8 cP), which has a lower viscosity than DOX (1.2 cP) yields an improved separation. The same is true for the lower viscosity solvents where MEK (0.38 cP), which has a lower viscosity than THF (0.46 cP), yields an improved separation.

Of the various solvents it was found that CH shows the greatest fractionation power which is due to CH being a theta solvent for tBuMA but not nBuMA. Thus, the greater fractionating power of CH was found due to tBuMA experiencing enhanced retention in a theta solvent while, at the same time, nBuMA experiences normal retention in a thermodynamically good solvent. Furthermore, it was also shown that, unlike stereoregular PMMA, isotactic and syndiotactic poly(t-butyl methacrylate) are not separated in ThFFF.

These results demonstrated that ThFFF can successfully separate polymers based on molecular topology. Moreover, it was also shown that solvent polarity can have a significant influence on retention behaviour.

Communication Macromolecular Journals Macromolecular Rapid Communications

Fractionation of Poly(butyl methacrylate) by Molecular Topology Using Multidetector Thermal Field-Flow Fractionation

Guilaume Greyling, Harald Pasch*

Thermal field-flow fractionation (ThFFF) is an interesting alternative to column-based fractionation being able to address different molecular parameters including size and composition. Until today it has not been shown to be able to fractionate polymers of similar molar masses and chemical compositions by molecular topology. The present study demonstrates that poly(butyl methacrylates) with identical molar masses can be fractionated by ThFFF according to the topology of the butyl group. The influence of the solvent polarity on the thermal diffusion behavior of these polymers is presented and it is shown to have a significant influence on the fractionation of poly(n-butyl methacrylate) and poly(t-butyl methacrylate). Fractionation improves with increasing solvent polarity and solvent polarity may have a greater influence on fractionation than solvent viscosity. It is found that the thermal diffusion coefficient, D_T, as well as the hydrodynamic diameter, D_h, exhibit increasing trends with increasing solvent polarity. The solvent quality has a significant influence on the fractionation. It is found that cyclohexane, being a theta solvent for poly(t-butyl methacrylate) but not for poly(n-butyl methacrylate), significantly improves the fractionation of the samples by decreasing the diffusion rate of the former but not the latter.

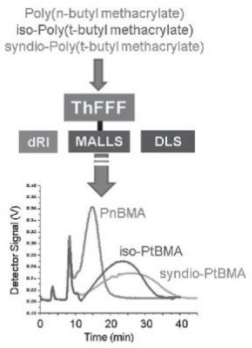

1. Introduction

Thermal field-flow fractionation (ThFFF) is a channel-based fractionation technique that applies a temperature gradient perpendicular to a carrier liquid flowing through an open, ribbon-like channel in order to fractionate analytes according to size, chemical composition, or microstructure.[1–3] The applied temperature gradient induces analytes to migrate from the hot to the cold wall (accumulation wall) of the channel. Such a temperature-induced migration is termed thermal diffusion and is characterized by the thermal diffusion coefficient, DT.[4]

G. Greyling, Prof. H. Pasch
Department of Chemistry and Polymer Science
University of Stellenbosch
Private Bag X1, 7602 Matieland, South Africa
E-mail: hpasch@sun.ac.za

Thermal diffusion is balanced by normal diffusion which is the migration of analytes away from the accumulation wall toward the center of the channel due to increasing analyte concentration (Figure S1 in the Supporting Information).[1,5] Normal diffusion is described by the normal diffusion coefficient, D.

Laminar flow conditions within the channel result in a parabolic flow velocity profile with faster flow streams toward the center of the channel and slower flow streams near the channel walls.[1] Elution from the channel is determined by the analyte's position in the parabolic flow velocity profile and therefore its average distance from the accumulation wall.[1] Thus, the farther the analytes are from the accumulation wall (faster flow streams), the shorter the retention time. The average distance from the accumulation wall is determined by the interplay between D_T and D and this interplay is described by the Soret coefficient, S_T, where $S_T = D_T/D$.[6] Therefore, analytes with

Macromol. Rapid Commun. **2015**, *36*, 2143–2148

DOI: 10.1002/marc.201500429

similar S_T values will reside in similar flow streams and co-elute. Furthermore, D is dependent on the size of the analyte in solution, whereas D_T is dependent on the chemical nature of the analyte and the solvent.[7] ThFFF can thus fractionate analytes according to size (D) as well as chemical composition (D_T) and, as a consequence, has been applied to the characterization of a variety of polymers.[8,9]

The capabilities of ThFFF in separating polymers according to tacticity and microstructure have been discussed recently.[2,3] The influence of solvent composition on polymer retention behavior has been extensively studied and it was demonstrated that solvent composition, as well as viscosity, can have a significant influence.[10–13] Moreover, it was reported that solvent viscosity is the dominating and only relevant solvent parameter that influences D_T as it is the only parameter that varies significantly between solvents.[14] Although this conclusion was based on the degree to which certain solvent parameters (such as solvent density, viscosity, and activation energy) vary between solvents, the study did not take into account the influence of solvent polarity. Moreover, despite this conclusion, the influence of solvent polarity on D_T has only been published for a single study. It was found that polymer latex particles undergo increased retention with increasing solvent polarity, whereas no clear trend was observed for silica particles.[15]

To date, the influence of solvent polarity on the thermal diffusion behavior of polymers has yet to be determined and in the present study we shall show that solvent polarity can play a significant role in the fractionation of poly(butyl methacrylates). Moreover, it will be shown that solvent polarity greatly influences both D_T and the hydrodynamic size of the samples. This study, for the first time, describes the use of ThFFF coupled on-line to multiangle laser light scattering (MALLS), differential refractive index (dRI), and dynamic light scattering (DLS) detection to investigate the influence of the solvent polarity on D_T and the fractionation of poly(butyl methacrylate) according to the topology of the butyl group. This is demonstrated for poly(t-butyl methacrylate) and poly(n-butyl methacrylate) having identical molar masses. The multidetector setup allows for the simultaneous on-line determination of the molar mass distributions by MALLS as well as the determination of D (and subsequently D_T) by DLS. The dRI detector was required as universal concentration detector. Such investigation has not been conducted before and, therefore, these first results require further more detailed studies.

2. Experimental Section

2.1. Materials

The isotactic (122 kDa) and syndiotactic (116 kDa) poly(t-butyl methacrylate) as well as the poly(n-butyl methacrylate) (128 kDa) and poly(methyl methacrylate) (139 kDa) standards were purchased from Polymer Source Inc. (Montreal, Canada) and prepared in 3 mg mL^{-1} concentrations using HPLC grade cyclohexane (CH), dichloromethane (DCM), tetrahydrofuran (THF), methyl ethyl ketone (MEK), dioxane (DOX), and dimethylformamide (DMF) purchased from Sigma-Aldrich (South Africa). Furthermore, molar mass data obtained from MALLS in each solvent corresponded well with the nominal molar masses reported by the manufacturer.

2.2. Thermal Field-Flow Fractionation

The thermal FFF system TF2000 (Postnova Analytics, Landsberg, Germany) was coupled online to MALLS (PN 3070, Postnova Analytics), dRI (PN 3150, Postnova Analytics), and DLS detectors (Zen 1600, Malvern Instruments, Worcestershire, UK). The experimental details of ThFFF are summarized in the Supporting Information. Furthermore, dn/dc values were obtained from the Polymer Data Handbook.[16]

3. Results and Discussion

Initial analysis in THF (a low viscosity, thermodynamically good solvent for all samples) showed that poly(t-butyl methacrylate) (tBuMA), poly(methyl methacrylate) (PMMA), and poly(n-butyl methacrylate) (nBuMA) samples exhibit distinctively different retention behaviors, thus illustrating the technique's sensitivity toward chemical composition (Figure 1A). Although PMMA does not form part of the study, it is included to demonstrate the chemical composition sensitivity of ThFFF.

Figure 1A shows the superimposed dRI fractograms of PMMA, tBuMA, and nBuMA in THF, while Tables 1 and 2 show the D_T and D values for the samples in THF, respectively.

Figure 1A also shows that, unlike stereoregular PMMA, the isotactic and syndiotactic tBuMA samples show identical elution behavior in THF.[3] Furthermore, the difference in retention times between the tBuMA and nBuMA samples is 4.5 min.

While the fractionation of PMMA and the poly(butyl methacrylate) samples is due to differences in chemical compositions, the fractionation of nBuMA and tBuMA is due to differences in molecular topology which affects the stiffness of the polymer chains. It has been reported that nBuMA is less rigid than tBuMA as they exhibit different characteristic ratios (C_∞) of 8.8 and 10.2, respectively.[17,18] Furthermore, it has been shown that D_T increases with increasing polymer rigidity, and from Table 1 it can be seen that nBuMA exhibits a smaller D_T value than tBuMA in THF.[17,19] Since the samples exhibit similar D values but different S_T values (Table S1, Supporting Information), fractionation is due to differences in D_T and, therefore, molecular rigidity. Additionally, as D_T can be used

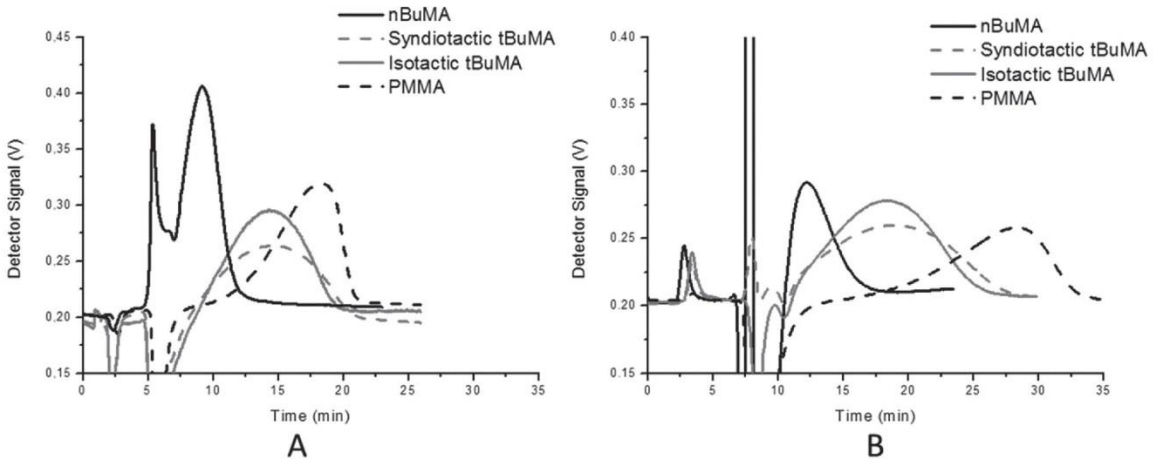

Figure 1. Superimposed dRI fractograms of poly(n-butyl methacrylate) (black), poly(methyl methacrylate) (black dash) as well as isotactic (grey) and syndiotactic (grey dash) poly(t-butyl methacrylate) in A) THF and B) DOX.

to estimate the relative rigidity of polymers, it can be seen from Table 1 that isotactic and syndiotactic tBuMA exhibit similar D_T values and are therefore equally rigid. Thus, in contrast to isotactic and syndiotactic PMMA, tacticity does not appear to influence the chain rigidity of tBuMA.[3,20]

In an attempt to improve the fractionation of nBuMA and tBuMA, the solvent viscosity was increased as it was reported to be the only solvent parameter to influence D_T and thus retention.[14] Dioxane (DOX) was selected as a high viscosity, thermodynamically good solvent and Tables 1 and 2 show the D_T and D values for the samples in DOX, respectively. Figure 1B shows the superimposed PMMA, tBuMA, and nBuMA dRI fractograms in DOX.

Figure 1B shows that the isotactic and syndiotactic tBuMA samples still co-elute in DOX. Furthermore, the difference in retention times between the PMMA and tBuMA samples increased from 3.7 min in THF to 9.4 min in DOX while the difference in retention times between the nBuMA and tBuMA samples increased from 4.5 min in THF to 6.3 min in DOX. The almost 3-fold increase in retention time differences between the PMMA and tBuMA samples with a 3-fold increase in viscosity is as expected (viscosity of THF is 0.46cP and DOX is 1.2 cP). However, the increase in retention time difference between the nBuMA and tBuMA samples was found to be relatively low as the significant increase in viscosity only improved fractionation by 1.8 min. Viscosity can, therefore, not be the primary solvent parameter influencing the fractionation of nBuMA and tBuMA.

It was reported that tBuMA and nBuMA exhibit different Hildebrand solubility parameters (δ) of 16.9 and 17.8 $MPa^{1/2}$, respectively.[21] The Hildebrand solubility parameter, which is a numerical estimate of the degree of intermolecular interactions, can be used to describe a polymer's solubility and relative polarity.[21] Therefore, the different δ values for tBuMA and nBuMA indicate that the samples exhibit different polarities. Consequently, the retention behaviors in ThFFF could be influenced by solvent polarity rather than solvent viscosity.

In order to determine the influence of solvent polarity on the fractionation of nBuMA and tBuMA in ThFFF, solvents

Table 1. Thermal diffusion coefficients (D_T) of the poly(n-butyl methacrylate) as well as isotactic and syndiotactic poly(t-butyl methacrylate) samples in the various solvents.

Sample[a)]	D_T [10^{-7} cm^2 s^{-1} K^{-1}]					
	CH	DCM	THF	MEK	DOX	DMF
Isotactic tBuMA	0.722 ± 0.017	0.813 ± 0.015	1.22 ± 0.02	1.77 ± 0.07	0.544 ± 0.010	0.711 ± 0.022
Syndiotactic tBuMA	0.711 ± 0.016	0.797 ± 0.024	1.23 ± 0.01	1.61 ± 0.07	0.549 ± 0.014	0.693 ± 0.025
nBuMA	0.517 ± 0.022	0.671 ± 0.022	0.883 ± 0.050	1.11 ± 0.06	0.317 ± 0.014	0.475 ± 0.019

[a)]Molar masses of the samples: nBuMA, 128 kDa; isotactic tBuMA, 122 kDa; and syndiotactic tBuMA, 116 kDa.

Table 2. Diffusion coefficients (D) of poly(n-butyl methacrylate) as well as isotactic and syndiotactic poly(t-butyl methacrylate) in the various solvents.

Sample[a)]	D [10^{-7} cm^2 s^{-1}]					
	CH	DCM	THF	MEK	DOX	DMF
Isotactic tBuMA	2.16 ± 0.11	4.34 ± 0.23	4.04 ± 0.11	4.73 ± 0.22	1.89 ± 0.22	2.72 ± 0.11
Syndiotactic tBuMA	2.29 ± 0.10	4.18 ± 0.14	4.12 ± 0.25	4.67 ± 0.23	2.10 ± 0.26	2.68 ± 0.14
nBuMA	2.72 ± 0.11	4.42 ± 0.25	4.20 ± 0.23	4.90 ± 0.24	2.10 ± 0.19	2.84 ± 0.12

[a)]Molar masses of the samples: nBuMA, 128 kDa; isotactic tBuMA, 122 kDa; and syndiotactic tBuMA, 116 kDa.

of various polarities and viscosities were selected. The solvents selected for the study are listed in Table S2 (Supporting Information) and include CH, DCM, THF, MEK, DOX, and DMF. Table S2 also lists the Snyder polarity index (P') as well as the viscosity of each of the respective solvents. The Snyder polarity index is a unitless parameter that ranks solvents according to relative polarity as determined from theoretical calculations.[22] Low P' values correspond to a low polarity solvents, while high P' values correspond to high polarity solvents. In addition to the thermodynamically good solvents, CH was also included as it is reported to be a theta solvent for tBuMA but not for nBuMA.

Figure 2 shows the superimposed nBuMA and tBuMA dRI fractograms in each solvent.

The fractograms are presented in order of increasing solvent polarity and, therefore, fractograms A, B, C, D, E, and F correspond to analysis in CH, DCM, THF, MEK, DOX, and DMF, respectively. Figure 2 shows that as the polarities of the solvent increase, the retention times of the samples increase and that the fractionation of nBuMA and tBuMA also improves. Furthermore, Tables 1 and 2 show the D_T and D values for the samples in each solvent.

Table 1 shows an important trend in D_T as a function of solvent polarity. Table 1 shows that, with the exception of CH, both the low viscosity solvents (DCM, THF, and MEK) as well as the high viscosity solvents (DOX and DMF) exhibit an increasing trend in D_T with increasing solvent polarity. Furthermore, a similar increasing trend for D_h with increasing solvent polarity was observed (Table S3, Supporting Information).

Comparing the retention time differences between nBuMA and tBuMA in each solvent, it is clear that the fractionation of nBuMA and tBuMA improves with increasing solvent polarity. The fractionation improves in order of DCM–THF–MEK–DOX–DMF which show increasing differences in retention times of 3.2, 4.5, 5.1, 6.3, and 7.2 min, respectively (Table S4, Supporting Information). More importantly, this trend shows that solvent polarity can influence polymer retention behavior to a greater extent than solvent viscosity as DMF (0.8 cP) which a lower viscosity than DOX (1.2 cP) yields an improved fractionation. The same is true for the lower viscosity solvents where MEK (0.38 cP), which has a lower viscosity than THF (0.46 cP), yields an improved fractionation. This trend, however, does not hold true for CH as it yields the best fractionation of nBuMA and tBuMA but is the least polar solvent. Moreover, only CH appears to exhibit some degree of selectivity toward tacticity as it yields the largest difference in retention times (2.2 min) between isotactic and syndiotactic tBuMA (Table S4, Supporting Information). This exception to the trend can be explained by bearing in mind that CH is a theta solvent for tBuMA.

In a theta solvent it is expected that a polymer forms a more compact conformation than in a thermodynamically "good" solvent. Thus, in a theta solvent the polymer should exhibit a smaller size and consequently larger D value than in a "good" solvent of similar viscosity. The larger D values should, in turn, yield shorter retention times. However, Table S4 (Supporting Information) shows that the samples exhibit longer retention times in CH than in DMF, while Table 2 shows that D values for tBuMA samples are smaller for CH than for DMF (viscosities CH and DMF are 0.9 and 0.8 cP, respectively). The DLS data suggest that, unexpectedly, the tBuMA samples are diffusing slower in CH than in DMF as the samples take on a more expanded conformation and larger size in the theta solvent than the "good" solvent (Table S3, Supporting Information). However, it is more plausible that the weak solvent–polymer interactions of the theta solvent are obstructing diffusion in CH and thus erroneously yielding larger D_h and smaller D values than expected.

The suppression of D in CH explains the enhanced retention relative to DMF. As the polymer's diffusion away from the cold wall is suppressed, the molecules are confined to the slower flow streams which result in longer retention times. Moreover, the similar D_T values for the tBuMA samples in CH and DMF further show that the enhanced retention in CH is due to D and not due to changes in DT.

This suppression of D is not seen for nBuMA as CH is a "good" solvent and not a theta solvent. This is

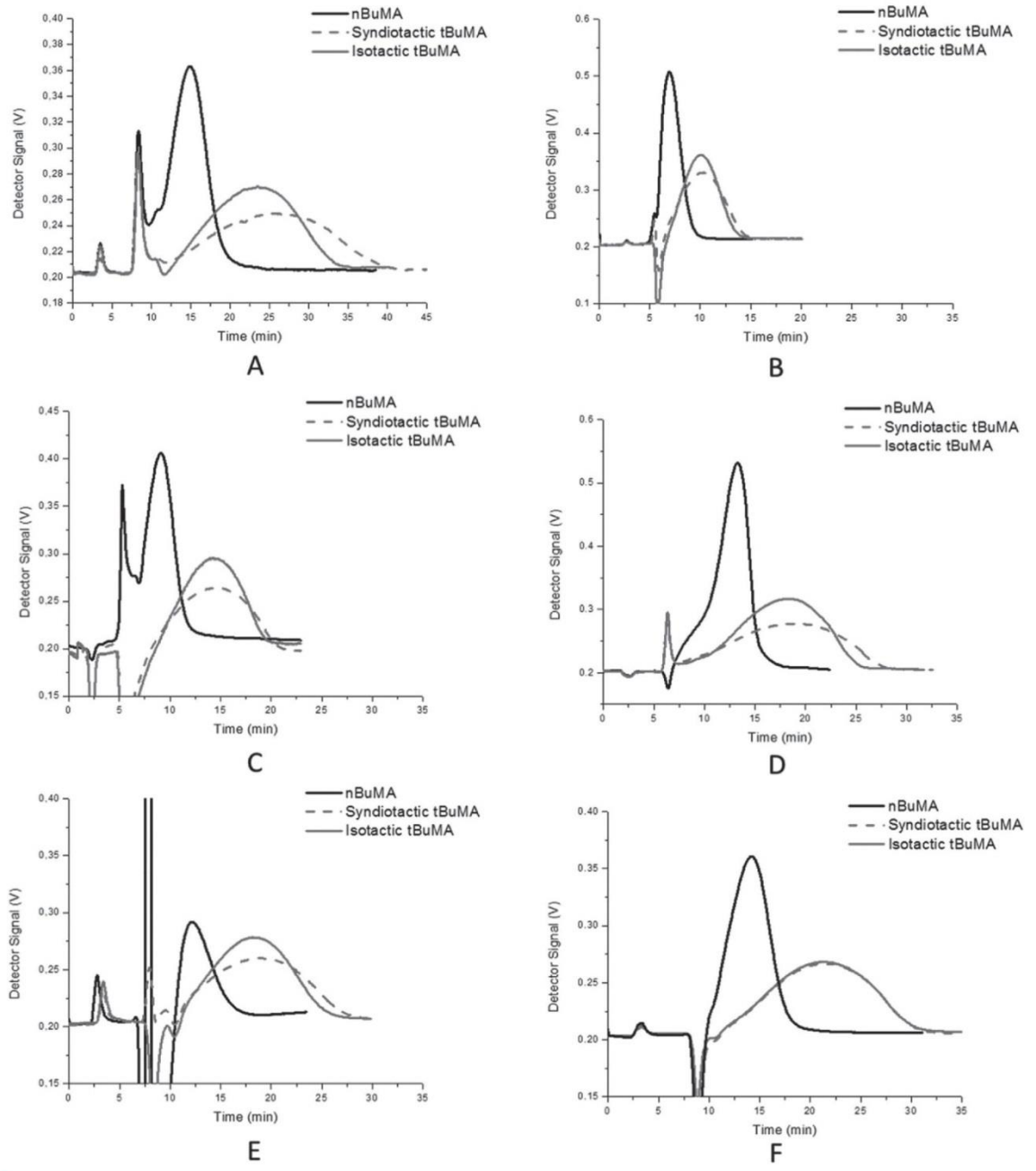

Figure 2. Superimposed dRI fractograms of poly(n-butyl methacrylate) (black) as well as isotactic (grey) and syndiotactic (grey dash) poly(t-butyl methacrylate) in the various solvents. A) CH, B) DCM, C) THF, D) MEK, E) DOX, and F) DMF.

demonstrated by the similar values for D in CH and DMF (Table 2). Moreover, with the exception of CH, the nBuMA and tBuMA samples show similar D values but different D_T values in each solvent. Similar D values are expected as the samples exhibit similar sizes while the differences in D_T values are due to the relative rigidity of tBuMA and nBuMA. Therefore, the greater fractionation power of CH is due to tBuMA experiencing enhanced retention in a theta solvent, while, at the same time, nBuMA experiences normal retention in a "good" solvent.

4. Conclusions

For the first time it has been demonstrated that ThFFF can fractionate poly(n-butyl methacrylate) and poly(t-butyl methacrylate) having identical molar masses based on the topology of the butyl group. It was shown that solvent polarity can have a significant influence on the retention behavior, size, and thermal diffusion of the polymers. It was also shown that, unlike stereoregular PMMA, isotactic and syndiotactic poly(t-butyl methacrylate)s are not separated in ThFFF. Furthermore, the best fractionation of poly(t-butyl methacrylate) and poly(n-butyl methacrylate) was obtained in cyclohexane which is a theta solvent for the former but a good solvent for the latter.

It is known that the interaction of the macromolecules with the solvent depends on temperature. In different layers of the ThFFF channel, the polymer coils could possess different conformations depending on the solvent type. It will be interesting to compare how fast the change of solvent viscosity with temperature and how fast the change of polymer conformation in certain solvents will be. This could explain the observed behavior, however, as to date no work investigated the rate of change in the conformation of tBuMA or nBuMA as a function of temperature in a ThFFF channel, molecular dynamic calculations would need to be employed which would fall outside the scope of the current work.

Supporting Information

Supporting Information is available from the Wiley Online Library or from the author.

Received: July 21, 2015; Revised: September 15, 2015; Published online: October 19, 2015; DOI: 10.1002/marc.201500429

Keywords: poly(n-butyl methacrylate); poly(t-butyl methacrylate); solvent polarity; thermal diffusion; thermal field-flow fractionation

[1] M. E. Schimpf, J. C. Giddings, K. Caldwell, *Field-Flow Fractionation Handbook*, Wiley-Interscience, New York **2000**.
[2] G. Greyling, H. Pasch, *Macromol. Rapid Commun.* **2014**, *35*, 1846.
[3] G. Greyling, H. Pasch, *Anal. Chem.* **2015**, *87*, 3011.
[4] M. E. Schimpf, *J. Chromatogr. A* **1990**, *517*, 405.
[5] J. R. Runyon, S. K. R. Williams, *J. Chromatogr. A* **2011**, *1218*, 7016.
[6] J. Runyon, S. Williams, *Polym. Prepr.* **2011**, *52*, 230.
[7] S. K. R. Williams, D. Lee, *J. Sep. Sci.* **2006**, *29*, 1720.
[8] A. C. Makan, P. Sinha, N. Ngaza, W. van Aswegen, H. Pasch, *Anal. Bioanal. Chem.* **2013**, *405*, 9041.
[9] J. R. Runyon, S. K. R. Williams, *J. Chromatogr. A* **2011**, *1218*, 6774.
[10] G. E. Kassalainen, S. K. R. Williams, *J. Chromatogr. A* **2003**, *988*, 285.
[11] R. M. Sisson, J. C. Giddings, *Anal. Chem.* **1994**, *66*, 4043.
[12] C. A. Rue, M. E. Schimpf, *Anal. Chem.* **1994**, *66*, 4054.
[13] J. J. Kirkland, L. S. Boone, W. W. Yau, *J. Chromatogr. A* **1990**, *517*, 377.
[14] M. Hartung, J. Rauch, W. K hler, *J. Chem. Phys.* **2006**, *125*, 214904.
[15] G. Liu, J. C. Giddings, *Chromatographia* **1992**, *34*, 483.
[16] J. E. Mark, *Polymer Data Handbook*, Oxford University Press, Oxford **1999**.
[17] A. Karandinos, J. Mays, N. Hadjichristidis, *Polym. Bull.* **1990**, *24*, 251.
[18] A. Karandinos, S. Nan, J. W. Mays, N. Hadjichristidis, *Macromolecules* **1991**, *24*, 2007.
[19] D. Stadelmaier, W. K hler, *Macromolecules* **2009**, *42*, 9147.
[20] U. Apel, R. Hentschke, J. Helfrich, *Macromolecules* **1995**, *28*, 1778.
[21] D. Koshal, *Manufacturing Engineer's Reference Book*, Butterworth-Heinemann, Oxford **1993**.
[22] R. E. Schirmer, *Modern Methods of Pharmaceutical Analysis*, 2nd ed., CRC Press, Boston **1990**.

4.2 Fractionation of Micelles According to Corona Composition

G. Greyling, H. Pasch, *J. Chromatogr. A* **2015**, *1414*, 163–172.

The second part of this study describes the characterisation and separation of poly(methyl methacrylate)-polystyrene (PMMA-PS) micelles with isotactic and syndiotactic coronas according to corona composition.

PMMA-PS micelles with isotactic (iPMMA-PS) and syndiotactic (sPMMA-PS) coronas were prepared in ACN by both the co-solvent and nanoprecipitation methods. As expected, the tacticity of the corona influenced the critical micelle concentration (CMC) values whereas the preparation method was found to have no significant influence on the CMC values. Similar results were reported for amphiphilic poly(lactic acid)-block-poly(ethylene glycol) copolymers.[75] Moreover, it was found that the sPMMA-PS micelles exhibited lower CMC values than the iPMMA-PS micelles. The lower CMC values for the sPMMA-PS micelles were attributed to the more flexible syndiotactic PMMA blocks which could pack together in the corona more easily than the less flexible isotactic PMMA blocks and, therefore, form micelles at lower concentrations. In contrast to the CMC, the critical micelle temperature (CMT) was found to remain unaffected by the microstructure of the corona.

During the study, several ThFFF conditions using increasing temperature gradients were selected for the characterisation of micelles. The ThFFF conditions were chosen such that the micelles would experience increased retention while remaining intact up to temperature gradient of $\Delta T = 25$ degrees. It was found that not all the micelles remained intact at a temperature gradient of $\Delta T = 30$ degrees.

It was demonstrated that ThFFF can successfully characterise micelles by simultaneously determining important micelle characteristics such as size, shape, aggregation number, diffusion, thermal diffusion and Soret coefficients as a function of temperature, from a single injection. Furthermore, ThFFF was able to yield valuable information regarding size distributions and morphology changes as a function of temperature which is not possible by other techniques. With regards to thermal diffusion of micelles, it was also found that micelles exhibit an unique decreasing trend in D_T which is not observed for either high molecular weight polymers or aggregates and that this trend is independent of the microstructure of the corona and the preparation method.

Upon comparing the ThFFF data of the sPMMA-PS and iPMMA-PS micelles it was found that the various micelles exhibited different S_T values at each analysis condition. A difference in S_T is indicative of a possible separation. Moreover, such a separation would be due to corona composition as the micelles exhibited similar sizes. Superimposing the fractograms of the various micelles revealed that a separation based on corona composition could potentially be achieved with temperature gradients up to $\Delta T = 20$ degrees.

However, a separation could not be experimentally achieved as the micelles aggregated upon mixing due to stereocomplexation of the PMMA coronas in ACN.[76] Although a separation according to corona composition could not be demonstrated for PMMA-PS micelles in ACN, it was demonstrated that ThFFF is a powerful tool to study and characterise dynamic self-assemblies (such as micelles) with different compositions.

Journal of Chromatography A, 1414 (2015) 163–172

Contents lists available at ScienceDirect

Journal of Chromatography A

journal homepage: www.elsevier.com/locate/chroma

Multidetector thermal field-flow fractionation as a unique tool for the tacticity-based separation of poly(methyl methacrylate)-polystyrene block copolymer micelles

Guilaume Greyling, Harald Pasch*

Department of Chemistry and Polymer Science, University of Stellenbosch, Private Bag X1, 7602 Stellenbosch, South Africa

ARTICLE INFO

Article history:
Received 19 June 2015
Received in revised form 4 August 2015
Accepted 12 August 2015
Available online 15 August 2015

Keywords:
Thermal field-flow fractionation
Thermal diffusion
Micelle
Block copolymer
Tacticity

ABSTRACT

Poly(methyl methacrylate)-polystyrene (PMMA-PS) micelles with isotactic and syndiotactic coronas are prepared in acetonitrile and subjected to thermal field-flow fractionation (ThFFF) analysis at various conditions of increasing temperature gradients. It is shown for the first time that multidetector ThFFF provides comprehensive information on important micelle characteristics such as size (D_h), shape (R_g/R_h), aggregation number (Z), thermal diffusion (D_T) and Soret coefficients (S_T) as a function of temperature from a single injection. Moreover, it is found that micelles exhibit a unique decreasing trend in D_T as a function of temperature which is independent of the tacticity of the corona and the micelle preparation method used. It is also demonstrated that ThFFF can monitor micelle to vesicle transitions as a function of temperature. In addition to ThFFF, it is found from DLS analysis that the tacticity of the corona influences the critical micelle concentration and the magnitude to which micelles expand/contract with temperature. The tacticity does not, however, influence the critical micelle temperature. Furthermore, the separation of micelles based on the tacticity of the corona highlight the unique capabilities of ThFFF.

1. Introduction

Thermal field-flow fractionation (ThFFF) is a subtechnique of field-flow fractionation that employs a temperature gradient across an open, ribbon-like channel to fractionate analyte molecules according to size or chemical composition [1,2]. Analytes subjected to a temperature gradient migrate from the hot to the cold wall (accumulation wall) of the channel. Such a lateral migration of analytes due to a temperature gradient is characterised by the thermal diffusion coefficient, D_T. Thermal diffusion is counteracted by normal diffusion which is the migration of analyte molecules away from the accumulation wall towards the center of the channel due to increasing analyte concentration. Normal diffusion is characterised by the normal diffusion coefficient, D [3]. Furthermore, diffusion is dependent on the size of the analyte molecules in solution, whereas thermal diffusion is independent of size and dependent on, among other factors, the chemical nature of the analyte molecules and the solvent [1,4].

Within the channel with the flowing carrier, a parabolic flow velocity profile forms which results in faster flow streams towards the center of the channel and slower streams towards the accumulation wall [1]. Retention is determined by the average position of the analyte molecules in the flow velocity profile and therefore by their mean distance from the accumulation wall [4]. Thus, the further the analyte molecules are from the accumulation wall (faster flow streams), the shorter the retention time. The average distance from the accumulation wall is determined by the interplay between D_T and D. This interplay is described by the Soret coefficient, S_T, where $S_T = D_T/D$ [1,5]. Therefore, analyte molecules with similar S_T values will reside in similar flow streams and co-elute. Furthermore, D_T appears to be dominated by the monomers preferentially located in the outer region of solvated polymer molecules [6]. As with all FFF techniques (operating in normal mode), ThFFF elution order is from small to large size analytes [1,4].

ThFFF is predominantly used in the characterization of analytes in organic solvents and it has been demonstrated that ThFFF can be used for the characterization of a variety of analytes such as homopolymers, polymer blends, copolymers, microgel samples, particles, colloids and aggregates [1,2,7–11]. It has also been demonstrated that the fractionation capabilities of ThFFF are not limited to size and chemical composition but extend to polymer microstructure [12,13]. ThFFF is a powerful alternative to commonly used column-based techniques, such as size exclusion chromatography (SEC), as the relatively gentle fractionation conditions

* Corresponding author. Tel.: +27 21 808 3173; fax: +27 21 808 4967.
E-mail address: hpasch@sun.ac.za (H. Pasch).

http://dx.doi.org/10.1016/j.chroma.2015.08.023
0021-9673/

and the absence of a stationary phase enable ThFFF to readily fractionate a variety of high molecular weight and fragile compounds without degradation taking place [4]. Moreover, sample preparation steps such as filtering, which could affect sample composition, are not often required prior to ThFFF analysis.

The unique features of ThFFF make it a suitable technique for the characterization of high molecular weight self-assemblies such as micelles. Micelles are formed by the self-assembly of e.g. block copolymers that are dissolved in a selective solvent. A selective solvent is a thermodynamically good solvent for one of the blocks but a poor solvent/precipitant for the other [6,14–16]. Block copolymer micelles consist of a core formed by the insoluble block and a corona formed by the soluble block. The critical concentration at which the block copolymers start to self-assemble into micelles is called the critical micelle concentration, CMC. Below the CMC only molecularly dissolved copolymer chains, or unimers, are found whereas above the CMC, micelles are in equilibrium with unimers [15,17]. Closely related to the CMC is the critical micelle temperature, CMT. The CMT is the temperature above which micelles disassemble into unimers due to decreasing solvent selectivity with increasing temperature [15,18]. Other important micelle characteristics include Z (aggregation number), R_g (radius of gyration), R_h (hydrodynamic radius) (or hydrodynamic diameter, D_h) and R_g/R_h (shape factor).[17]

Micelles are appealing for applications in fields such as colloid stabilization, drug delivery, coating and microreactor applications due to their stability and versatility and are characterised by various techniques [19–21]. These include techniques such as electron microscopy (SEM and TEM), atomic force microscopy (AFM), NMR, fluorescence spectroscopy, dynamic light scattering (DLS), static light scattering (SLS) and SEC [15,22,23]. For electron microscopy the sample is dried and only observed over a narrow scale range. Furthermore, although information regarding size and size distributions can be obtained, information regarding corona chemical composition cannot. AFM suffers from the shape and size of the micelles being affected by tip-convolution effects, specific interactions between the substrate the block copolymer or by the flattening of the micelles on the substrate while fluorescence spectroscopy is not suitable for routine use and care must be taken to avoid aggregation between the probe and unimers below the CMC [15,24].

DLS and SLS enables the analysis of analytes in solution but only information regarding size and size distributions can be obtained whereas NMR yields information regarding the average corona chemical composition but it cannot reveal any information regarding size and size distributions present in the sample. Lastly, SEC has been employed to characterize the unimer-micelle equilibrium and also to determine molecular weights of micelles [14,15]. However, several studies have shown that strong perturbation in the unimer-micelle equilibrium, disassembly of micelles, analyte trapping in the column and adsorption on the column packing occur during analysis [14,15].

Recently, flow field-flow fractionation (FlFFF) and asymmetric flow field-flow fractionation (AF4) have been used to characterize micelles and other self-assemblies, such as polymersomes, according to size, shape and molecular weight [22,23,25,26]. Moreover, it was demonstrated that in some instances only AF4 could reveal the presence of size distributions that were not observed by traditional techniques such as DLS [23,25]. In addition to AF4, ThFFF has also been shown to be a suitable technique for the analysis of micelles with different core compositions [27].

To date, the question whether it is possible to fractionate micelles based solely on differences in the tacticity of the corona has yet to be investigated. This is a pertinent question as anisotropic micelles with mixed corona compositions, such as patchy, multicompartment and Janus micelles, have attracted significant attention in recent years due to their unique morphologies and potential applications [28]. Moreover, these self-assemblies lack suitable analytical techniques to provide comprehensive information on both corona composition as well as on size and shape distributions [28].

In the present study, for the first time it is demonstrated that, in addition to determining important micelle characteristics such as size, shape and aggregation number as a function of temperature, ThFFF is capable of fractionating micelles based on differences in the tacticity of the corona. This study describes the application of ThFFF coupled online to ultraviolet (UV), multiangle laser light scattering (MALLS), differential refractive index (dRI) and dynamic light scattering (DLS) detectors to simultaneously determine changes in micelle characteristics such as R_g/R_h, D_h, R_g, Z, D_T and S_T as a function of temperature for PMMA-PS micelles with different corona tacticities.

2. Materials and methods

2.1. Materials

PMMA-PS block copolymers with different PMMA tacticities were purchased from Polymer Source Inc. (Montreal, Canada). HPLC grade acetonitrile (ACN) was purchased from Sigma–Aldrich (South Africa).

2.2. Micelle preparation

PMMA-PS block copolymers with high isotactic (iPMMA-PS) and high syndiotactic (sPMMA-PS) PMMA content were used to prepare micelles in ACN by both the co-solvent and nanoprecipitation methods reported in the Supplementary material [25,29]. ACN is a theta solvent for PMMA and a non-solvent for PS. Samples prepared by the nanoprecipitation method are indicated hereafter by the notation (N). Furthermore, micelle formation was confirmed by ^{1}H NMR as described in the literature [15,29].

2.3. Thermal field flow fractionation

The thermal FFF system TF2000 (Postnova Analytics, Landsberg, Germany) was coupled online to an UV (PN 3212 at 254 nm, Postnova Analytics), MALLS (PN 3070, Postnova Analytics), dRI (PN 3150, Postnova Analytics) and DLS detectors (Zen 1600, Malvern Instruments, Worcestershire, UK). The TF2000 channel had a tip-to-tip length of 45.6 cm, breadth of 2 cm, thickness of 127 μm and void volume of 1.14 mL. Carrier flow is generated by a isocratic pump (PN 1130, Postnova Analytics) and the samples are introduced into the channel via a Rheodyne manual injection valve. Values for S_T were calculated as shown in the introduction while values for D_T were calculated according to [1]:

$$D_T = \frac{6Dt_r}{\Delta T t^\circ}$$

Where t^o is the void time, t_r is the retention time of the sample and ΔT is the temperature difference between the hot and cold wall. D_h and D values were determined by DLS analysis. ACN was used as carrier liquid with a flow rate of 0.3 mL min^{-1} and a dn/dc value of 0.136 mL g^{-1} for PMMA in ACN was used for the micelles [10]. Samples were injected through a 100 μL capillary sample loop and triplicate analysis of each sample was performed under non-overloading sample concentrations.

2.4. ^{1}H NMR

The NMR experiments were conducted on a 400 MHz Varian Unity Inova spectrometer (Agilent/Varian, Palo Alto, California,

Table 1
Molecular weights and tacticities of the block copolymers. Tacticity was determined by ^{1}H NMR.

	Batch number	Molecular weight [kg mol^{-1}]			Tacticity content [mol %]		
		PS	PMMA	Total	Isotactic	Atactic	Syndiotactic
iPMMA-PS	P8805-SMMAiso	60	85	145	92.6	2.8	4.6
sPMMA-PS	P10474-SMMA	60	83	143	1.6	17.1	81.3

USA). The experimental details of ^{1}H NMR are summarised in the Supplementary material.

3. Results and discussion

iPMMA-PS and sPMMA-PS block copolymers with similar block sizes were selected to yield micelles of comparable sizes but different corona microstructures. The molecular weights of the respective block copolymers as well as the tacticity of the PMMA blocks are shown in Table 1.

The micelles were prepared by both the co-solvent and nanoprecipitation methods as the former yielded iPMMA-PS and sPMMA-PS micelles of significantly different sizes. The co-solvent method yielded iPMMA-PS and sPMMA-PS micelles with hydrodynamic diameters, D_h, of 123.7 ± 0.6 nm and 176 ± 0.9 nm, respectively. In contrast, the nanoprecipitation method yielded micelles of comparative sizes namely 133.4 ± 0.6 nm and 118.2 ± 0.2 nm for the iPMMA-PS and sPMMA-PS micelles, respectively. It has been shown that the preparation process can influence micelle characteristics such as size [30]. In order to determine if the preparation method also had an influence on the ThFFF retention behaviour, each of the four samples was analysed by ThFFF in ACN. Furthermore, offline DLS data were obtained that showed monodisperse unimodal patterns in all cases (Fig. S-1, Supplementary material).

The CMC values for each of the micelle samples are reported in Table 2. It was found that, irrespective of the preparation method, the sPMMA-PS micelles exhibit lower CMC values than the iPMMA-PS micelles. Furthermore, it can also be seen that the various preparation methods did not significantly influence the CMC values. CMC is determined graphically by a sharp change in D_h as a function of concentration while the CMT is determined graphically by a sharp change in D_h as a function of temperature.

The lower CMC values for the sPMMA-PS micelles are due to the less rigid syndiotactic PMMA molecules in the corona. It has been demonstrated by molecular dynamic calculations as well as by experimental data that syndiotactic PMMA is less rigid than isotactic PMMA [12,31]. Therefore, the difference in rigidity allows for the less rigid syndiotactic PMMA blocks to readily pack together in the corona and, therefore, form micelles at lower concentrations. These results demonstrate that the tacticity of a copolymer, and thus of the corona, can influence micelle stability. Similar results were obtained for amphiphilic poly(lactic acid)-block-poly(ethylene glycol) copolymers [32]. Also shown in Table 2 are the CMT values. The similar CMT values show that neither the tacticity content of the corona nor the preparation method influences the CMT.

In order to determine if the temperature has a permanent effect on micelle size that would influence ThFFF retention behaviour, the micelles were heated from 25 to 80 °C by 10 °C increments and subsequently cooled from 80 to 25 °C by 10 °C increments. Fig. 1 shows the superimposed offline DLS data for heating and cooling and it can be seen that a perfect overlap occurs indicating that no deviations in size were found for the micelles. Thus, temperature does not have a permanent effect on micelle size that could influence ThFFF retention behaviour.

Also shown in Fig. 1 are linear regression lines. The slopes of the regression lines indicate the rates at which the sizes of the micelles change with temperature. When comparing the slopes of the linear regression lines, it can be seen that the various micelles expand (upon heating) and contract (upon cooling) to different extents in response to temperature changes. Thus, the sPMMA-PS micelles (Fig. 1A and C) exhibit greater changes in size as a function of temperature than the iPMMA-PS micelles (Fig. 1B and D) as they exhibit larger values for the slopes. Therefore, the tacticity content of the corona influences the magnitude to which micelles expand and contract in response to temperature changes.

After determining the CMT values of the various micelles, several ThFFF conditions using increasing temperature gradients were selected for the analysis of the micelles. The conditions selected for the experiments are listed in Table 3. The analysis conditions are labelled by the notation $T_{\text{cold wall},\,\Delta T}$ where the first and second subscripts refer to the temperatures of the cold wall and the temperature gradient, respectively. Thus, $T_{19,\,10}$ refers to analysis conditions with a cold wall temperature of 19 °C and a temperature gradient of 10 °C.

The ThFFF conditions were chosen such that the micelle would experience increased retention while remaining intact up to $T_{21,\,25}$. At $T_{22,\,30}$ the micelles are expected to disassemble into unimers as the hot wall temperature exceeds the CMT.

3.1. ThFFF analysis of iPMMA-PS micelles

The iPMMA-PS micelles were subjected to ThFFF analysis at each of the analysis conditions listed in Table 3. Fig. 2 shows the superimposed UV, dRI and MALLS fractograms of each ThFFF condition.

Fig. 2A and B exhibit bimodal elution profiles that are characteristic for the unimers (and any other unretained low molecular weight molecules) that elute at 5–10 min and the micelles that elute at 15–40 min. The elution patterns clearly show that as the temperature gradient increases, the micelle retention time increases up to $T_{22,\,30}$ where no micelle peak is found in the various fractograms. This is most evident in the MALLS 90° fractogram where there is no micelle peak but a relatively large unimer peak at 5–10 min. The UV fractogram confirms that the peaks at 5–10 min correspond

Table 2
Critical micelle concentration (CMC) and critical micelle temperature (CMT) for the various micelles as determined from offline DLS data.

Micelle sample[a]	CMC [mg mL^{-1}]	CMT [°C]
iPMMA-PS	0.23 ± 0.01	48.4 ± 0.5
iPMMA-PS (N)	0.20 ± 0.02	48.5 ± 0.8
sPMMA-PS	0.11 ± 0.01	48.3 ± 0.7
sPMMA-PS (N)	0.09 ± 0.01	48.3 ± 1.0

[a] micelles prepared by the nanoprecipitation method are indicated by (N).

Table 3
Hot and cold wall temperatures as well as the temperature gradients used for the analysis of the PMMA-PS micelles.

Analysis condition [$T_{\text{cold wall},\,\Delta T}$]	Cold wall temperature [°C]	Hot wall temperature [°C]	ΔT [°C]
$T_{19,\,10}$	19.0 ± 0.1	29.4 ± 0.1	10.4 ± 0.1
$T_{20,\,15}$	19.7 ± 0.1	34.9 ± 0.2	15.2 ± 0.1
$T_{21,\,20}$	20.5 ± 0.2	40.9 ± 0.1	20.4 ± 0.1
$T_{21,\,25}$	21.3 ± 0.1	47.0 ± 0.1	25.7 ± 0.1
$T_{22,\,30}$	22.0 ± 0.1	53.6 ± 0.2	31.6 ± 0.1

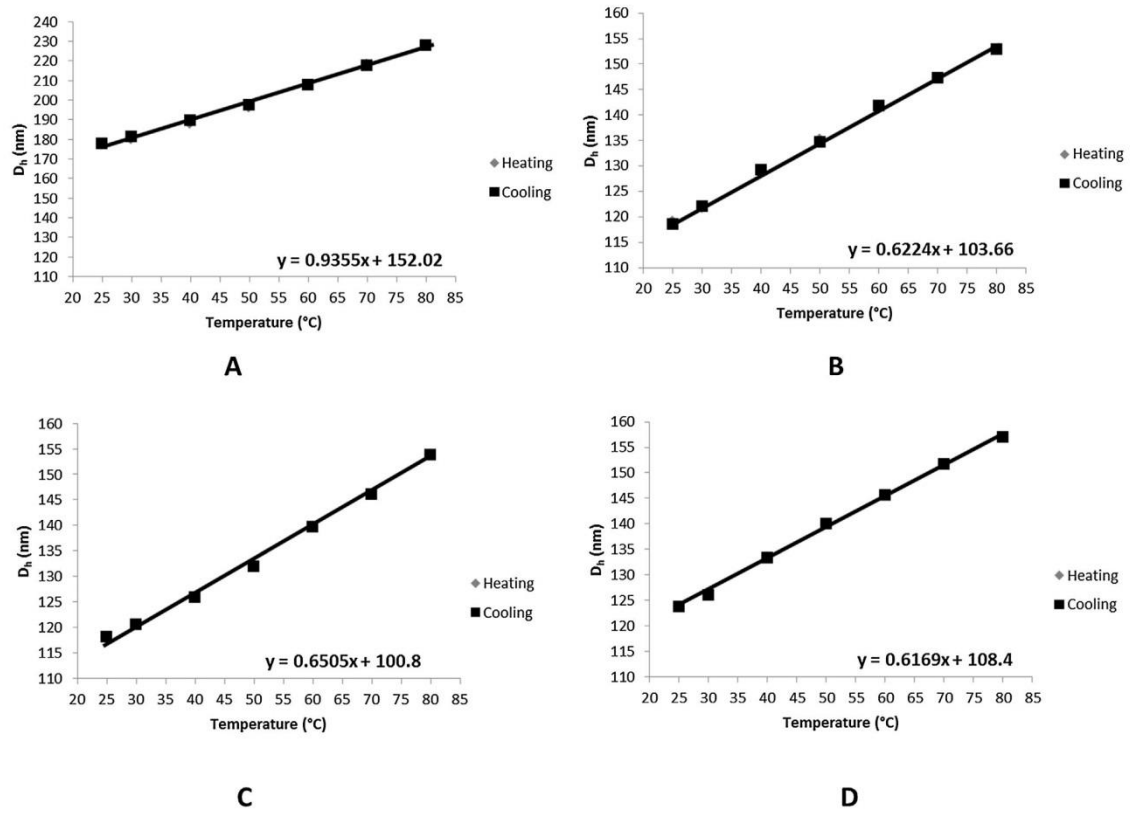

Fig. 1. Superimposed heating (diamonds) and cooling (squares) DLS data for the various micelles between 25 and 80 °C. (A) sPMMA-PS, (B) iPMMA-PS, (C) sPMMA-PS (N) and (D) iPMMA-PS (N). Linear regression lines are shown to aid interpretation of the data and to show general trends as a function of temperature.

to unretained low molecular weight molecules such as unimers. The relatively small micelle peaks in the UV and dRI fractograms are due to the use of low micelle concentrations in order to avoid self-aggregation of the PMMA coronas in ACN. ACN is a strongly complexing solvent for PMMA [33]. The UV fractograms collected at the various ThFFF conditions, showed that the size of the unimer peak increases from $T_{19,10}$ to $T_{20,15}$ where it remains constant until $T_{22,30}$. At $T_{22,30}$, the unimer peak reaches a maximum intensity which corresponds to the disassembly of micelles into unimers (Fig. S-2, Supplementary material).

In addition to the UV, MALLS and dRI fractograms, the DLS data also show an increase in retention time with increasing temperature gradient as well as the absences of a micelle peak at $T_{22,30}$ (Fig. S-3, Supplementary material). Furthermore, the D_h and D values determined from the DLS data are shown in Table 4 and it can be seen that D_h increases with increasing temperature while D decreases accordingly. The increase in D_h is expected. As the solvent selectivity decreases with increasing temperature the micelle core swells which, in turn, increases D_h.

In addition to the expected size increase, the micelles exhibit an unexpected decreasing trend in both D_T and S_T with increasing temperature gradient (Table 4). The decrease in S_T is primarily due to the decrease in D_T as D remains relatively constant with increasing temperature gradient. This trend in D_T appears to be unique to micelles as it has been shown that for polymers (high molecular weight polymers and aggregates), D_T is independent of molecular weight, channel hardware and the temperature gradient (at the same cold wall temperature).[1,34]

The Z and R_g/R_h values as a function of temperature are presented in Table 4 and it can be seen that Z increases with temperature from $T_{19,10}$ to $T_{21,20}$ whereafter it decreases from $T_{21,20}$ to $T_{21,25}$. The increase in Z as a function of temperature could be explained by the increased thermal motion of the copolymer molecules in the micelle which create space for the insertion of more unimers into the micelle. A similar trend in Z was observed with PEO-PPO micelles [35]. At $T_{21,25}$ the selectivity of the solvent has sufficiently decreased to shift the unimer-micelle equilibrium towards unimers, resulting in the decrease in Z. Additionally,

Table 4
Retention time (t_r), hydrodynamic diameter (D_h), diffusion (D), thermal diffusion (D_T), Soret (S_T) coefficients, aggregation number (Z) and shape factor (R_g/R_h) of iPMMA-PS micelles determined at various ThFFF conditions.

Analysis condition [$T_{cold\ wall}$, ΔT]	t_r [min]	D_h [nm]	D [10^{-7} cm^2 s^{-1}]	D_T [10^{-7} cm^2 s^{-1} K^{-1}]	S_T [K^{-1}]	Z	R_g/R_h
$T_{19,10}$	21.4 ± 0.2	120.1 ± 1.7	1.06 ± 0.01	2.45 ± 0.01	2.32 ± 0.01	676 ± 6	0.835
$T_{20,15}$	24.3 ± 0.3	124.0 ± 1.5	1.02 ± 0.02	1.78 ± 0.01	1.75 ± 0.01	752 ± 8	0.656
$T_{21,20}$	27.9 ± 0.7	126.1 ± 1.5	1.00 ± 0.02	1.57 ± 0.02	1.56 ± 0.01	765 ± 7	0.768
$T_{21,25}$	29.7 ± 0.5	131.0 ± 1.6	0.97 ± 0.01	1.26 ± 0.02	1.29 ± 0.01	693 ± 7	1.16

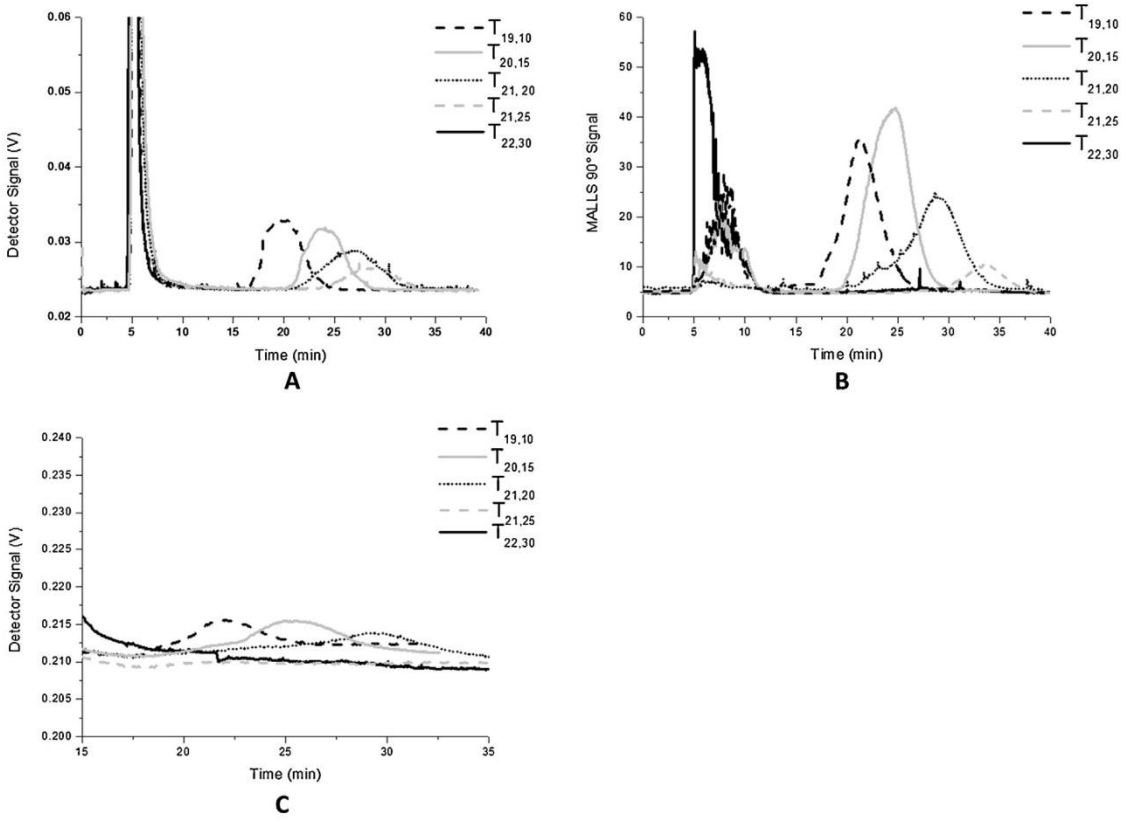

Fig. 2. Superimposed fractograms of iPMMA-PS micelles analysed under various ThFFF conditions. ThFFF conditions $T_{19,10}$, $T_{20,15}$, $T_{21,20}$, $T_{21,25}$ and $T_{22,30}$ are indicated as black, grey, red, green and blue (or as black dash, grey solid, black dotted, grey dash and black solid lines in black and white print), respectively. Detectors: UV (A), MALLS 90° (B) and dRI (C).

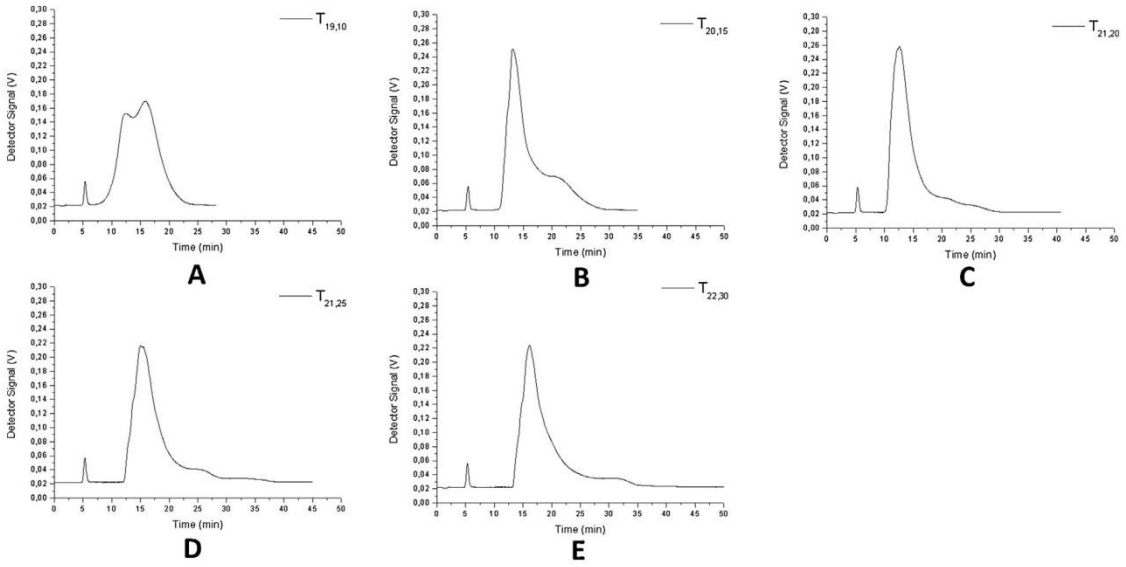

Fig. 3. UV fractograms of sPMMA-PS micelles analysed under various ThFFF conditions. (A) $T_{19,10}$, (B) $T_{20,15}$, (C) $T_{21,20}$, (D) $T_{21,25}$ and (E) $T_{22,30}$.

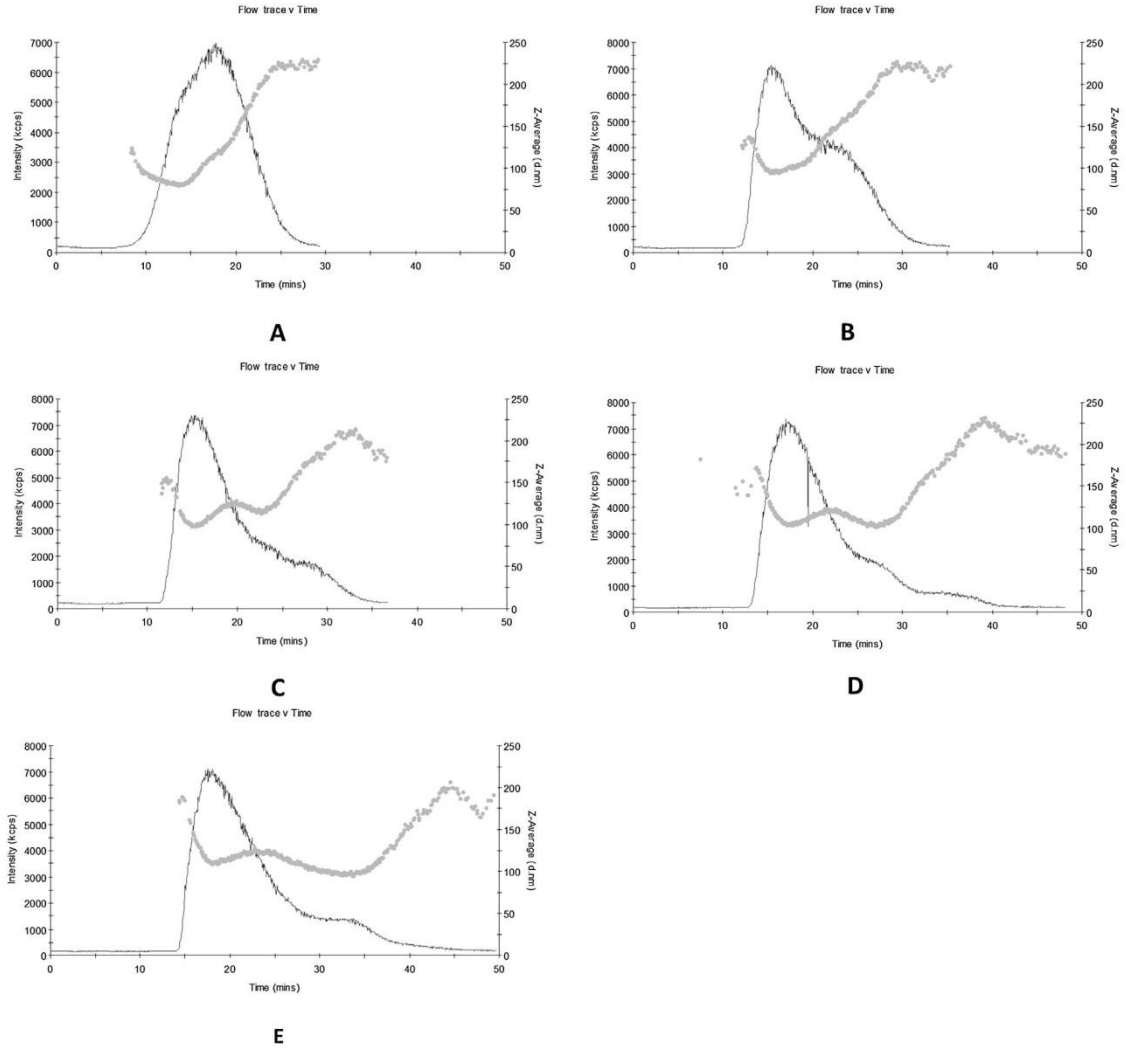

Fig. 4. DLS flow data of the sPMMA-PS micelles subjected to various ThFFF conditions. (A) $T_{19,10}$, (B) $T_{20,15}$, (C) $T_{21,20}$, (D) $T_{21,25}$ and (E) $T_{22,30}$. The dots represent the Z-average size (D_h) and the solid lines show the corresponding elution profile.

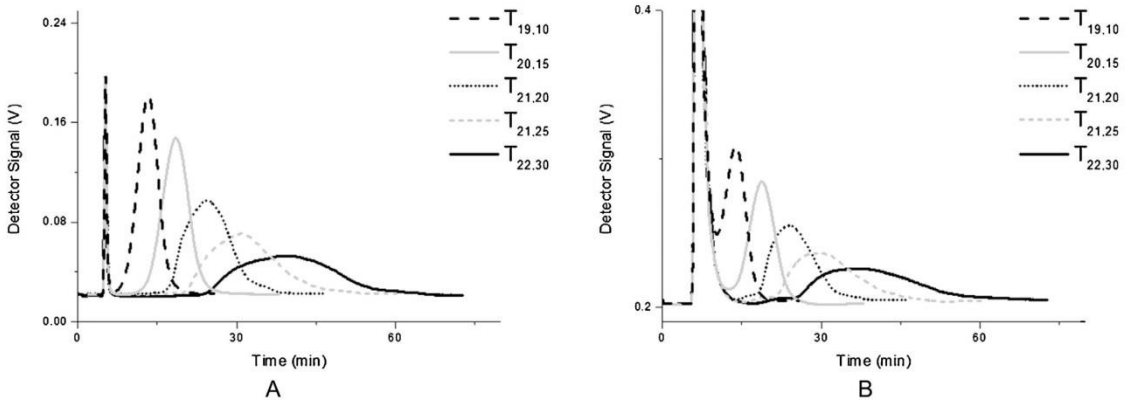

Fig. 5. Superimposed fractograms of sPMMA-PS (N) micelles analysed under various ThFFF conditions. ThFFF conditions $T_{19,10}$, $T_{20,15}$, $T_{21,20}$, $T_{21,25}$ and $T_{22,30}$ are indicated as black, grey, red, green and blue (or as black dash, grey solid, black dotted, grey dash and black solid lines in black and white print), respectively. Detectors: UV (A) and dRI (B).

Table 5
Retention time (t_r), hydrodynamic diameter (D_h), diffusion (D), thermal diffusion (D_T), Soret (S_T) coefficients, aggregation number (Z) and the shape factor (R_g/R_h) of sPMMA-PS micelles determined at various ThFFF conditions.

Analysis condition [$T_{cold\ wall}$, ΔT]	t_r [min]	D_h [nm]	D [10^{-7} cm^2 s^{-1}]	D_T [10^{-7} cm^2 s^{-1} K^{-1}]	S_T [K^{-1}]	Z	R_g/R_h
$T_{19,10}$	12.5 ± 0.1	120.7 ± 0.5	1.05 ± 0.04	1.44 ± 0.02	1.36 ± 0.01	338 ± 4	0.989
$T_{20,15}$	13.6 ± 0.1	125.3 ± 0.9	1.02 ± 0.06	1.01 ± 0.01	0.989 ± 0.016	256 ± 5	0.704
$T_{21,20}$	12.9 ± 0.1	121.0 ± 0.5	1.05 ± 0.04	0.738 ± 0.009	0.704 ± 0.009	326 ± 4	0.795
$T_{21,25}$	16.2 ± 0.2	120.0 ± 0.8	1.06 ± 0.07	0.751 ± 0.008	0.708 ± 0.009	484 ± 9	1.35
$T_{22,30}$	17.1 ± 0.4	118.7 ± 0.9	1.07 ± 0.08	0.667 ± 0.015	0.621 ± 0.017	340 ± 6	1.21

Table 6
Retention time (t_r), hydrodynamic diameter (D_h), diffusion (D), thermal diffusion (D_T), Soret (S_T) coefficients, aggregation number (Z) and the shape factor (R_g/R_h) of sPMMA-PS (N) micelles determined at various ThFFF conditions.

Analysis condition [$T_{cold\ wall}$, ΔT]	t_r [min]	D_h [nm]	D [10^{-7} cm^2 s^{-1}]	D_T [10^{-7} cm^2 s^{-1} K^{-1}]	S_T [K^{-1}]	Z	R_g/R_h
$T_{19,10}$	13.6 ± 0.2	90.8 ± 0.2	1.40 ± 0.02	2.02 ± 0.01	1.44 ± 0.01	111 ± 2	0.771
$T_{20,15}$	19.2 ± 0.3	93.4 ± 0.2	1.36 ± 0.01	1.83 ± 0.01	1.34 ± 0.01	114 ± 1	0.766
$T_{21,20}$	24.6 ± 0.2	98.5 ± 0.1	1.29 ± 0.02	1.64 ± 0.01	1.27 ± 0.02	162 ± 5	0.785
$T_{21,25}$	31.0 ± 0.5	103.3 ± 0.5	1.23 ± 0.05	1.56 ± 0.02	1.26 ± 0.01	279 ± 6	0.973
$T_{22,30}$	39.4 ± 0.5	105.6 ± 0.5	1.20 ± 0.05	1.28 ± 0.02	1.28 ± 0.02	358 ± 8	1.143

the shape factor yields information on the morphology of the self-assembly being characterised with values of 0.774 and 1.0 corresponding to micelles and vesicles, respectively [25]. Table 4 shows that from $T_{19,10}$ to $T_{21,20}$ the micellar structure is the predominant self-assembly after which it appears to change to vesicle. However, at $T_{21,25}$ the swollen micelles only resemble the shape of vesicles as an increase and not a decrease in Z would be associated with the transition from micelle to vesicle.

After the iPMMA-PS micelles were characterised by ThFFF, the iPMMA-PS (N) micelles were analysed. Despite having similar CMC and CMT values, the iPMMA-PS (N) micelles disassembled into unimers in the channel as only the void peak was observed (Figs. S-4 and S-5, Supplementary material). Therefore, the preparation method had a significant effect on micelle stability for ThFFF analysis.

3.2. ThFFF analysis of sPMMA-PS micelles

The sPMMA-PS micelles prepared by the co-solvent method were subjected to the various ThFFF conditions. Figs. 3 and 4 show the UV fractograms and DLS data at the different ThFFF conditions and it can be seen that the micelles exhibit various size distributions. These size distributions were not detected by offline DLS that, therefore, demonstrates that similar to AF4, ThFFF yields valuable information on size distributions that is not accessible by other more traditional analysis techniques. Furthermore, the size distributions change with increasing temperature. The same behavior is mirrored in the dRI (Fig. S-6, Supplementary material) and MALLS 90° fractograms (not shown). The UV fractograms show that the size of the void peak remains unchanged indicating that concentration of unimers present in the sample does not change with temperature. There is, therefore, no shift in the unimer-micelle equilibrium with increasing temperature (Fig. 3). The ThFFF data also show that the sPMMA-PS micelles remain intact during the analysis performed at $T_{22,30}$ which has a hot wall temperature of 53.6 ± 0.2 °C that is well above the CMC of 48.3 ± 0.7 °C.

Table 5 shows the micelles' characteristics collected at various ThFFF conditions and it was found that the sPMMA-PS micelles exhibit a similar decreasing trend in D_T as the iPMMA-PS micelles. Thus, the trend in D_T is not dependent on the tacticity of the corona. The disperse nature of the sample is also evident from the wide range of aggregation numbers and shape factors which do not exhibit a clear trend as a function of temperature.

The sPMMA-PS (N) micelles were sufficiently stable to be analysed by ThFFF. Fig. 5 shows the superimposed UV and dRI fractograms at each analysis condition. From Fig. 5, it can be seen that as the temperature gradient increases, retention increases accordingly. Moreover, the micelles remain intact during the analysis performed at $T_{22,30}$ which has a hot wall temperature of 53.6 ± 0.2 °C that is well above the CMC of 48.3 ± 1.0 °C. Fig. 5 also shows that the peaks broaden significantly with increasing temperature, thus revealing the presence of various size distributions in the sample. These size distributions were not detected by offline DLS. Furthermore, from the UV fractograms collected at the various ThFFF conditions, it was found that the size of the void peak remains constant from $T_{19,10}$ to $T_{22,30}$. (Fig. S-7, Supplementary material).

The size distributions, and their changes as a function of temperature, are illustrated in the DLS data. Fig. 6 shows the DLS data collected at the various ThFFF conditions and it can be seen that as the temperature increases, the two distinct size distributions become less prominent and more spread out. The dispersed nature of the sample is also observed in the MALLS 90° fractograms (not shown).

Table 6 shows the micelles' characteristics collected at various ThFFF conditions indicating that the sPMMA-PS (N) micelles

Table 7
Diffusion (D), thermal diffusion (D_T) and Soret (S_T) coefficients for the iPMMA-PS and sPMMA-PS micelles determined at various ThFFF conditions.

Analysis condition [$T_{cold\ wall}$, ΔT]	D [10^{-7} cm^2 s^{-1}]		D_T [10^{-7} cm^2 s^{-1} K^{-1}]		S_T [K^{-1}]	
	iPMMA-PS	sPMMA-PS	iPMMA-PS	sPMMA-PS	iPMMA-PS	sPMMA-PS
$T_{19,10}$	1.06 ± 0.01	1.05 ± 0.04	2.45 ± 0.01	1.44 ± 0.02	2.32 ± 0.01	1.36 ± 0.01
$T_{20,15}$	1.02 ± 0.02	1.02 ± 0.06	1.78 ± 0.01	1.01 ± 0.01	1.75 ± 0.01	0.989 ± 0.016
$T_{21,20}$	1.00 ± 0.02	1.05 ± 0.04	1.57 ± 0.02	0.738 ± 0.009	1.56 ± 0.01	0.704 ± 0.009
$T_{21,25}$	0.97 ± 0.01	1.06 ± 0.07	1.26 ± 0.02	0.751 ± 0.008	1.29 ± 0.01	0.708 ± 0.009

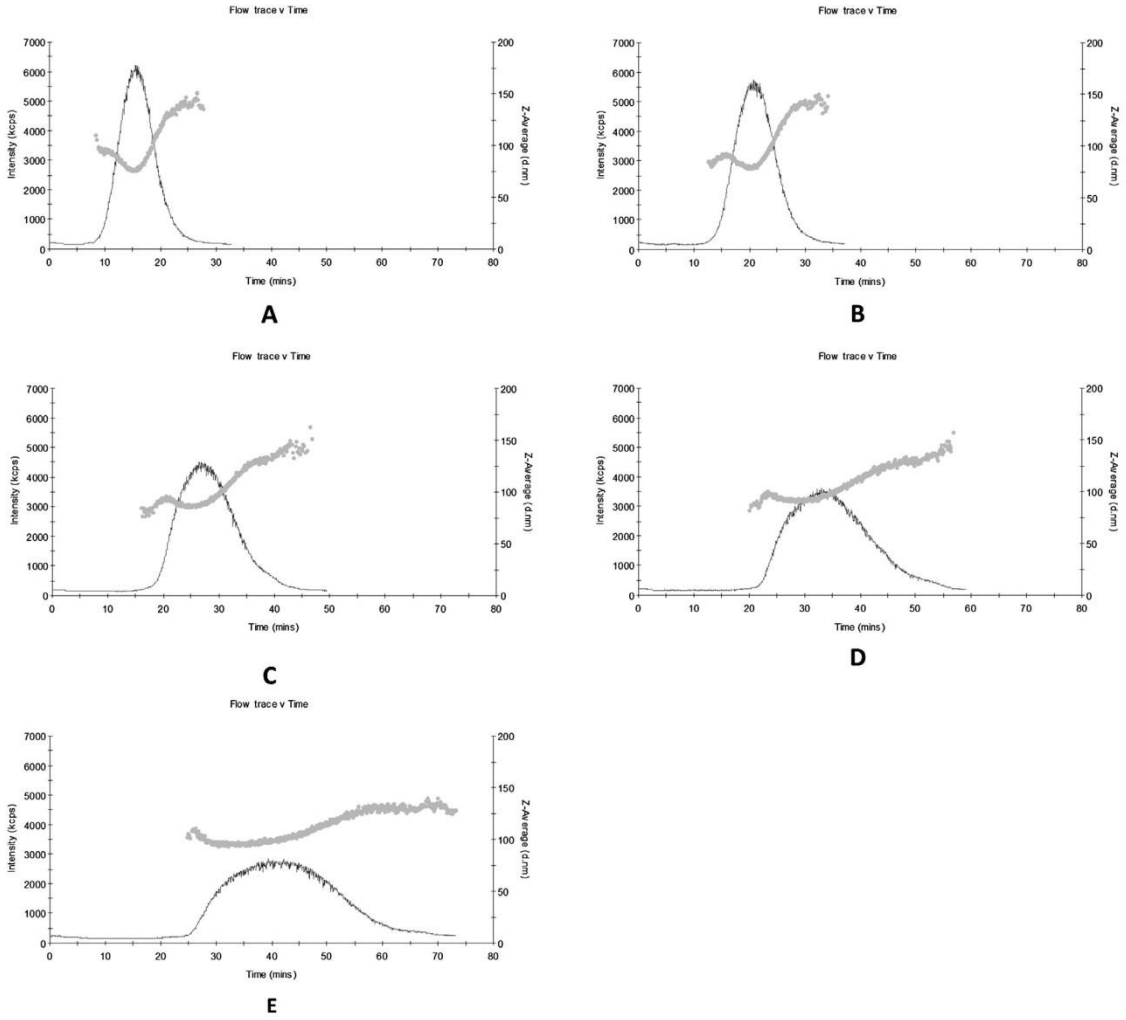

Fig. 6. DLS flow data of the sPMMA-PS (N) micelles subjected to various ThFFF conditions. (A) $T_{19,10}$, (B) $T_{20,15}$, (C) $T_{21,20}$, (D) $T_{21,25}$ and (E) $T_{22,30}$. The dots represent the Z-average size (D_h) and the solid lines show the corresponding elution profile.

exhibit similar trends in D_h, D_T and S_T as the iPMMA-PS and sPMMA-PS micelles. As expected, D_h increases with increasing temperature whereas D_T and S_T decrease with increasing temperature. Therefore, the unique decrease observed in D_T with increasing temperature gradient appears to be independent of the corona composition and the preparation method.

As seen with the iPMMA-PS micelles, the shape factor shows a micelle to vesicle transition with increasing temperature (Table 6). Moreover, the sPMMA-PS (N) micelles also show a significant increase in Z accompanying the change in shape factor. Therefore, in contrast to the iPMMA-PS micelles, the sPMMA-PS (N) micelles appear to reassemble into vesicles with increasing temperature.

In order to answer the question if ThFFF can fractionate micelles with regards to corona microstructure, the ThFFF data of the sPMMA-PS and iPMMA-PS micelles were compared. Table 7 lists the D_h, D, D_T, and S_T values for the sPMMA-PS and iPMMA-PS micelles at various ThFFF conditions.

Comparing the ThFFF data of the sPMMA-PS and iPMMA-PS micelles it can be seen that the S_T values of the micelles are different at each ThFFF condition. A difference in S_T is indicative of a possible separation. Moreover, a separation of the sPMMA-PS and iPMMA-PS micelles is based on the tacticity content of the corona as the micelles have similar D (and thus D_h) values. Fig. 7 shows the superimposed dRI fractograms of the sPMMA-PS and iPMMA-PS micelles. The dRI fractograms are drawn on a relative intensity scale as the injection concentration of the iPMMA-PS micelles was lower than that of the sPMMA-PS micelles. A lower injection concentration was used for the iPMMA-PS micelles to prevent aggregation.

Fig. 7 shows that a separation based on the tacticity content of the corona could be achieved under ThFFF conditions $T_{19,10}$, $T_{20,15}$ and $T_{21,20}$. Furthermore, the dispersed nature of the sPMMA-PS micelles should not influence the separation as the iPMMA-PS micelles elute after the shoulder of the sPMMA-PS micelle peak.

In light of these results, a blend of the sPMMA-PS and iPMMA-PS micelles was prepared in a 1:1 ratio. The mixture resulted in aggregations, irrespective of the ratio attempted. Furthermore, preparing 'mixed' micelles, where a single micelle consists of both sPMMA-PS and iPMMA-PS copolymers, also resulted in aggregation. The failed attempts to prepare 'mixed' and blended micelles are attributed to the stereocomplexation of the PMMA blocks in ACN.

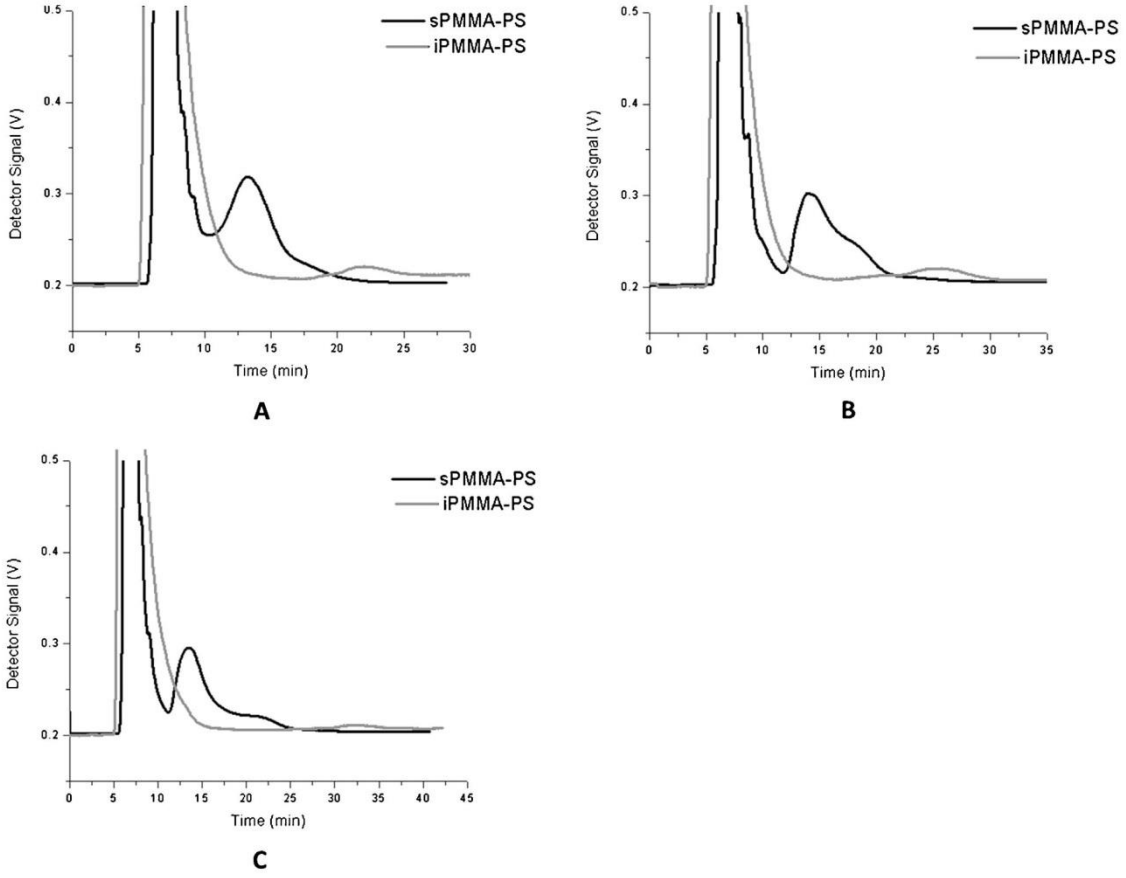

Fig. 7. Superimposed dRI fractograms of sPMMA-PS (black) and iPMMA-PS (red, as or grey in black and white print) micelles analysed under various ThFFF conditions. (A) $T_{19,10}$, (B) $T_{20,15}$ and (C) $T_{21,20}$.

4. Conclusions

PMMA-PS micelles with different corona tacticities were prepared by various methods. It was found that the tacticity of the corona not only influenced the CMC but also the extent to which micelles react to a temperature change. Furthermore, the CMT appeared to be unaffected by the tacticity of the corona. It has been shown that ThFFF coupled online to UV, MALLS, dRI and DLS detectors serve as a unique characterization platform to study and characterize dynamic self-assemblies such as micelles. The ThFFF multidetector setup can simultaneously determine important micelle characteristics such as D_h, Z, R_g, R_g/R_h, D, D_T and S_T as a function of temperature, from a single injection. It was also found that micelles exhibit a decreasing trend in D_T with increasing temperature gradient which is independent of the tacticity of the corona and the preparation method. Furthermore, ThFFF is able to yield valuable information regarding size distributions and morphology changes as a function of temperature which is not possible by other analysis techniques. It was also demonstrated that the capability of ThFFF to separate polymers with regards to tacticity can be extended to separate micelles based on the tacticity of the corona.

Appendix A. Supplementary data

Supplementary data associated with this article can be found, in the online version, at http://dx.doi.org/10.1016/j.chroma.2015.08.023.

References

[1] M.E. Schimpf, J.C. Giddings, K. Caldwell (Eds.), Field-Flow Fractionation Handbook, Wiley-Interscience, New York, 2000.
[2] F.A. Messaud, R.D. Sanderson, J.R. Runyon, T. Otte, H. Pasch, S.K.R. Williams, An overview on field-flow fractionation techniques and their applications in the separation and characterization of polymers, Prog. Polym. Sci. 34 (2009) 351–368, http://dx.doi.org/10.1016/j.progpolymsci.2008.11.001.
[3] C.A. Rue, M.E. Schimpf, Thermal diffusion in liquid mixtures and its effect on polymer retention in thermal field-flow fractionation, Anal. Chem. 66 (1994) 4054–4062, http://dx.doi.org/10.1021/ac00094a030.
[4] M.E. Schimpf, Characterization of polymers by thermal field-flow fractionation, J. Chromatogr. A 517 (1990) 405–421, http://dx.doi.org/10.1016/S0021-9673(01)95737-1.
[5] J.R. Runyon, S.K.R. Williams, Characterization of complex polymers using thermal field-flow fractionation coupled with online multiangle and dynamic light scattering and differential refractive index detection, Polym. Prepr. 52 (2011) 230–231.
[6] M.E. Schimpf, J.C. Giddings, Characterization of thermal diffusion of copolymers in solution by thermal field-flow fractionation, J. Polym. Sci. B Polym. Phys. 28 (1990) 2673–2680, http://dx.doi.org/10.1002/polb.1990.090281313.
[7] W. Hiller, W. van Aswegen, M. Hehn, H. Pasch, Online ThFFF–NMR: A novel tool for molar mass and chemical composition analysis of complex macromolecules, Macromolecules 46 (2013) 2544–2552, http://dx.doi.org/10.1021/ma400350y.
[8] P.M. Shiundu, J.C. Giddings, Influence of bulk and surface composition on the retention of colloidal particles in thermal field-flow fractionation, J. Chromatogr. A 715 (1995) 117–126, http://dx.doi.org/10.1016/0021-9673(95)00572-5.
[9] S. Kim Ratanathanawongs, P.M. Shiundu, J. Calvin Giddings, Size and compositional studies of core-shell latexes using flow and thermal field-flow fractionation, Colloids Surf. A Physiochem. Eng. Asp. 105 (1995) 243–250, http://dx.doi.org/10.1016/0927-7757(95)03315-7.

[10] D. Lee, S.K.R. Williams, Thermal field-flow fractionation and multiangle light scattering of polyvinyl acetate with broad polydispersity and ultrahigh molecular weight microgel components, J. Chromatogr. A 1217 (2010) 1667–1673, http://dx.doi.org/10.1016/j.chroma.2010.01.035.
[11] S. Lee, A. Molnar, Determination of molecular weight and gel content of natural rubber using thermal field-flow fractionation, Macromolecules 28 (1995) 6354–6356, http://pubs.acs.org/doi/abs/10.1021/ma00122a050 (accessed August 12, 2014).
[12] G. Greyling, H. Pasch, Tacticity separation of poly(methyl methacrylate) by multidetector thermal field-flow fractionation, Anal. Chem. 87 (2015) 3011–3018, http://dx.doi.org/10.1021/ac504651p.
[13] G. Greyling, H. Pasch, Multidetector thermal field-flow fractionation as a novel tool for the microstructure separation of polyisoprene and polybutadiene, Macromol. Rapid Commun. 35 (2014) 1846–1851, http://dx.doi.org/10.1002/marc.201400405.
[14] Z. Grubišć-Gallot, Y. Gallot, J. Sedláček, Study of polystyrene-block-poly(methyl methacrylate) micelles by size exclusion chromatography/low-angle laser light scattering, 1. Influence of copolymer concentration and flow rate, Macromol. Chem. Phys. 195 (1994) 781–791, http://dx.doi.org/10.1002/macp.1994.021950234.
[15] J.-F. Gohy, Block copolymer micelles, in: V. Abetz (Ed.), Block Copolym. II, Springer-Verlag, Berlin/Heidelberg, 2005, pp. 65–136, http://dx.doi.org/10.1007/12_048.
[16] I. Larue, M. Adam, M. Pitsikalis, N. Hadjichristidis, M. Rubinstein, S.S. Sheiko, Reversible morphological transitions of polystyrene- b -polyisoprene micelles, Macromolecules 39 (2006) 309–314, http://dx.doi.org/10.1021/ma051548z.
[17] G. Riess, Micellization of block copolymers, Prog. Polym. Sci. 28 (2003) 1107–1170, http://dx.doi.org/10.1016/S0079-6700(03)00015-7.
[18] J. Bang, K. Viswanathan, T.P. Lodge, M.J. Park, K. Char, Temperature-dependent micellar structures in poly(styrene-b-isoprene) diblock copolymer solutions near the critical micelle temperature, J. Chem. Phys. 121 (2004) 11489–11500, http://dx.doi.org/10.1063/1.1812753.
[19] S. Pispas, N. Hadjichristidis, I. Potemkin, A. Khokhlov, Effect of architecture on the micellization properties of block copolymers: A 2 B Miktoarm Stars vs AB Diblocks, Macromolecules 33 (2000) 1741–1746, http://dx.doi.org/10.1021/ma991636h.
[20] S.C. Owen, D.P.Y. Chan, M.S. Shoichet, Polymeric micelle stability, Nano Today 7 (2012) 53–65, http://dx.doi.org/10.1016/j.nantod.2012.01.002.
[21] A.B. Ebrahim Attia, Z.Y. Ong, J.L. Hedrick, P.P. Lee, P.L.R. Ee, P.T. Hammond, et al., Mixed micelles self-assembled from block copolymers for drug delivery, Curr. Opin. Colloid Interface Sci. 16 (2011) 182–194, http://dx.doi.org/10.1016/j.cocis.2010.10.003.
[22] M.A. Awan, V.L. Dimonie, Solution properties of diblock copolymers of polystyrene- block -polybutadiene, Langmuir 13 (1997) 140–146.
[23] J. Ehrhart, A.-F. Mingotaud, F. Violleau, Asymmetrical flow field-flow fractionation with multi-angle light scattering and quasi elastic light scattering for characterization of poly(ethyleneglycol-b-ε-caprolactone) block copolymer self-assemblies used as drug carriers for photodynamic therapy, J. Chromatogr. A 1218 (2011) 4249–4256, http://dx.doi.org/10.1016/j.chroma.2011.01.048.
[24] Ö. Topel, B.A. Çakır, L. Budama, N. Hoda, Determination of critical micelle concentration of polybutadiene-block-poly(ethyleneoxide) diblock copolymer by fluorescence spectroscopy and dynamic light scattering, J. Mol. Liq. 177 (2013) 40–43, http://dx.doi.org/10.1016/j.molliq.2012.10.013.
[25] U. Till, M. Gaucher-Delmas, P. Saint-Aguet, G. Hamon, J. Marty, C. Chassenieux, et al., Asymmetrical flow field-flow fractionation with multi-angle light scattering and quasi-elastic light scattering for characterization of polymersomes: comparison with classical techniques, Anal. Bioanal. Chem. 406 (2014) 7841–7853, http://dx.doi.org/10.1007/s00216-014-7891-8.
[26] A. Zattoni, B. Roda, F. Borghi, V. Marassi, P. Reschiglian, Flow field-flow fractionation for the analysis of nanoparticles used in drug delivery, J. Pharm. Biomed. Anal. 87 (2014) 53–61, http://dx.doi.org/10.1016/j.jpba.2013.08.018.
[27] M. Antonietti, A. Briel, C. Tank, Chromatographic characterization of complex polymer systems with thermal field-flow fractionation, Acta Polym. 46 (1995) 254–260, http://dx.doi.org/10.1002/actp.1995.010460307.
[28] J. Du, R.K. O'Reilly, Anisotropic particles with patchy, multicompartment and Janus architectures: preparation and application., Chem, Soc. Rev. 40 (2011) 2402–2416, http://dx.doi.org/10.1039/C0CS00216J.
[29] L. Oranli, P. Bahadur, G. Riess, Hydrodynamic studies on micellar solutions of styrene-butadiene block copolymers in selective solvents, Can. J. Chem. 63 (1985) 2691–2696.
[30] V.K. Mourya, N. Inamdar, R.B. Nawale, S.S. Kulthe, Polymeric micelles: General considerations and their applications, Indian J. Pharm. Educ. Res. 45 (2011) 128–138.
[31] U. Apel, R. Hentschke, J. Helfrich, Molecular dynamics simulation of syndio-and isotactic poly (methyl methacrylate) in benzene, Macromolecules 28 (1995) 1778–1785.
[32] C. Agatemor, M.P. Shaver, Tacticity-induced changes in the micellization and degradation properties of poly(lactic acid)- block -poly(ethylene glycol) copolymers, Biomacromolecules 14 (2013) 699–708, http://dx.doi.org/10.1021/bm400060x.
[33] G. Wypych, Handbook of Solvents, ChemTec Publishing, Toronto-New York, 2001.
[34] J.R. Runyon, S.K.R. Williams, Composition and molecular weight analysis of styrene-acrylic copolymers using thermal field-flow fractionation, J. Chromatogr. A 1218 (2011) 6774–6779, http://dx.doi.org/10.1016/j.chroma.2011.07.076.
[35] P. Alexandridis, T. Alan Hatton, Poly(ethylene oxide)-poly(propylene oxide)-poly(ethylene oxide) block copolymer surfactants in aqueous solutions and at interfaces: thermodynamics, structure, dynamics, and modeling, Colloids Surf. A Physicochem. Eng. Asp. 96 (1995) 1–46, http://dx.doi.org/10.1016/0927-7757(94)03028-X.

4.3 Characterisation of Mixed Micelle Formation

G. Greyling, H. Pasch, *Angew. Chemie Int. Ed.* **2015**, Submitted.

The third part of this study describes the characterisation and separation of polybutadiene-polystyrene (PB-PS) micelles with 1,2-polybutadiene and 1,4-polybutadiene coronas according to corona composition as well as the characterisation of mixed micelles formation in terms of size, molecular weight and composition.

PB-PS micelles with 1,2-polybutadiene (1,2 PB-PS) and 1,4-polybutadiene (1,4 PB-PS) coronas were prepared in heptane. The various PB-PS micelles were each characterised by ThFFF under similar conditions of increasing temperature gradient used for the PMMA-PS micelles. When the ThFFF data of the various PB-PS micelles were compared, it was found that a separation according to corona composition could be possible. Thus, in order to determine if the micelles could be separated, a 1:1 blend of the 1,4 and 1,2 PB-PS micelles was analysed by ThFFF with a temperature gradient of $\Delta T = 30$ degrees and it was clearly demonstrated that ThFFF can indeed separate micelles according to corona composition. The separation was also subsequently proven by ^{1}H NMR.

After successfully demonstrating that ThFFF can separate micelles based on corona composition, the characterisation of mixed micelle formation in terms of size, molecular weight, chemical composition and their respective distributions was addressed. Consequently, a 1:1 blend of the 1,4 and 1,2 PB-PS micelles was prepared and analysed at various time intervals over a period of a week. The various fractograms showed a decrease in the 1,4 PB-PS micelles content with an increase in the mixed micelle content. However, trends in the 1,2 PB-PS micelles content

could not be determined as the 1,2 PB-PS and mixed micelles were shown to coelute. The various fractograms also showed that after a week virtually all the 1,4 PB-PS micelles were reassembled into mixed micelles. Moreover, trends in the size and molecular weight data agreed with the observed changes in micelle peak intensities and also revealed changes in several distributions as a function of time.

Furthermore, chemical composition information was obtained by a novel approach of coupling ThFFF to FTIR via a LC-Transform. This method enabled the determination of chemical composition as a function of elution time and it was found that the FTIR data correlated well with the changes in size and molecular weight distributions.

These results demonstrated that ThFFF is an unique characterisation platform which is capable of fractionating micelles according to corona composition while simultaneously providing comprehensive information on important micelle characteristics such as size, molecular weight, chemical composition as well as their respective distributions, from a single injection.

COMMUNICATION WILEY-VCH

Separation and Characterization of Mixed Micelles by Multidetector Thermal Field-Flow Fractionation

Guilaume Greyling and Harald Pasch *

Abstract: Polymeric micelles have attracted much attention as a versatile platform that can readily be modified for a wide range of applications. However, current analytical techniques are not suitable to provide comprehensive information regarding size, molar mass, chemical composition and their respective distributions. It is shown by the analysis of polybutadiene-polystyrene micelles with various corona compositions that, in contrast to current techniques, multidetector thermal field-flow fractionation (ThFFF) is capable of separating micelles according to corona composition while providing comprehensive information on important micelle characteristics such as size, molar mass, chemical composition as well as their respective distributions from a single injection. Moreover, it is shown that ThFFF is a suitable technique to monitor the formation of mixed micelles in terms of size, molar mass, chemical composition and their respective distributions.

The ability of block copolymers to self-assemble into various nanostructures, such as micelles, when dissolved in a selective solvent, i.e. a good solvent for one of the blocks but a precipitant for the other, has attracted much attention as polymeric micelles provide a versatile platform that can readily be modified for a wide range of applications.[1–3] Block copolymer micelles consist of a core formed by the insoluble block and a corona formed by the soluble block.[4] Micelles are appealing for applications in fields such as colloid stabilization, microreactor, drug delivery and biomedical applications due to their stability, versatility and relative ease of preparation.[2–5] Furthermore, micelles containing two or more different copolymers and thus mixed compositions, i.e. mixed micelles, have attracted significant attention in recent years as a convenient method to improve micelle stability and prepare micelles with unique morphologies and properties.[5,6] Moreover, mixed micelles enable the incorporation of various functionalities without the synthetic challenge of preparing a single copolymer with the desired functionalities.[5]

To successfully utilize micelles, these nanostructures must be comprehensively characterized in terms of size, aggregation number, morphology, corona composition and molar mass.[3,5] In addition, determining particle size (PSD), molar mass (MMD) and corona composition (CCD) distributions are of great importance as these parameters significantly influence applications.[5,7] However, current characterization techniques such as electron microscopy (SEM and TEM), atomic force microscopy and dynamic and static light scattering are suitable to determine particle size and PSD but not molar mass, chemical composition or their respective distributions.[8] Furthermore, although corona composition and number average molar mass can be probed by NMR and fluorescence spectroscopy, these techniques yield no information regarding their distributions.[6,9,10] Moreover, the suitability of current techniques diminishes for samples exhibiting complex or multiple size, molar mass or composition distributions.[7] Consequently, a method to directly determine size, PSD, molar mass, MMD and CCD is highly desirable.[6,8]

To this end, techniques such as field-flow fractionation (FFF) and size exclusion chromatography (SEC) have been used to separate and characterize micelles. However, SEC showed analyte trapping in the column, disassembly of micelles and adsorption on the column packing occurring during analysis.[4,11] On the other hand, FFF subtechniques such as flow field-flow fractionation (FlFFF), asymmetric flow field-flow fractionation (AF4) and thermal field-flow fractionation (ThFFF) have been shown to be suitable techniques for the characterization of self-assemblies such as micelles.[7,12,13] It was shown that FlFFF, AF4 and ThFFF can determine size, PSD, morphology, molar mass and MMD of micelles and other self-assemblies, such as polymersomes, and that they can reveal size distributions not observed by traditional techniques such as DLS.[7,12,13] However, although FlFFF, AF4 and ThFFF can all separate analytes according to size, only ThFFF can additionally separate analytes according to chemical composition.[14–16]

In ThFFF a temperature gradient is applied across an open, ribbon-like channel to separate analytes according to size, microstructure or chemical composition.[14,17–19] The temperature gradient induces analytes to migrate from the hot to the cold wall of the channel. This temperature induced migration is characterized by the thermal diffusion coefficient, D_T, which is independent of the size of the analytes but dependent on the chemical nature of the analytes and the solvent.[14,16] Opposing D_T is normal diffusion which is the concentration induced migration of analytes away from the cold wall towards the center of the channel. Normal diffusion is characterized by the normal diffusion coefficient, D, which is dependent on the size of the analytes in solution.[14–16] Retention in ThFFF is determined by the interplay between D_T and D and therefore, ThFFF is able to separate analytes according to size (D) and chemical composition (D_T).[14,15,20] For interested readers, more in-depth explanations on retention in ThFFF can be found in various publications.[14,15,17,20]

The lack of stationary phase, relatively gentle separation conditions and the capability to separate analytes according to chemical composition makes ThFFF a suitable technique for the

[*] Prof. H. Pasch
Department of Chemistry and Polymer Science
University of Stellenbosch
Private bag X1, 7602, Matieland
E-mail: hpasch@sun.ac.za
G. Greyling
Department of Chemistry and Polymer Science
University of Stellenbosch
Private bag X1, 7602, Matieland

Supporting information for this article is given via a link at the end of the document.

characterization of self-assemblies such as micelles. Indeed, previous work on poly(methyl methacrylate)-polystyrene (PMMA-PS) micelles with different corona compositions showed that ThFFF could, in addition to determining important micelle characteristics, potentially separate micelles based on corona composition.[12] However, due to aggregation, separation was not experimentally achieved.

This study shows, for the first time, that ThFFF is capable of separating micelles based on corona composition. Moreover, it will be shown that the formation of mixed micelles can be monitored and characterized in terms of size, PSD, molar mass, MMD and CCD. This study describes the application of ThFFF coupled online to ultraviolet (UV), multiangle laser light scattering (MALLS), differential refractive index (dRI), dynamic light scattering (DLS) and FTIR (via LC transform approach) detectors to separate and determine size, PSD, molar mass, MMD and CCD for polybutadiene-polystyrene (PB-PS) micelles with various corona compositions.

PB-PS block copolymers with high 1,4-PB (1,4 PB-PS) and high 1,2-PB (1,2 PB-PS) isomeric content were used to prepare micelles with different corona compositions in heptane (Supporting Information). In addition to the 1,4 and 1,2 PB-PS micelles, mixed PB-PS micelles with mixed corona compositions were also prepared for comparison. The various PB-PS micelles were each characterized by ThFFF under similar conditions previously used for PMMA-PS micelles and the results are reported in the Supporting Information.[12]

Comparing the ThFFF data of the various PB-PS micelles, it can be seen that a separation according to corona composition could be possible as the superimposed fractograms in Figure 1 A shows a significant difference in the retention behaviors of the 1,4 and 1,2 PB-PS micelles with a temperature gradient of 30 °C. Furthermore, Figure 1 A also shows that the 1,2 and mixed PB-PS micelles exhibit similar retention behaviors and would co-elute. In order to determine if a separation can be achieved, a 1:1 blend of the 1,4 and 1,2 PB-PS micelles was analyzed by ThFFF with a temperature gradient of 30 °C and the resulting bimodal elution profile shown in Figure 1 B shows that ThFFF can separated micelles according to corona composition.

Moreover, the micelle blend was fractionated into five fractions which were subsequently sent for ^{1}H NMR analysis. The NMR data showed that the 1,4-PB isomer content decreased across the elution profile while the 1,2-PB isomer content increased. These trends in PB isomer content correlate well with the ThFFF retention data, thus further demonstrating that a separation according to corona composition is indeed achieved.

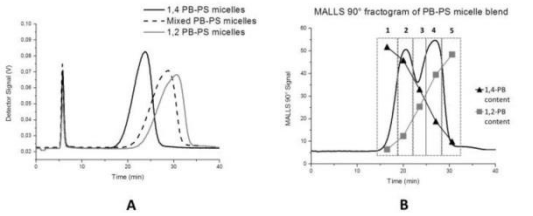

Figure 1. A) Superimposed UV fractograms of the 1,4 PB-PS (black line), 1,2 PB-PS (grey line) and mixed PB-PS micelles (black dashes). B) Fractionation of the micelle blend by ThFFF in heptane for ^{1}H NMR analysis. General trends in the 1,4-PB (triangle) and 1,2-PB (square) content are superimposed on the MALLS 90° fractogram.

After determining that ThFFF can separate micelles based on corona composition, the question whether ThFFF could monitor the formation of mixed micelles, as well as the accompanying changes in size, PSD, molar mass, MMD and CCD, was addressed. Consequently, a 1:1 micelle blend of the 1,4 and 1,2 PB-PS micelles was prepared and analyzed by ThFFF at various time intervals of T = 0, 2, 12 and 24 hours as well as at T = 1 week.

Figure 2 shows the UV fractograms of the micelle blend collected at the various time intervals. For clarity, the first peak in the bimodal elution profile will be referred to as the 1,4 PB-PS peak while the second peak will be referred to as the mPB-PS peak. This notation is used as Figure 1 A shows that the 1,2 and mixed PB-PS micelles co-elute. Thus, the mPB-PS peak contains both 1,2 and mixed PB-PS micelles.

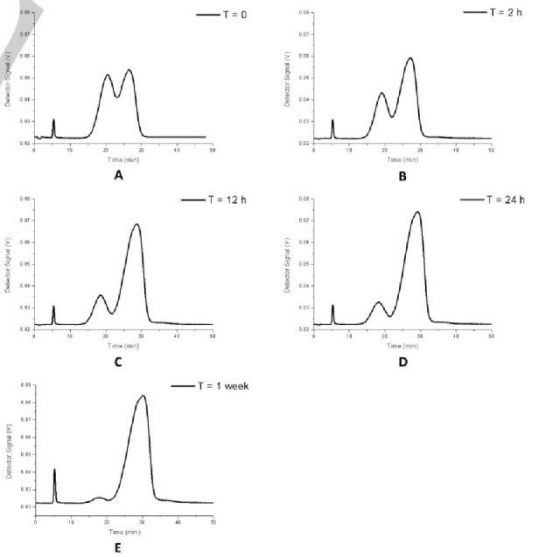

Figure 2. UV fractograms of the micelle blend taken at various time intervals. A) T = 0, B) T = 2 h, C) T = 12 h, D) T = 24 h and E) T = 1 week.

Figure 2 shows that, as expected, the 1,4 PB-PS peak intensity decreases while the mPB-PS peak intensity increase as a function of time. Moreover, Figure 1 E shows that after a week almost all of the 1,4 PB-PS micelles have reassembled into mixed micelles.

Figure 3 shows the MALLS 90° fractograms of the micelle blend at the various time intervals and as expected, the 1,4 PB-PS peak intensity decreases as a function of time while the mPB-PS peak intensity increases. Thus, there is a mass transport from the 1,4 PB-PS peak to the mPB-PS peak which is indicative of the formation of mixed micelles. Moreover, Figure 3 E also shows that after a week almost all the 1,4 PB-PS micelles have reassembled into mixed micelles.

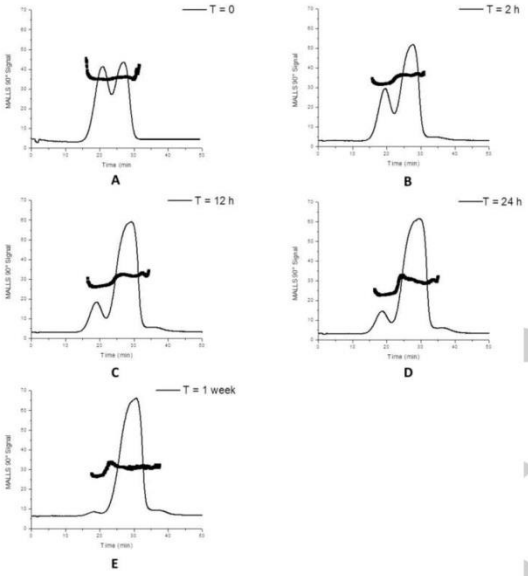

Figure 3. MALLS 90° fractograms of the micelle blend taken at various time intervals. A) T = 0, B) T = 2 h, C) T = 12 h, D) T = 24 h and E) T = 1 week. Also shown are the superimposed molar mass distributions.

Also shown in Figure 3 are the superimposed MMD at each time interval. Figure 3 shows that at T = 0 a relatively uniform size distribution is obtained which is as expected as the 1,4 and 1,2 PB-PS micelles exhibit relatively similar molar masses of 8732 and 8974 kg mol^{-1} respectively. Moreover, from T = 2 h to T = 1 week several size distributions become more evident which show that the 1,4 PB-PS and mPB-PS peaks contain micelles of various sizes. Additionally, the molar mass values for the 1,4 PB-PS peak show a decreasing trend in molar mass while the mPB-PS peak show an increasing trend in molar mass as a function of time, as expected (Table S2 in the Supporting Information).

Figure 4 shows the online DLS data collected at the various time intervals and it can be seen that multiple size distributions become more evident as a function of time. These results correlate well with the MMD data obtained from MALLS.

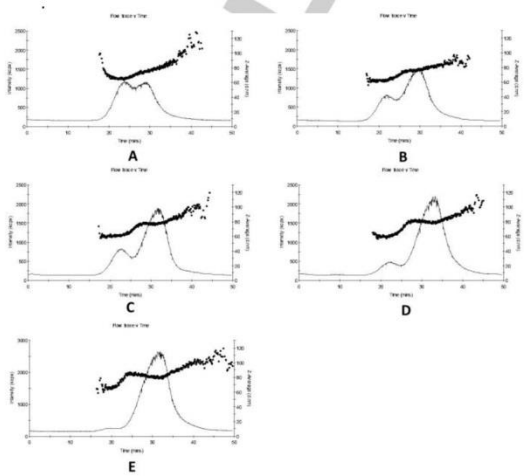

Figure 4. Online DLS data of the micelle blend taken at various time intervals. A) T = 0, B) T = 2 h, C) T = 12 h, D) T = 24 h and E) T = 1 week. The dots represent the Z-average size (D_h) and the solid lines show the corresponding elution profile.

Table 1 shows the various sizes of the 1,4 PB-PS and mPB-PS peaks as determined from the online DLS data. Table 1 clearly shows that the micelles in the 1,4 PB-PS peak decrease in size as a function of time while the micelles in the mPB-PS peak increase in size. This correlates well with the trends seen in the molar mass data obtained from MALLS (Supporting Information).

Also shown in Table 1 are the aggregation number (Z) and shape factor (R_g/R_h) of the 1,4 PB-PS and mPB-PS peaks as a function of time. Z is an indication of the number of copolymer molecules in the micelles while the R_g/R_h yields information on morphology with values of 0.774 and 1.0 corresponding to micelles and vesicles, respectively.[21] Table 1 shows that the 1,4 PB-PS peak exhibits a decreasing trend in Z while the mPB-PS exhibit an increasing trend in Z as a function of time. Furthermore, the R_g/R_h values show that the predominant self-assembly in the 1,4 PB-PS peak is micelle at each time interval whereas the predominant self-assembly in the mPB-PS peak changes from micelle to vesicle as a function of time.

Table 1. Hydrodynamic diameter (D_h), aggregation number (Z) and shape factor (R_g/R_h) of the 1,4 PB-PS and mPB-PS peaks in the blend.

Time interval [hours]	D_h [nm]		Z		R_g/R_h	
	1,4 PB-PS	mPB-PS	1,4 PB-PS	mPB-PS	1,4 PB-PS	mPB-PS
0	67.6 ± 0.9	78.6 ± 0.7	146 ± 5	103 ± 3	0.789	0.636
2	64.2 ± 0.8	78.2 ± 0.9	126 ± 4	117 ± 4	0.872	0.931
12	61.7 ± 1.2	77.7 ± 0.9	114 ± 6	120 ± 2	0.810	1.18
24	59.6 ± 0.5	80.1 ± 1.3	108 ± 4	134 ± 5	0.851	1.57
1 week	56.1 ± 0.8	82.2 ± 0.8	102 ± 2	143 ± 3	0.877	1.83

After determining size, PSD, molar mass and MMD, the CCD of the micelle blend was determined by ThFFF coupled to FTIR via a LC transform approach. Using the LC transform approach, composition as a function of retention time can be determined by monitoring the specific wavenumbers for the 1,4- and 1,2-PB isomers at 966 cm^{-1} and 912 cm^{-1}, respectively.[22] Thus, monitoring the PB isomer content as a function of retention time gives direct information regarding the corona composition of the eluting analyte and CCD.

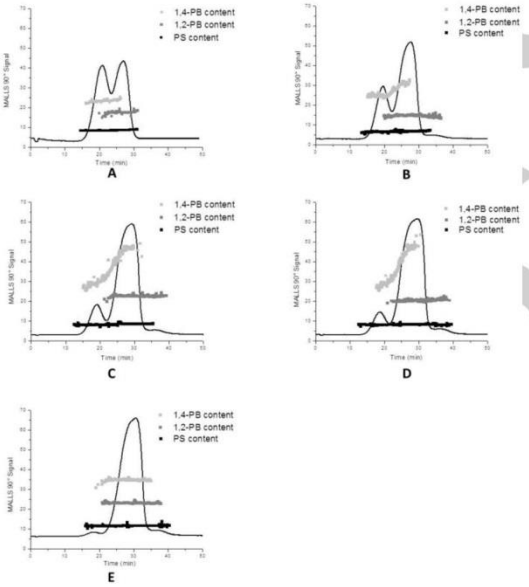

Figure 5. Changes in the FTIR signal intensities of the 1,4-PB (light grey) and 1,2-PB (dark grey) isomers as well as of polystyrene (black) across the elution profile of the micelle blend at various time intervals. A) T = 0, B) T = 2 h, C) T = 12 h, D) T = 24 h and E) T = 1 week. The FTIR signal intensities for the 1,4- and 1,2-PB isomers are show relative to the FTIR signal intensity of polystyrene.

Figure 5 shows the FTIR data collected at the various time intervals and it can be seen that the 1,4- and 1,2-PB isomer distributions remain relatively uniform at T = 0, which correlates well with the previous results. Furthermore, Figure 5 B – D show that the 1,4-PB isomer content increases across the elution profile while the 1,2-PB isomer content remains relatively constant. This shows that the 1,4 PB-PS micelles are reassembling into mixed micelles which elute at longer retention times. Figure 5 B – D also show that the formation of mixed micelles is more prominent as a function of time, which is as expected. Furthermore, Figure 5 E shows that after a week the 1,4-PB content is concentrated in the mPB-PS peak. Thus, as seen from the UV, MALLS and DLS data, practically all of the 1,4 PB-PS micelles have been reassembled into mixed micelles after a week.

It was shown by the analysis of PB-PS micelles with various coronas compositions that, to date, multidetector ThFFF is the only characterization platform which is capable of separating micelles according to corona composition while providing comprehensive information on important micelle characteristics such as size, molar mass, corona composition as well as their respective distributions, from a single injection.

Experimental Section

See Supporting Information

Keywords: Micelles • Block copolymers • Thermal Field-Flow Fractionation • Thermal diffusion

[1] A. Blanazs, S. P. Armes, A. J. Ryan, *Macromol. Rapid Commun.* **2009**, *30*, 267–77.

[2] S. C. Owen, D. P. Y. Chan, M. S. Shoichet, *Nano Today* **2012**, *7*, 53–65.

[3] G. Riess, *Prog. Polym. Sci.* **2003**, *28*, 1107–1170.

[4] J.-F. Gohy, in *Block Copolym. II* (Ed.: V. Abetz), Springer-Verlag, Berlin/Heidelberg, **2005**, pp. 65–136.

[5] A. B. Ebrahim Attia, Z. Y. Ong, J. L. Hedrick, P. P. Lee, P. L. R. Ee, P. T. Hammond, Y.-Y. Yang, *Curr. Opin. Colloid Interface Sci.* **2011**, *16*, 182–194.

[6] J. Du, R. K. O'Reilly, *Chem. Soc. Rev.* **2011**, *40*, 2402–2416.

[7] J. Ehrhart, A.-F. Mingotaud, F. Violleau, *J. Chromatogr. A* **2011**, *1218*, 4249–56.

[8] T. Doussineau, C. Y. Bao, R. Antoine, P. Dugourd, W. Zhang, F. D'Agosto, B. Charleux, *ACS Macro Lett.* **2012**, *1*, 414–417.

[9] M. Štěpánek, J. Humpolíčková, K. Procházka, M. Hof, Z. Tuzar, M. Špirková, T. Wolff, *Collect. Czechoslov. Chem. Commun.* **2003**, *68*, 2120–2138.

[10] J. U. Izunobi, C. L. Higginbotham, *J. Chem. Educ.* **2011**, *88*, 1098–1104.

[11] Z. Grubišć-Gallot, Y. Gallot, J. Sedláček, *Macromol. Chem. Phys.* **1994**, *195*, 781–791.

[12] G. Greyling, H. Pasch, *J. Chromatogr. A* **2015**, *1414*, 163–172.

[13] M. A. Awan, V. L. Dimonie, *Langmuir* **1997**, *13*, 140–146.

[14] M. E. Schimpf, J. C. Giddings, K. Caldwell, *Field-Flow Fractionation Handbook*, Wiley-Interscience, New York, **2000**.

[15] C. A. Rue, M. E. Schimpf, *Anal. Chem.* **1994**, *66*, 4054–4062.

[16] M. E. Schimpf, *J. Chromatogr. A* **1990**, *517*, 405–421.

[17] F. A. Messaud, R. D. Sanderson, J. R. Runyon, T. Otte, H. Pasch, S. K. R. Williams, *Prog. Polym. Sci.* **2009**, *34*, 351–368.

[18] G. Greyling, H. Pasch, *Anal. Chem.* **2015**, *87*, 3011–3018.

[19] G. Greyling, H. Pasch, *Macromol. Rapid Commun.* **2014**, *35*, 1846–1851.

[20] J. J. Kirkland, L. S. Boone, W. W. Yau, *J. Chromatogr. A* **1990**, *517*, 377–393.

[21] U. Till, M. Gaucher-Delmas, P. Saint-Aguet, G. Hamon, J. Marty, C. Chassenieux, B. Payré, D. Goudounèche, A. Mingotaud, F. Violleau, *Anal. Bioanal. Chem.* **2014**, *406*, 7841–53.

[22] G. M. M. Sadeghi, M. Barikani, J. Morshedian, F. A. Taromi, *Iran. Polym. J.* **2003**, *12*, 515–521.

Chapter 5

Conclusions and Future Work

In this study it was demonstrated that ThFFF is a suitable technique for the microstructure-based separation of polymers and their self-assemblies.

The results for the current dissertation are summarised as follow:

In the first part of this study, it was shown that in addition to size and chemical composition, ThFFF is capable of separating polymers based on microstructure. This was demonstrated by the successful separation of PI and PB based on microstructure, the separation PMMA based on tacticity and the separation of BuMA based on topology. It was also shown that solvent parameters (such as viscosity and polarity) can have a significant influence on retention behaviour and that ThFFF be applied to probe relative polymer chain stiffness.

In the second part, the suitability of ThFFF to characterise micelles with various corona compositions was successfully demonstrated. It was shown by the analysis of PMMA-PS micelles that ThFFF can yield valuable information on important micelle characteristics such as size, shape, aggregation number, diffusion, thermal diffusion and Soret coefficients as a function of temperature, from a single injection. Additionally, ThFFF revealed information regarding size distributions and morphology changes as a function of temperature which is not possible by other analysis techniques. Furthermore, the potential of ThFFF to separate micelles based on corona composition was also shown.

In the next step the potential of ThFFF to separate micelles based on corona composition was realised by the successful separation of PB-PS micelles according

to corona microstructure. It was demonstrated that not only can ThFFF be applied to characterise mixed micelle formation in terms of size, molecular weight and their distributions, but a novel approach of coupling ThFFF to FTIR (via a LC-Transform interface) enables the determination of composition distributions as well. Consequently, ThFFF is currently the only characterisation platform capable of separating micelles according to corona composition while simultaneously providing comprehensive information on important micelle characteristics and their respective distributions.

The overall results demonstrate that ThFFF is a powerful analytical tool which is capable of not only separating polymers according to microstructure but also capable of separating micelles according to corona composition while simultaneously determining important micelle characteristics.

Suggested future work includes further investigation into determining the sensitivity of ThFFF towards chemical composition as preliminary results show that D_T is influenced by the isotope content of deuterated polystyrene homopolymers. Furthermore, the capabilities of ThFFF could be applied to the characterisation of triblock copolymers, cyclic polymers and star polymers (with arms of various compositions) in solution.

Chapter 6

References

[1] H. Pasch, *Polym. Chem.* **2013**, *4*, 2628–2650.

[2] H. Pasch, *Polym. Adv. Technol.* **2015**, *26*, 771–784.

[3] S. Podzimek, *Light Scattering, Size Exclusion Chromatography and Asymmetric Flow Field Flow Fractionation: Powerful Tools for the Characterization of Polymers, Proteins and Nanopoarticles*, John Wiley & Sons Inc., New Jersey, **2011**.

[4] J. C. Salamone, *Polymeric Materials Encyclopedia, Twelve Volume Set*, CRC Press, **1996**.

[5] G. E. Zaikov, R. Kozlowski, *Chemical and Physical Properties of Polymers*, Nova Science Publishers, New York, **2005**.

[6] M. Hehn, W. Hiller, T. Wagner, J. Thiel, H. Pasch, *Macromol. Chem. Phys.* **2012**, *213*, 401–410.

[7] P. Sinha, W. Hiller, V. Bellas, H. Pasch, *J. Sep. Sci.* **2012**, *35*, 1731–40.

[8] H. Pasch, B. Trathnigg, *Multidimensional HPLC of Polymers*, Springer-Verlag, Berlin-Heidelberg-New York, **2013**.

[9] M. I. Malik, G. W. Harding, M. E. Grabowsky, H. Pasch, *J. Chromatogr. A* **2012**, *1244*, 77–87.

[10] H. Pasch, A. C. Makan, H. Chirowodza, N. Ngaza, W. Hiller, N. Ngaza, W. Hiller, *Anal. Bioanal. Chem. Anal.* **2013**, *406*, 1585–96.

[11] Y. S. Gao, K. D. Caldwell, M. N. Myers, J. C. Giddings, *Macromolecules* **1985**, *18*, 1272–1277.

[12] M. E. Schimpf, J. C. Giddings, K. Caldwell, *Field-Flow Fractionation Handbook*, Wiley-Interscience, New York, **2000**.

[13] S. K. R. Williams, J. R. Runyon, A. A. Ashames, *Anal. Chem.* **2011**, *83*, 634–

642.

[14] W. Hiller, W. van Aswegen, M. Hehn, H. Pasch, *Macromolecules* **2013**, *46*, 2544–2552.

[15] P. M. Shiundu, J. C. Giddings, *J. Chromatogr. A* **1995**, *715*, 117–126.

[16] S. Kim Ratanathanawongs, P. M. Shiundu, J. Calvin Giddings, *Colloids Surfaces A Physicochem. Eng. Asp.* **1995**, *105*, 243–250.

[17] D. Lee, S. K. R. Williams, *J. Chromatogr. A* **2010**, *1217*, 1667–73.

[18] F. A. Messaud, R. D. Sanderson, J. R. Runyon, T. Otte, H. Pasch, S. K. R. Williams, *Prog. Polym. Sci.* **2009**, *34*, 351–368.

[19] S. Lee, A. Molnar, *Macromolecules* **1995**, *28*, 6354–6356.

[20] A. Blanazs, S. P. Armes, A. J. Ryan, *Macromol. Rapid Commun.* **2009**, *30*, 267–77.

[21] S. C. Owen, D. P. Y. Chan, M. S. Shoichet, *Nano Today* **2012**, *7*, 53–65.

[22] G. Riess, *Prog. Polym. Sci.* **2003**, *28*, 1107–1170.

[23] J.-F. Gohy, in *Block Copolym. II* (Ed.: V. Abetz), Springer-Verlag, Berlin/Heidelberg, **2005**, pp. 65–136.

[24] J. Bang, K. Viswanathan, T. P. Lodge, M. J. Park, K. Char, *J. Chem. Phys.* **2004**, *121*, 11489–500.

[25] A. B. Ebrahim Attia, Z. Y. Ong, J. L. Hedrick, P. P. Lee, P. L. R. Ee, P. T. Hammond, Y.-Y. Yang, *Curr. Opin. Colloid Interface Sci.* **2011**, *16*, 182–194.

[26] J. Du, R. K. O'Reilly, *Chem. Soc. Rev.* **2011**, *40*, 2402–2416.

[27] J. Ehrhart, A.-F. Mingotaud, F. Violleau, *J. Chromatogr. A* **2011**, *1218*, 4249–56.

[28] T. Doussineau, C. Y. Bao, R. Antoine, P. Dugourd, W. Zhang, F. D'Agosto, B. Charleux, *ACS Macro Lett.* **2012**, *1*, 414–417.

[29] M. Štěpánek, J. Humpolíčková, K. Procházka, M. Hof, Z. Tuzar, M. Špírková,

T. Wolff, *Collect. Czechoslov. Chem. Commun.* **2003**, *68*, 2120–2138.

[30] J. U. Izunobi, C. L. Higginbotham, *J. Chem. Educ.* **2011**, *88*, 1098–1104.

[31] R. Erhardt, M. Zhang, A. Böker, H. Zettl, C. Abetz, P. Frederik, G. Krausch, V. Abetz, A. H. E. Müller, *J. Am. Chem. Soc.* **2003**, *125*, 3260–3267.

[32] Z. Grubišć-Gallot, Y. Gallot, J. Sedláček, *Macromol. Chem. Phys.* **1994**, *195*, 781–791.

[33] M. Antonietti, A. Briel, C. Tank, *Acta Polym.* **1995**, *46*, 254–260.

[34] M. A. Awan, V. L. Dimonie, *Langmuir* **1997**, *13*, 140–146.

[35] C. A. Rue, M. E. Schimpf, *Anal. Chem.* **1994**, *66*, 4054–4062.

[36] M. E. Schimpf, *J. Chromatogr. A* **1990**, *517*, 405–421.

[37] J. C. Giddings, *J. Sep. Sci.* **1966**, *1*, 123–125.

[38] M. Wagner, S. Holzschuh, A. Traeger, A. Fahr, U. S. Schubert, *Anal. Chem.* **2014**, *86*, 5201–5210.

[39] P. Reschiglian, A. Zattoni, B. Roda, E. Michelini, A. Roda, *Trends Biotechnol.* **2005**, *23*, 475–483.

[40] S. K. Ratanathanawongs Williams, D. Lee, *J. Sep. Sci.* **2006**, *29*, 1720–1732.

[41] B. Roda, A. Zattoni, P. Reschiglian, M. H. Moon, M. Mirasoli, E. Michelini, A. Roda, *Anal. Chim. Acta* **2009**, *635*, 132–43.

[42] J. Giddings, *Science (80-.).* **1993**, *260*, 1456–1465.

[43] K. Wahlund, *J. Chromatogr. A* **2013**, *1287*, 97–112.

[44] J. Janča, *J. Liq. Chromatogr. Relat. Technol.* **2002**, *25*, 683–704.

[45] J. Janča, J.-F. Berneron, R. Boutin, *J. Colloid Interface Sci.* **2003**, *260*, 317–323.

[46] L. Pasti, S. Agnolet, F. Dondi, *Anal. Chem.* **2007**, *79*, 5284–5296.

[47] A. Van Asten, E. Venema, W. Kok, H. Poppe, *J. Chromatogr. A* **1993**, *644*, 83–94.

[48] H. Cölfen, M. Antonietti, H. Pasch, H. Engelhardt, G. O, *New Developments in Polymer Analytics I*, Springer Berlin Heidelberg, **2000**.

[49] A. C. Van Asten, W. T. Kok, R. Tjissen, H. Poppe, *J. Polym. Sci. Part B Polym. Phys.* **1996**, *34*, 283–295.

[50] R. M. Sisson, J. C. Giddings, *Anal. Chem.* **1994**, *66*, 4043–4053.

[51] M. E. Schimpf, J. C. Giddings, *J. Polym. Sci. Part B Polym. Phys.* **1989**, *27*, 1317–1332.

[52] M. E. Schimpf, J. C. Giddings, *J. Polym. Sci. Part B Polym. Phys.* **1990**, *28*, 2673–2680.

[53] C. Van Batten, M. Hoyos, M. Martin, *Chromatographia* **1997**, *45*, 121–126.

[54] M. E. Schimpf, L. M. Wheeler, P. F. Romeo, in *Chromatogr. Polym. Charact. by SEC FFF* (Ed.: T. Provder), ACS Symposium Series, Washington, DC, **1993**, pp. 63–76.

[55] D. Stadelmaier, W. Köhler, *Macromolecules* **2009**, *42*, 9147–9152.

[56] J. J. Kirkland, L. S. Boone, W. W. Yau, *J. Chromatogr. A* **1990**, *517*, 377–393.

[57] J. R. Runyon, S. K. R. Williams, *J. Chromatogr. A* **2011**, *1218*, 6774–9.

[58] A. C. Van Asten, R. J. van Dam, W. T. Kok, R. Tijssen, H. Poppe, *J. Chromatogr. A* **1995**, *703*, 245–263.

[59] K.-H. Cho, Y. H. Park, S. J. Jeon, W.-S. Kim, D. W. Lee, *J. Liq. Chromatogr. Relat. Technol.* **1997**, *20*, 2741–2756.

[60] J. J. Gunderson, J. C. Giddings, *Macromolecules* **1986**, *19*, 2618–2621.

[61] G. E. Kassalainen, S. K. R. Williams, *J. Chromatogr. A* **2003**, *988*, 285–295.

[62] J. C. Giddings, M. N. Myers, J. Janča, *J. Chromatogr. A* **1979**, *186*, 37–44.

[63] C. A. Ponyik, D. T. Wu, S. K. R. Williams, *Anal. Bioanal. Chem.* **2013**, *405*, 9033–40.

[64] W. van Aswegen, W. Hiller, M. Hehn, H. Pasch, *Macromol. Rapid Commun.* **2013**, *34*, 1098–103.

[65] J. R. Runyon, S. K. R. Williams, *Polym. Prepr.* **2011**, *52*, 230–231.

[66] Y. J. Choi, S. T. Kim, S. H. Lee, A.-J. Kim, G. Kwag, S. Lee, *J. Chromatogr. A* **2013**, *1314*, 306–12.

[67] P. M. Shiundu, S. M. Munguti, S. K. Ratanathanawongs Williams, *J. Chromatogr. A* **2003**, *983*, 163–176.

[68] P. M. Shiundu, S. M. Munguti, S. K. Ratanathanawongs Williams, *J. Chromatogr. A* **2003**, *984*, 67–79.

[69] B. Wunderlich, *Thermal Analysis of Polymeric Materials*, Springer-Verlag, Berlin-Heidelberg, **2005**.

[70] J. Cowie, I. McEwen, *J. Chem. Soc. Faraday Trans. 1* **1976**, *72*, 526–533.

[71] U. Apel, R. Hentschke, J. Helfrich, *Macromolecules* **1995**, *28*, 1778–1785.

[72] A. Karandinos, J. Mays, N. Hadjichristidis, *Polym. Bull.* **1990**, *24*, 251–254.

[73] A. Karandinos, S. Nan, J. W. Mays, N. Hadjichristidis, *Macromolecules* **1991**, *24*, 2007–2010.

[74] D. Koshal, *Manufacturing Engineer's Reference Book*, Butterworth-Heinemann, Oxford, **1993**.

[75] C. Agatemor, M. P. Shaver, *Biomacromolecules* **2013**, *14*, 699–708.

[76] G. Wypych, *Handbook of Solvents*, ChemTec Publishing, Toronto-New York, **2001**.